

1993

Cellular Trafficking and Processing Pathways of the Alzheimer (β)/A4 Amyloid Precursor Protein

Gregg L. Caporaso

Follow this and additional works at: http://digitalcommons.rockefeller.edu/student_theses_and_dissertations



Part of the [Life Sciences Commons](#)

Recommended Citation

Caporaso, Gregg L., "Cellular Trafficking and Processing Pathways of the Alzheimer (β)/A4 Amyloid Precursor Protein" (1993). *Student Theses and Dissertations*. 354.
http://digitalcommons.rockefeller.edu/student_theses_and_dissertations/354

This Thesis is brought to you for free and open access by Digital Commons @ RU. It has been accepted for inclusion in Student Theses and Dissertations by an authorized administrator of Digital Commons @ RU. For more information, please contact mcsweej@mail.rockefeller.edu.



**Cellular Trafficking and Processing Pathways of the
Alzheimer β /A4 Amyloid Precursor Protein**

A thesis submitted to the Faculty of
The Rockefeller University
in partial fulfillment of the requirements
for the degree of Doctor of Philosophy

by

Gregg L. Caporaso

January 1993
The Rockefeller University
New York

To My Parents

Thus it seemed that this one hillside illustrated the principle of all the operations of Nature. The Maker of this earth but patented a leaf. What Champollion will decipher this hieroglyphic for us, that we may turn over a new leaf at last?

—H. D. T.

Acknowledgements

I am grateful to all those people who have helped make my graduate years productive and enjoyable. While there are probably no members of the Laboratory of Molecular and Cellular Neuroscience whom I have not sought out for assistance at one time or another, several individuals merit special attention. I thank Kerstin Iverfeldt and Talvinder Sihra for teaching me many of the basic techniques that were indispensable for most of my projects, as well as the abundant advice and the camaraderie they have provided. I also thank Joseph Buxbaum and Fred Gorelick, whose own projects were instrumental to the success of my efforts. In addition to being valued friends, Christer Nordstedt and Triprayar Ramabhadran were perennial sources of novel ideas and scientific exchange. Finally, every graduate student should be fortunate enough to encounter senior laboratory researchers like Andrew Czernik and Angus Nairn who, in addition to being seemingly limitless founts of biochemical knowledge, were always willing to share their learning with an eager student.

I would also like to thank Pietro De Camilli, with whom I had the great pleasure and privilege of working for several months. He and the members of his laboratory were exceedingly gracious in offering to me their professional expertise and their friendship.

I must also thank Alan Aderem, Günter Blobel, Juan Bonifacino, and William Muller, who undertook the selfless task of serving on my thesis committee.

To be sure, I reserve my greatest appreciation for my research advisors, Paul Greengard and Samuel Gandy. I was honored to spend countless hours with Paul poring over manuscripts and discussing fresh approaches to problems. With his attention and insight, Paul never failed to give me an example to which I might aspire. Lastly, I thank Sam who, in addition to being my advisor, has been a good friend throughout my graduate studies. Without Sam's unflagging support and sincere kindness, this project would never have reached completion.

Table of Contents

	Page
Acknowledgements	v
Table of Contents	vii
List of Figures	viii
List of Tables	xi
Abbreviations	xii
Abstract	1
Chapter 1. Introduction	3
Chapter 2. Experimental Methods	35
Chapter 3. Separate Processing Pathways for APP Secretion and Proteolytic Degradation	45
Chapter 4. Regulation of APP Secretion by Protein Phosphorylation	76
Chapter 5. Cellular Transport of APP via Clathrin-Coated Vesicles	102
Chapter 6. Correlation Between the Subcellular Localization of APP and Its Biochemical Processing	120
Chapter 7. Concluding Remarks	162
References	168

List of Figures

	Page
Figure 1. Neurofibrillary tangles and paired helical filaments.	8
Figure 2. Bielschowsky silver staining of a senile plaque.	13
Figure 3. Birefringence of a senile plaque stained with Congo red and viewed by polarized light.	16
Figure 4. Distribution of senile plaques in the hippocampus and entorhinal cortex of the brain from an individual suffering from Alzheimer disease.	21
Figure 5. Structure of the Alzheimer β /A4 amyloid precursor protein.	25
Figure 6. Identification of APP species in PC12 cells by immunoprecipitation with domain-specific antibodies.	48
Figure 7. Model of lysosomal pH maintenance and the uptake of weak bases.	51
Figure 8. Neutralization of acidic compartments in chloroquine-treated cells.	53
Figure 9. Effects of chloroquine on APP processing.	56
Figure 10. Effect of chloroquine on APP maturation.	59
Figure 11. Effect of chloroquine on the turnover of mature APP.	61
Figure 12. Effect of chloroquine on APP secretion.	65
Figure 13. Effect of chloroquine on the turnover of the carboxyl-terminal APP fragment.	67
Figure 14. Effects of monensin on APP maturation and secretory processing.	70

Figure 15. Comparative effects of monensin and brefeldin A on APP maturation and secretion.	73
Figure 16. Comparison of the protein kinase C phosphorylation sites of APP and the receptors for EGF and IL-2.	78
Figure 17. Effect of phorbol ester on APP maturation.	82
Figure 18. Effect of phorbol ester on the turnover of mature APP.	84
Figure 19. Effect of phorbol ester on the turnover of the carboxyl-terminal APP fragment.	85
Figure 20. Effect of phorbol ester on APP secretion (autoradiogram).	87
Figure 21. Effect of phorbol ester on APP secretion (quantitation).	90
Figure 22. Effect of an inactive phorbol ester on APP secretion.	92
Figure 23. Comparative effects of phorbol ester and okadaic acid on APP secretion.	95
Figure 24. Proposed scheme for the cellular trafficking and proteolytic processing of APP.	100
Figure 25. Co-purification of APP and transferrin receptor with clathrin-coated vesicles fractionated by density-equilibrium centrifugation.	107
Figure 26. Co-purification of APP with clathrin-coated vesicles fractionated by gel-filtration chromatography.	111
Figure 27. Electron micrograph of clathrin-coated vesicles fractionated by gel-filtration chromatography.	114
Figure 28. Enrichment of APP in clathrin-coated vesicles.	117
Figure 29. Comparison of the subcellular localization of APP and GIMP _t in rat brain by immunofluorescence microscopy.	124

Figure 30. Localization of APP and SV2 in primary cultures of rat hippocampal neurons by immunofluorescence microscopy.	127
Figure 31. Localization of APP in rat brain tissue fragments by immunoelectron microscopy.	130
Figure 32. Immunofluorescence microscopy of various mammalian cell lines showing the juxtanuclear localization of APP.	133
Figure 33. Immunoblot analysis of APP in rat brain and mammalian cell lines.	136
Figure 34. Comparison of the distributions of APP and several Golgi complex markers by fluorescence microscopy in CHO cells.	139
Figure 35. Immunoblot analysis of CHO cells treated with BFA.	142
Figure 36. Comparison of the distributions of APP and Tf-R by immunofluorescence microscopy in control CHO cells and in CHO cells treated with BFA.	145
Figure 37. Comparison of the distributions of APP, Tf-R, and BiP by immunofluorescence microscopy in control COS cells and in COS cells treated with BFA.	148
Figure 38. Immunoblot analysis of CHO cells treated with phorbol ester.	151
Figure 39. Comparison of the distributions of APP and Igpl20 by immunofluorescence microscopy in control CHO cells and in CHO cells treated with chloroquine.	154
Figure 40. Immunoblot analysis of CHO cells treated with chloroquine.	157

List of Tables

	Page
Table 1. Diseases that cause dementia.	4
Table 2. Precursors of human amyloid fibril proteins.	17
Table 3. Comparison of APP isoforms and APP-related proteins.	27
Table 4. Summary of drug effects on the recovery of APP species.	97
Table 5. Cell-surface proteins whose cytoplasmic domains contain the consensus sequence NPXY.	104

Abbreviations

AD	Alzheimer disease
AMP	adenosine monophosphate
APP	amyloid precursor protein
ATP	adenosine triphosphate
BFA	brefeldin A
CCV	clathrin-coated vesicle
cDNA	complementary DNA
CSF	cerebrospinal fluid
CSF-1	colony-stimulating factor 1
DMEM	Dulbecco's modified Eagle's medium
DNA	deoxyribonucleic acid
DS	Down syndrome
EDTA	ethylenediaminetetraacetic acid
EGF	epidermal growth factor
EGTA	ethyleneglycoltetraacetic acid
ER	endoplasmic reticulum
FAD	familial Alzheimer disease
FBS	fetal bovine serum
FITC	fluorescein isothiocyanate
GMP	guanosine monophosphate
GSDB	goat serum dilution buffer
HBS	Hepes-buffered saline solution
HCHWA-D	hereditary cerebral hemorrhage with amyloidosis (Dutch type)

IL-2	interleukin 2
kDa	kilodalton
KPI	Kunitz-type protease inhibitor
KSPV	lysine-serine-proline-valine
MEM	Eagle's modified minimal essential medium
M _r	relative molecular mass
mRNA	messenger RNA
NFT	neurofibrillary tangle
NPXY	asparagine-proline-(<i>any amino acid</i>)-tyrosine
PAS	protein A Sepharose CL-4B
PBS	phosphate-buffered saline solution
PDBu	phorbol 12,13-dibutyrate
PHF	paired helical filament
PKC	protein kinase C
PN-II	protease nexin-II
RNA	ribonucleic acid
SDS	sodium dodecyl (lauryl) sulfate
TBST	Tris-buffered saline solution/Tween-20
Tf-R	transferrin receptor
TGF- α	transforming growth factor- α
TGN	<i>trans</i> -Golgi network
Tris	2-amino-2-hydroxymethyl-1,3-propanediol

Abstract

Extracellular deposition of the β /A4 amyloid peptide is a characteristic feature of the brain in patients with Alzheimer disease. β /A4 amyloid is derived from the integral membrane amyloid precursor protein (APP). Secreted truncated forms of APP found in blood plasma and cerebrospinal fluid arise by proteolytic cleavage of APP within the β /A4 amyloid domain, precluding the possibility of amyloidogenesis for that population of molecules.

The routes of APP processing were examined in metabolically-labeled PC12 cells treated with agents known to affect specific cellular functions. Treatment with either monensin or brefeldin A (BFA) prevented normal APP maturation (*N*- and *O*-glycosylation and tyrosine sulfation) and abolished APP secretion. Phorbol ester produced a several-fold increase in APP secretion, indicating that protein phosphorylation regulates intra- β /A4 amyloid cleavage and APP secretion. The lysosomotropic drug chloroquine exerted inhibitory effects on the degradation of mature APP holoprotein and of the carboxyl-terminal fragment resulting from secretory cleavage, but exhibited no effects on APP secretion. The results suggest that a substantial proportion of APP is degraded in an intracellular acidic compartment, but that the coupled APP cleavage/secretion event occurs in a chloroquine-insensitive compartment. Direct evidence that APP is targeted to the endosomal/lysosomal system was provided by the identification of APP in clathrin-coated vesicles, which mediate the transport of many proteins to endosomes.

The subcellular distribution of APP was examined by microscopy and correlated with its biochemical processing. As shown by immunofluorescence microscopy of rat brain sections, APP was concentrated in the Golgi complex and in proximal axon segments. By immunoelectron microscopy of rat brain tissue fragments, APP was found associated with Golgi elements and with medium-sized, invaginated vesicles in both axons and dendrites. Prominent localization of APP to the Golgi complex was also found in primary cultures of rat hippocampal neurons and in non-neuronal cell lines.

When cultured cells were treated with BFA, APP immunoreactivity changed from a Golgi-like to an ER-like distribution. No APP was detected in the BFA-induced reticulum identified by the transferrin receptor, indicating that concentration of APP in the Golgi does not reflect recycling between the *trans*-Golgi network and the early endosomal system. Although treatment with phorbol ester resulted in a marked elevation of APP secretion, no redistribution of APP immunoreactivity was apparent. Chloroquine induced APP co-localization with the lysosomal marker lgp120, whereas no co-localization was seen in untreated cells. Taken together, these results support a scheme in which APP is concentrated in the Golgi complex as it travels through the central vacuolar system *en route* to the plasma membrane for secretion and/or to lysosomes for degradation.

Chapter 1

Introduction

Perspective

Alzheimer disease (AD) is the fourth leading cause of death in the developed world, after heart disease, cancer, and stroke. Since it is a disease of the elderly, and because improving health care and medical technologies are extending human longevity, the social and fiscal burdens of AD will continue to increase.

The insidious memory loss, cognitive decline, and personality changes associated with AD lead to its categorization as a type of dementia, which may be defined clinically as an impairment in thought and intellect that is severe enough to interfere with normal social or occupational functioning (Kaplan and Sadock, 1988). Dementias historically were classified as "presenile" if they occur before, and as "senile" if they occur after, the age of 65 years (Tomlinson and Corsellis, 1984). Although many causes of dementia have been identified (Table 1), including brain neoplasms, infectious agents (*e.g.*, human immunodeficiency virus), prions (*e.g.*, in Creutzfeldt-Jakob disease), and systemic disorders (*e.g.*, multi-infarct dementia), AD is the most common dementing disease, accounting for more than half of all the cases of dementia (Katzman, 1986). Some dementias are readily treatable and sometimes reversible (*e.g.*, folate deficiency), but the etiology of AD is unknown and no effective treatment exists. The disease increases in severity over the course of

Table 1. Diseases that cause dementia (Kaplan and Sadock, 1988).

Parenchymatous diseases of the CNS	Systemic disorders
Alzheimer disease	Endocrine and metabolic disorders
Down syndrome	Thyroid disease*
Pick's disease	Parathyroid disease*
Gerstmann-Straussler syndrome	Pituitary-adrenal disorders*
Huntington's disease	Post-hypoglycemic states
Parkinson's disease*	Liver disease
Multiple sclerosis	Chronic progressive hepatic encephalopathy*
Deficiency states	Urinary tract disease
Cyanocobalamin deficiency*	Chronic uremic encephalopathy*
Folic acid deficiency*	Dialysis dementia*
Drugs and toxins*	Cardiovascular disease
Intracranial tumors and brain trauma*	Cerebral hypoxia or anoxia*
	Multi-infarct dementia*
	Cardiac arrhythmias*
	Inflammatory diseases of blood vessels*
Infectious processes	Pulmonary disease
Creutzfeldt-Jakob disease	Respiratory encephalopathy*
Kuru	
Cryptococcal meningitis*	Miscellaneous disorders
Neurosyphilis*	Hepatolenticular degeneration*
TB and fungal meningitides*	Hydrocephalic dementia*
Viral encephalitis*	Sarcoidosis*
HIV-related disorders	Normal pressure hydrocephalus*
(AIDS and ARC)	

*Conditions calling for therapeutic intervention. (Abbreviations: CNS, central nervous system; TB, tuberculosis; HIV, human immunodeficiency virus; AIDS, acquired immune deficiency syndrome; and ARC, AIDS-related complex.)

a decade, at the end of which time patients retain only vegetative neurologic function and typically succumb to secondary systemic processes such as infections (Katzman, 1986).

Accurate diagnosis of AD is, therefore, important in that misdiagnosis of a treatable form of dementia might result in useful therapy being withheld (Khachaturian, 1985). Since a definitive diagnosis of AD can only be made upon autopsy at present, physicians must instead arrive at a diagnosis of probable AD based upon a clinical history, a methodical cognitive evaluation of dementia, and the exclusion of other dementing disorders (McKhann *et al.*, 1984). Using such criteria, a group of researchers recently examined the elderly sector of one Massachusetts community and concluded that approximately 10% of people over the age of 65 years and more than 45% of people over the age of 85 years had probable AD (Evans *et al.*, 1989). If conservatively extrapolated to the entire United States population, these results would estimate that between three and four million Americans are afflicted with AD.

Historical introduction

In 1907, the Munich neuropathologist Alois Alzheimer reported the clinical presentation and the histopathological alterations in the brain of a 51-year-old woman who, he assessed, was afflicted with a novel neurological disease (Alzheimer, 1907). Over a span of less than five years, the patient suffered from progressive memory decline and dramatic alterations in personality that included paranoid delusions. Alzheimer's contribution to the disease that bears his name was to recognize that an association might exist

between these clinical symptoms and the startling microscopic brain pathology he found (Wilkins and Brody, 1969). Kraepelin (1910) identified these same pathological changes in the brains of patients clinically affected with dementia; he thus confirmed Alzheimer's report and first applied the name "Alzheimer's disease" to this clinicopathological entity.

Neurofibrillary tangles

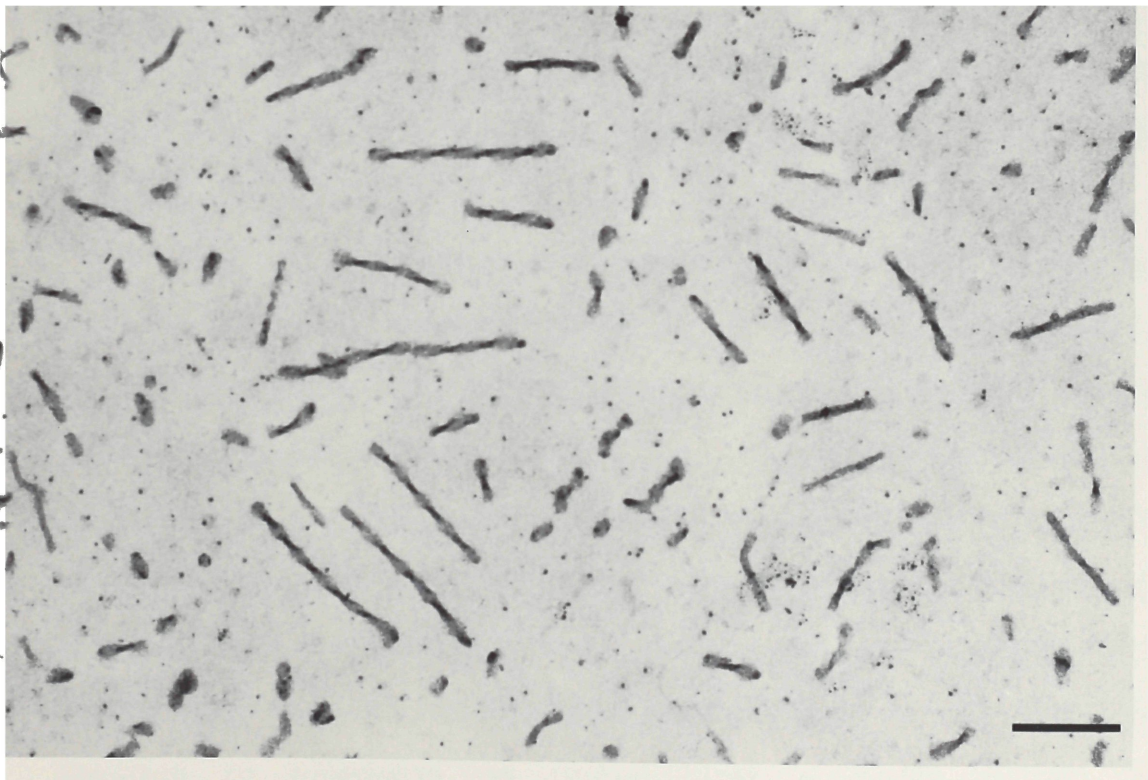
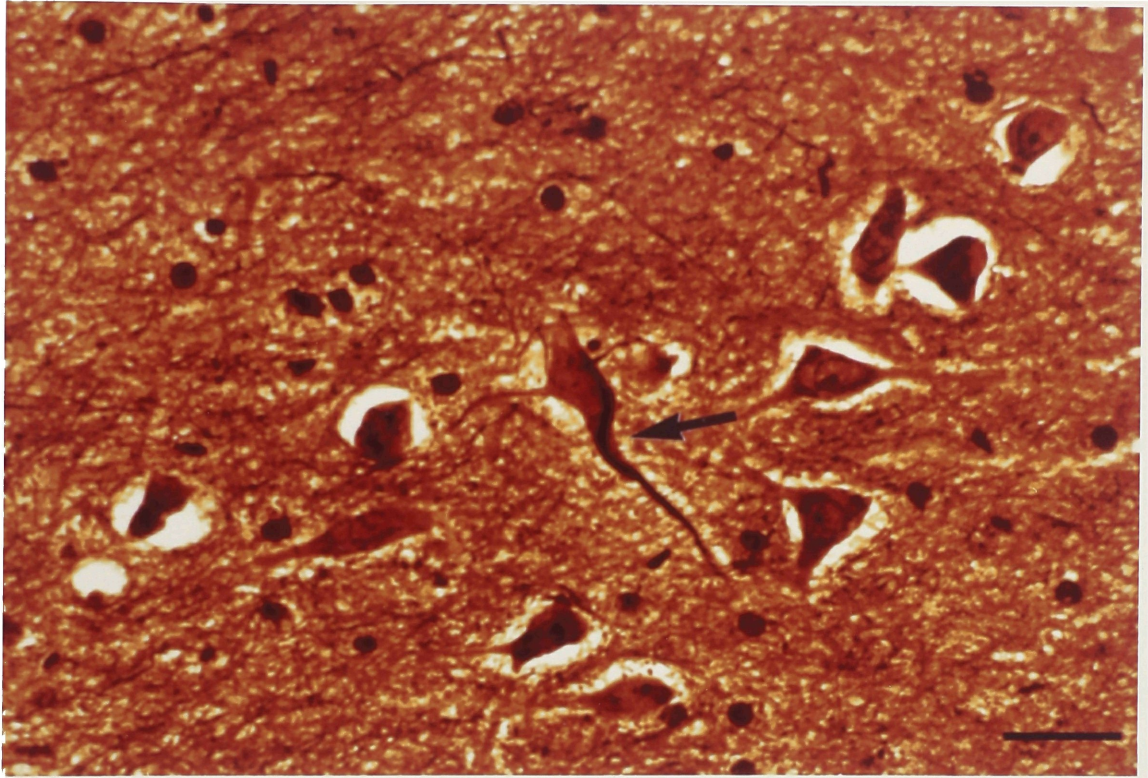
Using a histochemical staining technique based on silver impregnation, Alzheimer identified alterations in the neuronal cytoskeleton:

In the interior of a cell that otherwise appeared normal, one or several fibrils stood out due to their extraordinary thickness and impregnability . . . Since these fibrils could be stained with different dyes than normal, a chemical alteration of the fibrillar substance must have taken place (Alzheimer, 1907).

These intracellular structures, now known as neurofibrillary tangles (NFTs) (Figure 1, *top*), are most often found in the neurons of the cerebral cortex, hippocampus, amygdala, basal forebrain, and brainstem (Joachim and Selkoe, 1992). NFTs are not restricted to AD, but are also found in progressive supranuclear palsy, dementia pugilistica, and Guamanian-amyotrophic lateral sclerosis-Parkinsonism-dementia complex (Selkoe, 1989b). It is widely believed that the density of NFTs in affected areas of the brain correlates with the severity of dementia in AD (Blessed *et al.*, 1968).

When examined by electron microscopy, NFTs were found to be composed of paired helical filaments (PHFs), ~10-nm fibrils twisted in a double helix with a periodicity of 160 nm (Figure 1, *bottom*)

Figure 1. Neurofibrillary tangles and paired helical filaments. (*Top*) Bielschowsky silver staining of a section from the CA4 region of the hippocampus prepared upon the autopsy of a 68-year-old individual diagnosed with AD. A clearly defined NFT is indicated by the *arrow*. Scale bar represents 25 μm . (*Bottom*) Electron micrograph of PHFs purified from AD brain homogenates as described by Greenberg and Davies, 1990. Scale bar represents 200 nm. The silver-stained brain section in this figure, as well as those in Figures 2 and 4, and the electron micrograph were kind gifts from Li-wen Ko and Sharon Greenberg, respectively.



(Kidd, 1963). Biochemical analysis has proven more difficult, since most of the components of NFTs are extremely insoluble (Selkoe *et al.*, 1982). However, several constituents have been identified by immunological means in histopathological preparations and proteolytic digests of PHFs, including ubiquitin (Mori *et al.*, 1987; Manetto *et al.*, 1988) and microtubule-associated protein 5 (1B) (Hasegawa *et al.*, 1990). A principal soluble component of the PHFs was found to be the neuron-specific microtubule-associated protein tau (Kosik *et al.*, 1986; Goedert *et al.*, 1988; Wischik *et al.*, 1988a; Wischik *et al.*, 1988b). Tau represents a group of proteins with amino-terminal variability that arises by alternative splicing of a single gene (Himmler, 1989), and with a carboxyl-terminal region containing multiple repeats of a microtubule-binding domain (Himmler *et al.*, 1989). Antisense oligonucleotide experiments in neuronal cultures and baculovirus-mediated tau expression in Sf9 insect cells suggest that tau is involved in the formation and/or maintenance of axonal processes (Caceres and Kosik, 1990; Knops *et al.*, 1991).

Using several monoclonal antibodies that were raised against tau and that also recognize NFTs, Kosik *et al.* (1988) produced an epitope map of tau by screening an expression sublibrary of human tau complementary DNA (cDNA), and concluded that intact tau is present in NFTs. However, a monoclonal antibody called Alz-50 that labels NFTs in AD brains (Wolozin *et al.*, 1986), and which recognizes brain-derived tau (Nukina *et al.*, 1988), did not recognize any tau species expressed in the bacterial sublibrary. Alz-50 was initially reported to recognize on immunoblots a single protein (A68)

(Wolozin *et al.*, 1986), whose relative molecular mass (68 kDa) is comparable to that of tau. The results of these studies suggested that the tau in AD NFTs is post-translationally modified (Kosik *et al.*, 1988).

This hypothesis was strengthened when A68 was shown to share epitopes with tau, but to be different by several biochemical criteria, such as having a slightly higher molecular mass, more acidic isoelectric point, and decreased detergent solubility (Ksiezak-Reding *et al.*, 1990). Indeed, abnormally phosphorylated cytoskeletal components, including tau, had been identified in AD brain (Sternberger *et al.*, 1985; Grundke-Iqbal *et al.*, 1986), and Alz-50 was demonstrated to recognize a phosphorylated tau species (Uéda *et al.*, 1990). Subsequently, PHFs were shown to contain A68, and A68 was shown to be identical to the abnormally phosphorylated tau in NFTs (Lee *et al.*, 1991). When enzymatically dephosphorylated, the molecular mass and isoelectric point of A68 more closely resembled those of tau.

The aberrant phosphorylation of A68 was localized to the serine residue of a lysine-serine-proline-valine (KSPV) sequence in tau (Lee *et al.*, 1991). This sequence is a phosphorylation consensus motif for both *cdc2* kinase and proline-directed serine/threonine kinases, which comprise the mitogen-activated protein kinase and extracellular signal-regulated kinase families of enzymes (Shenoy *et al.*, 1989; Vulliet *et al.*, 1989), though phosphorylation of tau by these kinases *in vivo* has not yet been demonstrated. Recently, several groups have purified protein kinase activities based on their ability to produce an AD-like change in the phosphorylation state of tau.

These protein kinases have been shown *in vitro* to phosphorylate the serine residue of the KSPV site of tau, producing a change in the apparent molecular mass and antigenic characteristics of Alzheimer tau (Roder and Ingram, 1991; Biernat *et al.*, 1992; Ishiguro *et al.*, 1992; Drewes *et al.*, 1992). Aberrant regulation of tau phosphorylation could in theory produce cytoskeletal changes that result in PHFs and NFTs, since phosphorylated tau proteins have been shown *in vitro* to be less effective in promoting microtubule polymerization than non-phosphorylated forms (Lindwall and Cole, 1984).

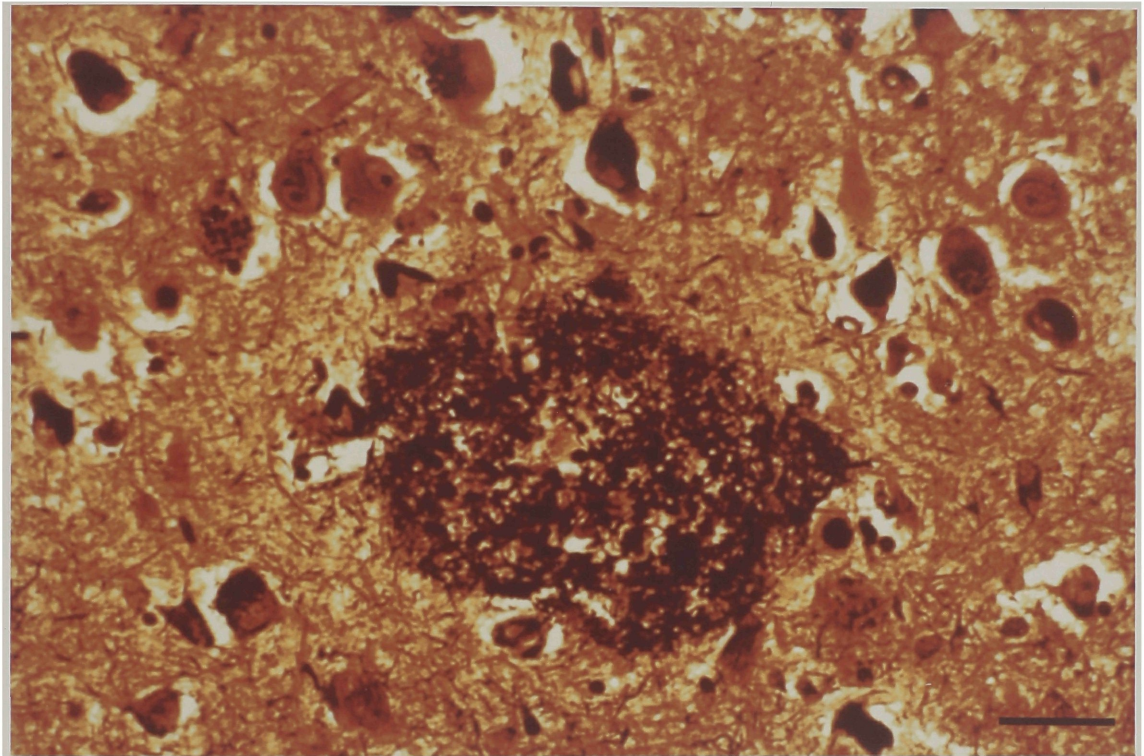
Senile plaques

Alzheimer also mentioned in his original report the cerebral atrophy that characterizes the brains of many demented patients and, more intriguingly, the identification of distinctive extracellular lesions:

Scattered through the entire cortex, especially in the upper layers, one found miliary foci that were caused by the deposition of a peculiar substance in the cerebral cortex. It could be recognized without staining, but was very refractory to dyes (Alzheimer, 1907).

Although he was not the first to observe these structures (Figure 2) (in 1892, Blocq and Marinesco described these lesions as "*nodules de sclérose névroglique*"), Alzheimer correlated this pathological finding with the clinical symptoms. As these structures are found in the brains of most elderly persons, but to a much lesser extent than in AD, Simchowicz (1911) termed the lesions "senile plaques." Also in 1911, Bielschowsky determined that the central core of the plaques

Figure 2. Bielschowsky silver staining of a senile plaque. Dystrophic neurites appear as black fibril-like structures, but the amyloid core of the plaque is not visible by this histochemical method. The microscopic field is from the CA1 hippocampal region of the individual described in Figure 1. Scale bar represents 25 μm .



was composed of an amyloid-like material.

The term "amyloid" was applied earlier by Virchow (1855) to describe deposits found upon autopsy in the brains of aged individuals. This designation was based upon the similarity of the substance to starch when viewed after iodine staining. However, brain amyloid was found to be composed of protein, not starch, when examined by chemical analysis shortly thereafter (Friedreich and Kekulé, 1859). Today, the amyloid deposits comprising the cores of senile plaques are accurately identified histopathologically by staining with the fluorescent dye thioflavin S or, more definitively, with the dye Congo red, which produces an apple-green birefringence when viewed with polarized light (Figure 3) (Schwartz *et al.*, 1965). The peptide fibrils constituting the primary component of the plaque-core amyloid are arranged in regular arrays of β -pleated sheets, which serve to orient the Congo red dye molecules in a regularly structured manner that is the basis of their characteristic appearance when viewed under polarized light (Sipe, 1992).

In addition to AD, there are several other diseases that involve amyloid deposition. However, these are biochemically distinguishable disorders whose only common feature is the accumulation in tissues of a normally soluble protein to form insoluble deposits, identifiable with the above-mentioned staining techniques (Sipe, 1992). Besides the amyloid of AD (see below, " β /A4 amyloid"), at least a dozen other amyloid proteins, along with their larger precursor molecules, have been characterized (Table 2). Some amyloid disorders affect multiple organs, such as the deposition of a protein called amyloid A in the spleen, liver, and

Figure 3. Birefringence of a senile plaque stained with Congo red and viewed by polarized light. The compact amyloid deposit comprising the core of a senile plaque appears as a "Maltese cross" pattern of birefringence.

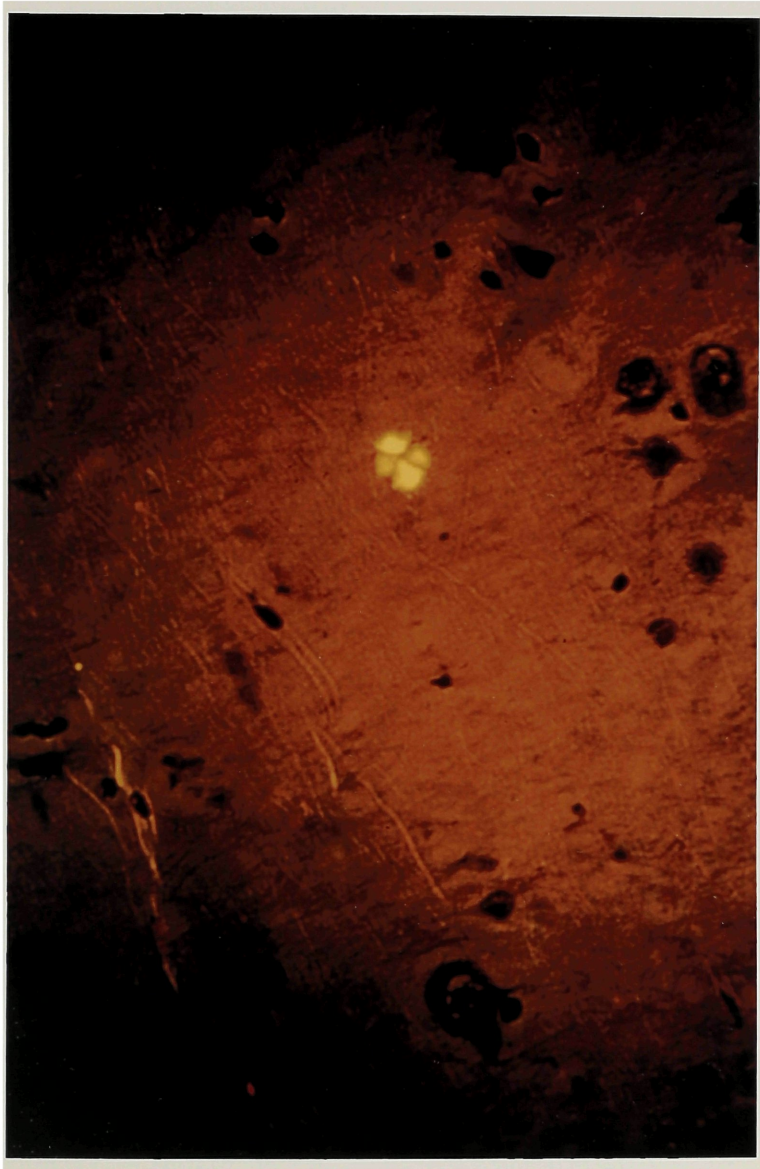


Table 2. Precursors of human amyloid fibril proteins (from Sipe, 1992).

Distribution	Protein	Size (kDa)	
		Fibril	Precursor
Systemic	Immunoglobulin	5-23	23
Systemic	Lipoproteins		
	Apo ^a -SAA ^b	8	12
	Apo-AI	9-11	26
	Apo-AII (mouse)	9	9
Systemic	TTR ^c /Prealbumin	5-14	14 (monomer)
Pancreas	IAPP ^d	4	9
Thyroid	Calcitonin	6	14.5
Heart	Atrial natriuretic factor	3-4	13
Musculoskeletal	β -2-microglobulin	12	12
Brain	β /A4 peptide	4-5	110-135
	Cystatin C	12	13
	Prion	27-30	30-35
Systemic	Gelsolin	7	90-93
Skin	Keratin	?	?

^aApolipoprotein. ^bSerum amyloid A. ^cTransthyretin. ^dIslet amyloid polypeptide.

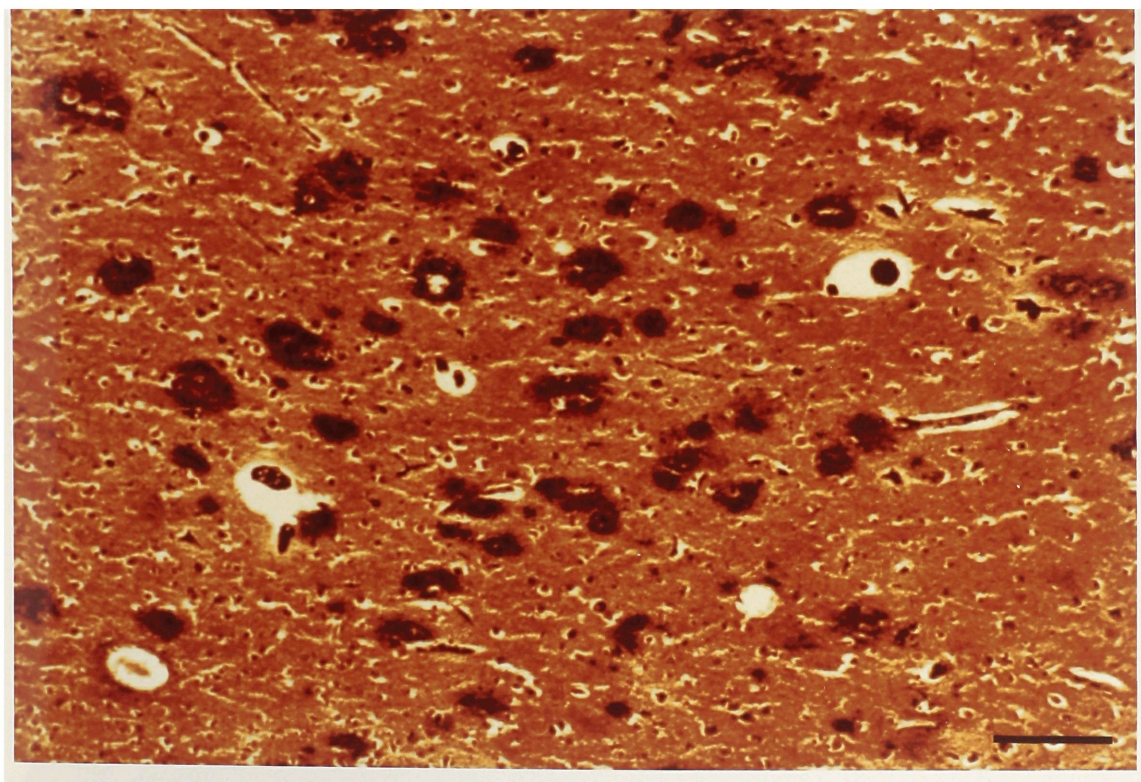
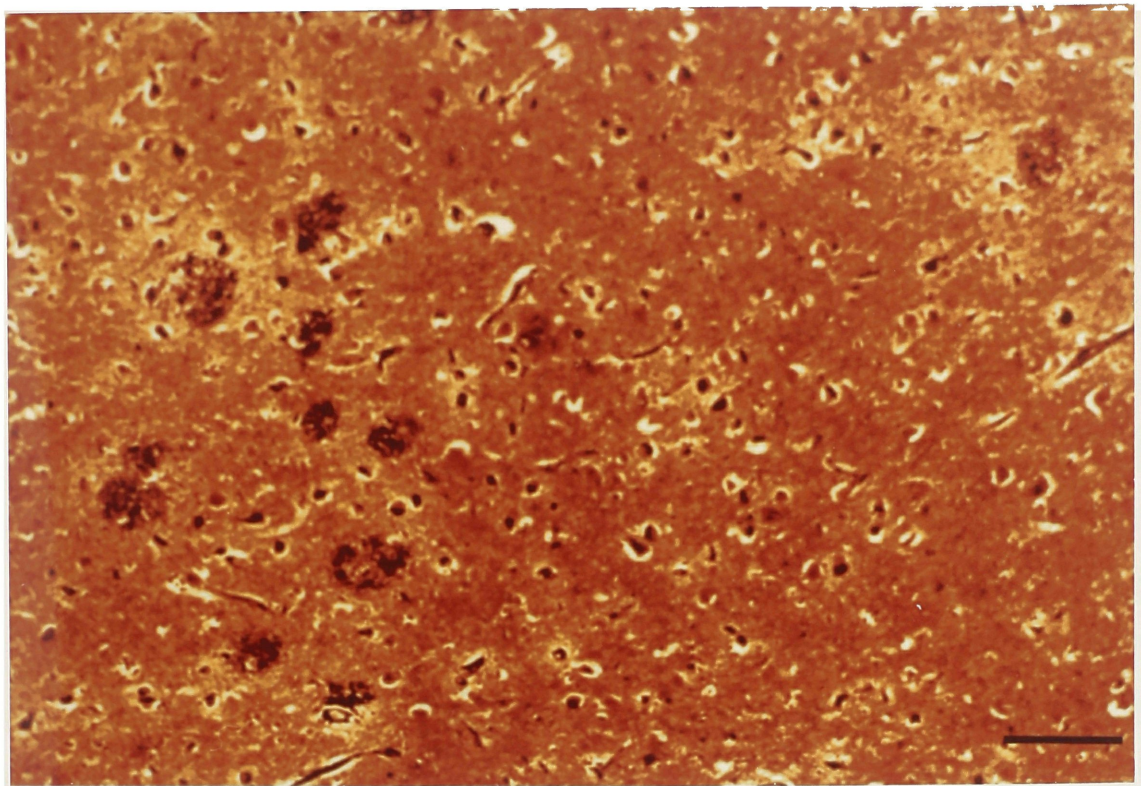
kidney; others affect particular organs, such as the pancreas in diabetes and the brain in AD (Sipe, 1992). In the case of the systemic disorders, the amyloid arises from the proteolysis of larger precursor proteins circulating in the blood; *e.g.*, amyloid A is generated from serum amyloid A, a protein released into the bloodstream during the acute phase response, although the mechanism whereby it is proteolyzed is not understood (Sipe, 1992).

Senile plaques were examined by electron microscopy in 1964 (Kidd, 1964). In addition to a central core of amyloid, senile plaques were found to be surrounded by dystrophic neurites, the degenerating remains of neuronal dendrites and axons (Figure 2). For this reason, senile plaques are sometimes referred to as neuritic plaques. Although an amyloid core is a distinctive feature of plaques, most amyloid deposits are not actually found in prototypical plaques, but rather exist as diffuse accumulations that may be refractory to Congo red or thioflavin S staining (Joachim and Selkoe, 1992). Evidence that these diffuse or "pre-amyloid" plaques are the precursors of mature senile plaques comes from examination of the brains of Down syndrome (DS) patients, who inevitably develop AD symptoms and pathology if they survive past the fourth decade of life (Wisniewski *et al.*, 1985). In younger Down patients (below the age of 40 years) the diffuse type of plaque predominates, whereas in older victims the neuritic type of plaque is more common (Giaccone *et al.*, 1989; Mann and Esiri, 1989; Rumble *et al.*, 1989). Accumulation of amyloid, therefore, might initiate neuritic dystrophy and possibly formation of NFTs, since PHFs are important components of dystrophic neurites (for review, see Trojanowski *et*

al., 1990).

Senile plaques are found primarily in association areas of the temporal and parietal cortices, with an especially high density of plaques in the hippocampus, entorhinal cortex, and amygdala, areas of the brain that are important for short-term and spatial memory (Figure 4) (Tomlinson and Corsellis, 1984; Katzman, 1986). In addition, diffuse amyloid deposits that do not go on to form neuritic plaques can be found in brain areas such as cerebellum, striatum, and thalamus (Joachim *et al.*, 1989; Ogomori *et al.*, 1989; Suenaga *et al.*, 1990), which argues that cerebral amyloid deposition does not invariably lead to neuritic dystrophy (Joachim and Selkoe, 1992). Although there is not a good correlation between brain areas of amyloid deposition and areas of synaptic loss, as indicated by a marker for the synaptic vesicle protein synaptophysin (Masliah *et al.*, 1990), this does not preclude a role for amyloid in the neuronal loss and cognitive deficits of AD (Joachim and Selkoe, 1992; see below, "Amyloid precursor protein"). Senile plaques are not abundant in subcortical nuclei, but are primarily concentrated in the cortex, hippocampus, and amygdala, regions containing the nerve terminals projected from NFT-prone subcortical areas (Price *et al.*, 1989; Selkoe, 1991). Plaque neurites represent the dystrophic terminals of cholinergic neurons (from the basal forebrain), serotonergic neurons (from the dorsal raphe nucleus), and noradrenergic neurons (from the locus coeruleus) (Powers *et al.*, 1988), as well as those of neurons that synthesize peptide neurotransmitters (Struble *et al.*, 1987). The involvement in AD of so many neurotransmitter systems has made difficult the rational design of effective therapies based on

Figure 4. Distribution of senile plaques in the hippocampus and entorhinal cortex of the brain from an individual suffering from Alzheimer disease. (*Top*) CA1 hippocampal region demonstrating adjacent areas of high and low plaque density. (*Bottom*) Entorhinal cortex containing a high concentration of senile plaques. Both microscopic fields are from a Bielschowsky silver-stained brain section of the individual described in Figure 1. Scale bars represent 100 μm .



transmitter replacement.

The source of the amyloid deposited in brain has not been determined. AD amyloid is found in the walls of blood vessels of the cerebral meninges, cerebral cortex, and hippocampus (collectively referred to as congophilic angiopathy) (Vinters and Gilbert, 1983), in addition to gray matter parenchyma. This has led some researchers to hypothesize that the source of AD amyloid is the bloodstream (Selkoe, 1989a), in analogy to systemic amyloid disorders. However, the brain-specific deposition of amyloid, the scarcity of amyloid in white matter, the association of neurites with amyloid in senile plaques, and high neuronal expression levels for the messenger RNAs (mRNAs) encoding the amyloid precursors (see below, "Amyloid precursor protein") strongly argue for a neuronal origin of deposited cerebral and cerebrovascular amyloid (Selkoe, 1989a).

β /A4 amyloid

Nearly 80 years after Alzheimer first characterized the disease that bears his name, Glenner and Wong (1984a) purified the protein component of AD cerebrovascular amyloid by solubilization with guanidine hydrochloride, and sequenced the peptides they recovered. They similarly purified amyloid from the brains of patients with DS, and demonstrated that this amyloid was composed of the same peptide, which they named β -amyloid, found in AD brains (Glenner and Wong, 1984b). The following year, other researchers purified the amyloid component of senile plaques, which they called A4 protein because of its ~4 kDa-mass, and showed that the protein sequence was nearly identical to the earlier described β -

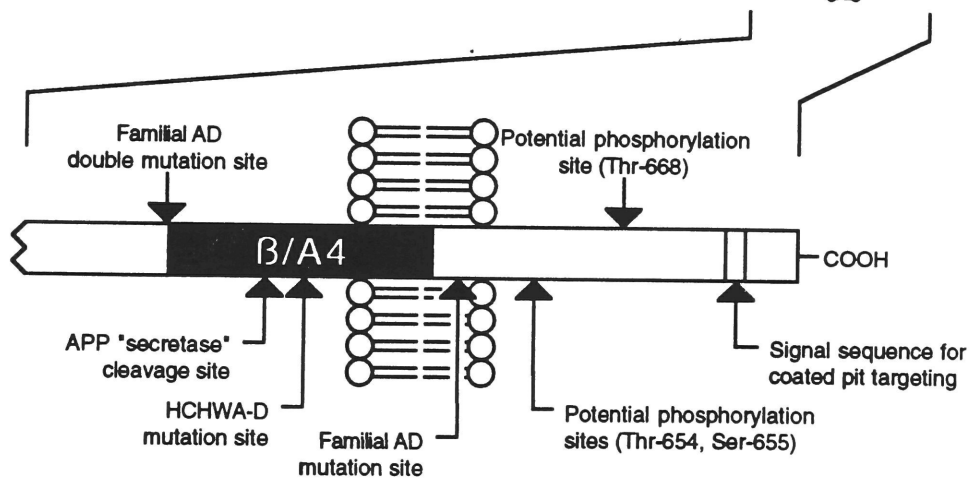
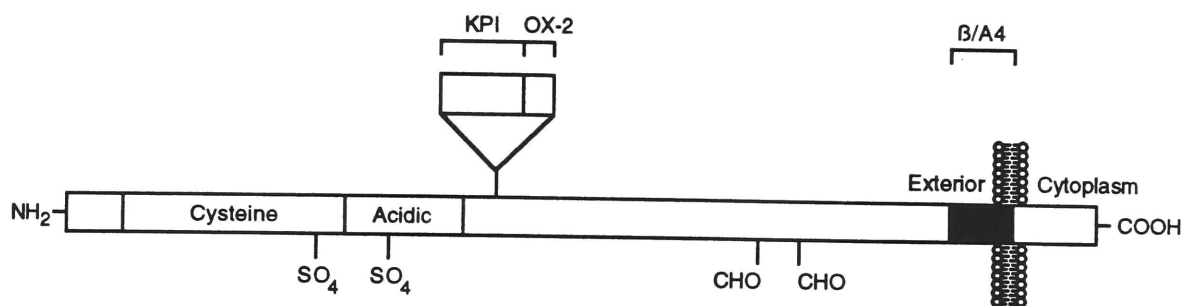
amyloid[†], with some heterogeneity present at the amino terminus (Masters *et al.*, 1985). The amyloid purified from plaque cores was 42-43 residues long, whereas that from the walls of blood vessels was only sequenced to residue number 24. It was subsequently shown that the cerebrovascular amyloid peptide is actually 39 residues long (*i.e.*, three residues are missing from the carboxyl terminus), and that the amino-terminal heterogeneity is minimal compared to that of plaque-core amyloid (Prelli *et al.*, 1988).

Amyloid precursor protein

Once the sequence of the β /A4 amyloid peptide was elucidated, researchers constructed "best guess" oligonucleotides corresponding to this sequence and screened brain cDNA libraries in an attempt to identify the gene that encodes β /A4 amyloid. Several groups of researchers independently cloned the gene simultaneously. Three groups isolated cDNAs that represented partial clones of the amyloid precursor and that mapped to chromosome 21 (Goldgaber *et al.*, 1987; Tanzi *et al.*, 1987; Robakis *et al.*, 1987). A fourth group isolated a full-length cDNA for the amyloid precursor protein (APP), a 695-amino acid protein that possesses a signal sequence for membrane insertion and a hydrophobic stretch of about 20 residues, suggesting that it is a transmembrane protein (Figure 5) (Kang *et al.*, 1987). In addition, the presence of a cysteine-rich domain, a stretch of residues abundant in aspartate and glutamate residues, and putative *N*-glycosylation sites suggested that APP might be a cell-

[†] The AD amyloid peptide will be referred to throughout this thesis as β /A4 amyloid or β /A4 peptide to acknowledge the contribution of the two research groups whose work led to discovery of the molecule.

Figure 5. Structure of the Alzheimer β /A4 amyloid precursor protein. The topology of APP in a cellular membrane, with the amino terminus (NH_2) oriented intraluminally and the carboxyl terminus ($COOH$) oriented cytoplasmically, is indicated. Other features of the APP molecule include: domains inserted by alternative splicing (*KPI* and *OX-2*); the β /A4 amyloid domain; regions enriched in the residue cysteine (*cysteine*), or in aspartate and glutamate (*acidic*); putative tyrosine-sulfation (SO_4) and *N*-glycosylation (*CHO*) sites; proteolytic cleavage site for the enzyme responsible for APP secretion ("secretase"); sites of APP genetic mutations; serine (*Ser-655*) and threonine (*Thr-654*, *Thr-668*) residues that can be phosphorylated (amino acids are identified for the 695-residue APP isoform); and an NPXY sequence that might be involved in the targeting of APP to clathrin-coated pits for endocytosis. See text for details. The lower half of the figure represents an expanded view of the indicated portion of the upper half.



surface receptor (Kang *et al.*, 1987). The localization of the gene for APP to chromosome 21 was consistent with the development of AD in Down syndrome (see above, "Senile plaques"), which is genetically characterized by triplication of this chromosome (*i.e.*, trisomy 21) or microduplication of the so-called "obligate Down's region" on chromosome 21. The APP gene is composed of 18 exons, with one intron interrupting the β /A4 amyloid domain (Lemaire *et al.*, 1989). This finding suggested that β /A4 peptide arises by aberrant APP proteolytic processing, rather than abnormal gene splicing.

Several isoforms of APP resulting from alternative splicing of the single APP gene were subsequently discovered (Table 3). Four isoforms (APP₃₆₅, APP₅₆₃, APP₇₅₁, and APP₇₇₀, where the subscript refers to the number of amino acids) possess a domain that bears close homology to the Kunitz family of protease inhibitors (KPI domain; members of this family include soybean trypsin inhibitor) (Ponte *et al.*, 1988; Tanzi *et al.*, 1988; Kitaguchi *et al.*, 1988; de Sauvage and Octave, 1989; Jacobsen *et al.*, 1991). The APP₇₅₁ and APP₇₇₀ isoforms have in fact been shown to be potent protease inhibitors (Oltersdorf *et al.*, 1989; Van Nostrand *et al.*, 1989). The APP₃₆₅ and APP₅₆₃ isoforms lack β /A4 amyloid, transmembrane, and cytoplasmic domains. Three isoforms--APP₃₆₅, APP₇₁₄ (Golde *et al.*, 1990), and APP₇₇₀--contain 19-residue inserts that resemble a region of a rat cell glycoprotein (MRC OX-2) present on the surface of neurons and certain types of leukocytes (Clark *et al.*, 1985). APP₆₉₅, APP₇₅₁, and APP₇₇₀ are the major isoforms of the protein, and are synthesized by all cell types so far examined, although very little APP₆₉₅ is expressed in non-neuronal cells (Neve *et al.*, 1988). These

Table 3. Comparison of APP isoforms and APP-related proteins.

Protein	Soluble ^f	KPI ^g	OX-2 ^h	β/A4 ⁱ	References
APP ₃₆₅ ^{a, b}	+	+	+	-	Jacobsen <i>et al.</i> , 1991
APP ₅₆₃ ^{a, b}	+	+	-	-	de Sauvage and Octave, 1989
APP ₆₉₅ ^a	-	-	-	+	Kang <i>et al.</i> , 1987
APP ₇₁₄ ^{a, b}	-	-	+	+	Golde <i>et al.</i> , 1990
APP ₇₅₁ ^a	-	+	-	+	Ponte <i>et al.</i> , 1988; Tanzi <i>et al.</i> , 1988
APP ₇₇₀ ^a	-	+	+	+	Kitaguchi <i>et al.</i> , 1988
APLP-1 ^c	-	-	-	-	Wasco <i>et al.</i> , 1992
APLP-2 ^c	-	-	-	-	unpublished ^j
APPL ^d	-	-	-	-	Rosen <i>et al.</i> , 1989
YWK-II ^e	-	-	-	-	Yan <i>et al.</i> , 1990

^aHuman APP species that result from alternative splicing of a single gene. Subscripts refer to the number of amino acids. ^bRNA message, but not protein, detected. ^cMammalian APP-like proteins. ^d*Drosophila melanogaster* homolog of APLP. ^eHuman sperm membrane protein whose transmembrane and cytoplasmic domains are highly homologous to those of APP. ^fDoes not possess transmembrane or cytoplasmic domains. ^gKunitz-type protease inhibitor domain. ^hDomain similar to one present in the rat MRC OX-2 glycoprotein found on the surface of neurons and some types of leukocytes (Clark *et al.*, 1985). ⁱβ/A4 amyloid peptide domain. ^jSangram Sisodia and Wilma Wasco, personal communications.

three species can undergo proteolytic cleavage within the β /A4 amyloid domain (Figure 5) (Sisodia *et al.*, 1990; Esch *et al.*, 1990), which results in the secretion of the APP ectodomain into the medium of cultured cells or into plasma and cerebrospinal fluid (CSF) (Weidemann *et al.*, 1989; Palmert *et al.*, 1989; Bush *et al.*, 1990).

In addition to the multiple APP isoforms, several APP-related integral membrane proteins encoded by different genes have been identified. All four proteins have cytoplasmic domains that are highly homologous to that of APP, although their extracellular domains differ to varying degrees and none possesses a β /A4 amyloid domain. The first was identified in the fruit fly *Drosophila melanogaster* and named APPL, for APP-like (Rosen *et al.*, 1989). The expression of APPL is neuron-specific (Luo *et al.*, 1990), and flies in which the gene for APPL has been deleted suffer a subtle phototactic deficit that can be rescued by insertion of the human APP gene (Luo *et al.*, 1992). Two mammalian versions of APPL--called APLP-1 and -2, for amyloid precursor-like proteins--were recently discovered and the gene of human APLP-1 was localized to chromosome 19 (Wasco *et al.*, 1992). The fourth APP-related protein is YWK-II, a molecule localized to the plasma membrane of human sperm (Yan *et al.*, 1990). The function of YWK-II is not known, but an antibody raised against it interferes with fertilization *in vitro*, suggesting a role in sperm-egg adherence.

That an abnormality in the metabolism of APP might give rise to AD is supported by several pieces of circumstantial evidence: β /A4 amyloid is deposited in memory-related and association areas of the brains of AD and DS patients; accumulation of β /A4 amyloid in

diffuse plaques precedes any other pathological changes, including NFTs and synapse loss, in the brains of DS victims; and senile plaques are lesions specific for AD and DS, unlike NFTs which are present in several seemingly unrelated disorders (see above, "Neurofibrillary tangles"). Definitive evidence for a role of APP in the etiology of AD has come from genetic studies of two rare disorders: hereditary cerebral hemorrhage with amyloidosis of the Dutch type (HCHWA-D) and familial AD (FAD).

HCHWA-D is an autosomal dominant disorder that only afflicts the members of four families living in two coastal villages in the Netherlands (Wattendorff *et al.*, 1982). The disease is characterized by the deposition of $\beta/A4$ in the walls of small cerebromeningeal and cortical blood vessels, which leads to fatal hemorrhages by the fifth or sixth decade of life. It is intriguing that a similar, but biochemically distinct, cerebral amyloid angiopathy which occurs mostly in Iceland results from cerebrovascular deposition of a fragment of the cysteine protease inhibitor cystatin C, causing death before the age of 30 years (Cohen *et al.*, 1983).

Unlike AD and DS patients, individuals with HCHWA-D do not develop NFTs or senile plaques, although they do develop diffuse parenchymal amyloid plaques (van Duinen *et al.*, 1987). Strong evidence for a causative role for APP in HCHWA-D came from restriction fragment length polymorphism studies of the four afflicted Dutch families, which showed a tight linkage (lod score > 7) between HCHWA-D and the APP gene (Van Broeckhoven *et al.*, 1990). When the two exons that code for the $\beta/A4$ amyloid domain were cloned and sequenced in these families, a single base transversion

(cytosine to guanosine) was discovered, which results in a glutamate to glutamine substitution at residue 22 of β /A4 (Figure 5) (Levy *et al.*, 1990). As the mutation was found in all individuals afflicted with HCHWA-D, these studies strongly suggest that a mutation in the APP gene can produce disease. A possible mechanism whereby this mutation might exert its pathogenetic effects has been provided by *in vitro* studies with synthetic β /A4 peptides, in which peptides containing the HCHWA-D mutation spontaneously aggregate and form fibrils more rapidly than wild-type peptides (Wisniewski *et al.*, 1991).

Shortly after this discovery in individuals with HCHWA-D, mutations in the APP gene were identified in the kindreds of AD patients suffering from early-onset (fifth or sixth decade), autosomal dominant heritable forms of the disease, called FAD. Genetic linkage analysis had implicated chromosome 21 in the etiology of some cases of FAD (St George-Hyslop *et al.*, 1987). However, most cases of AD are not linked to chromosome 21 (St George-Hyslop *et al.*, 1990), including normal-onset AD patients and one well-studied German kindred from the Volga River valley in Russia, now living in the United States, who develop FAD (Schellenberg *et al.*, 1988). For this reason, FAD kindreds demonstrating linkage to chromosome 21, for which no recombinational events had previously excluded APP as a disease gene, were chosen as the best candidates for repeating the HCHWA-D mutational studies.

The first discovered FAD mutation involves a valine-to-isoleucine substitution at codon 717 (APP₇₇₀ numbering scheme) (Goate *et al.*, 1991). Unlike in HCHWA-D, this mutation lies outside

the β /A4 amyloid region, at a residue in the transmembrane domain of APP (Figure 5). Two other mutations at the same codon (valine to phenylalanine or to glycine) were discovered soon after (Murrell *et al.*, 1991; Chartier-Harlin *et al.*, 1991), as well as another valine-to-isoleucine mutation in a Japanese FAD kindred unrelated to the original British and American kindreds (Naruse *et al.*, 1991). An interesting tandem amino-acid mutation has been identified in two large Swedish families with FAD, resulting in lysine-to-asparagine and methionine-to-leucine substitutions at codons 670 and 671 (APP₇₇₀ numbering scheme), respectively, which lie just upstream of the β /A4 amyloid domain (Figure 5) (Mullan *et al.*, 1992). Cultured cells that were transfected with an APP construct bearing this double mutation have been demonstrated to secrete more β /A4 peptide than cells expressing wild-type APP (Citron *et al.*, 1992). Finally, a Dutch family containing some members who develop FAD and other members who develop cerebral amyloidogenic hemorrhage (similar to HCHWA-D) possess an alanine-to-glycine mutation at codon 692 (APP₇₇₀ numbering scheme) within the β /A4 domain (Hendriks *et al.*, 1992).

Although genetic studies provide compelling evidence that a defect in the APP gene could give rise to AD, they have failed to find these or other APP mutations in all AD patients, both early- and late-onset. This reasoning and the linkage of some cases of FAD to chromosomes 14 and 19 (Schellenberg *et al.*, 1992b; Pericak-Vance *et al.*, 1991; Schellenberg *et al.*, 1992a) have led researchers to believe that defects in molecules that interact with APP and that regulate its metabolism might underlie some cases of AD. In order to

define such molecules, some AD investigators have focused on examining APP processing pathways and establishing the normal metabolism of APP. Other investigators have focused on experiments aimed at demonstrating whether β /A4 amyloid can exert deleterious effects on neurons. Study of the pathways of APP cellular trafficking and proteolytic processing will be dealt with in depth in later chapters, but before ending this chapter it may be worth while to summarize some of the studies on β /A4 toxicity.

It was initially suggested that β /A4 peptide might possess trophic, rather than toxic, effects on neurons. Experiments in brain-lesioned mice suggested that the neuritic dystrophy associated with senile plaques could represent aberrant neuronal sprouting in response to local injury (Geddes *et al.*, 1986). For this reason, the potential role of β /A4 amyloid as a growth regulator was examined *in vitro*. Rather than providing clear evidence either for or against β /A4 toxicity, such studies have engendered confusion and controversy in the research community. β /A4 has been reported by different groups to be both trophic and toxic to neurons, the latter effect supposedly being potentiated by nerve growth factor and antagonized by tachykinin agonists such as substance P (Whitson *et al.*, 1989; Yankner *et al.*, 1989, 1990a, and 1990b). A definitive role for β /A4 in regulating cell growth remains to be demonstrated, though minor differences in methodologies might explain some discrepancies in experimental results (Cotman *et al.*, 1992). Independent laboratories, though, have consistently implicated β /A4 amyloid in affecting the Ca^{2+} homeostasis of cultured neurons and, subsequently, increasing the vulnerability of these cells to

excitotoxins such as glutamate (Koh *et al.*, 1990; Mattson *et al.*, 1992).

Thesis proposal and outline

The purpose of the present study was to address the cellular trafficking and processing pathways of APP. Rather than directly examining the mechanism(s) whereby β /A4 peptide is generated from APP, an investigation of normal APP processing pathways was undertaken. The decision to study "normal," instead of "abnormal" or amyloidogenic, APP metabolism was based chiefly upon two considerations. First, AD represents the outcome of a pathologic process spanning more than half a century (or at least four decades in the case of DS patients, whose disease etiology is presumably a gene-dosage effect). In the absence of an animal model that replicates a rapid AD progression, a logical strategy for deducing the biological defect of AD might be to elucidate the normal processing pathways of APP and then to search for defects in these pathways in AD patients. Although a strong argument was made above for a causative role of APP in AD, if this presumption were false, this investigative strategy could still be useful in explaining the deposition of β /A4 peptide in the brains of AD patients. In addition, a comprehensive examination of APP cellular trafficking and proteolytic processing should facilitate future studies in cells or animals transfected with mutant-bearing APP constructs.

Second, the fact that the structure of APP is highly conserved across mammalian species (Yamada *et al.*, 1987; Shivers *et al.*, 1988) and possesses a homolog in invertebrates (Rosen *et al.*, 1989), that all cell types examined so far produce APP, that the APP gene transcript

is alternatively spliced to yield several protein isoforms with potentially different functions, and that APP is secreted from cells into CSF and blood (Weidemann *et al.*, 1989; Palmert *et al.*, 1989; Bush *et al.*, 1990) suggests that APP is an important protein worthy of careful study. Investigation of normal APP processing pathways could provide insights into its function. Further, elucidation of certain aspects of APP processing could be applicable to the study of other cellular proteins.

This thesis is organized into four investigative divisions. Chapter 3 describes the effects on APP metabolism of several reagents known to alter different aspects of cellular protein processing and trafficking. Chapter 4 describes the modulation of APP secretion by compounds that regulate the level of protein phosphorylation in the cell. The investigations of Chapter 5 deal with the identification of APP in clathrin-coated vesicles and discuss the implications of this finding for the trafficking and processing of APP. In Chapter 6, microscopic localization of APP is performed in a variety of tissues and cell types, and an attempt is made to correlate the subcellular distribution of APP with aspects of its biochemical processing.

Chapter 2

Experimental Methods

The contents of this section also appear in Caporaso *et al.* (1992a; 1992b; 1993) and Nordstedt *et al.* (1993).

Antibodies

The preparation of affinity-purified rabbit anti-carboxyl-terminal APP antibody 369A has been described previously (Buxbaum *et al.*, 1990). The anti-amino-terminal APP monoclonal antibody 22C11 (Weidemann *et al.*, 1989) was the gift of Konrad Beyreuther (University of Heidelberg, Heidelberg, Germany). A monoclonal antibody against the KPI domain of APP_{751/770} (Wunderlich *et al.*, 1992) was provided by Triprayar Ramabhadran (our laboratory). A murine monoclonal antibody against rat transferrin receptor (Tf-R) used for immunoblotting was purchased from Chemicon International, Inc. (Temecula, CA).

Antibodies used for microscopy studies were generous gifts, as follows: polyclonal rabbit serum against the carboxyl terminus of APP (C7; Dennis Selkoe, Harvard Medical School, Boston, MA); a monoclonal antibody that recognizes an integral membrane protein of the *trans*-Golgi and the *trans*-Golgi network (GIMP_t) (Ignacio Sandoval, Universidad Autónoma de Madrid, Cantoblanco, Madrid, Spain); a monoclonal antibody against the synaptic vesicle protein SV2 (Kathleen Buckley, Harvard Medical School, Boston, MA); a rabbit

polyclonal antibody against mannosidase II (Kelley Moremen, Massachusetts Institute of Technology, Cambridge, MA); a monoclonal antibody against the cytoplasmic domain of human Tf-R (Ian Trowbridge, Salk Institute, San Diego, CA); a monoclonal antibody that recognizes the endoplasmic reticulum marker BiP (David Bole, University of Michigan, Ann Arbor, MI); and a monoclonal antibody against the lysosomal marker lgp120 (Ira Mellman, Yale University School of Medicine, New Haven, CT).

Fluorescein isothiocyanate (FITC)-conjugated goat anti-mouse antibody was obtained from Sigma Chemical Co. (St. Louis, MO) and rhodamine-conjugated goat anti-rabbit antibody was obtained from Boehringer Mannheim Biochemicals (Indianapolis, IN). FITC-conjugated wheat germ agglutinin was obtained from Vector Laboratories, Inc. (Burlingame, CA). FITC-conjugated lentil lectin was obtained from E-Y Laboratories (San Mateo, CA). Protein A-gold particles were prepared according to the method of Slot and Geuze (1985). Donkey anti-rabbit and sheep anti-mouse horseradish peroxidase-coupled secondary antibodies were purchased from Amersham Corp. (Arlington Heights, IL). Agarose-coupled anti-mouse and anti-rabbit secondary antibodies were purchased from HyClone Laboratories, Inc. (Logan, UT). Protein A Sepharose CL-4B (PAS) was obtained from Pharmacia LKB (Uppsala, Sweden).

Pharmacological reagents

Chloroquine and ammonium chloride were purchased from Sigma Chemical Co., monensin was purchased from Calbiochem (San Diego, CA), and brefeldin A (BFA) was purchased from Epicentre

Technologies (Madison, WI). Phorbol 12,13-dibutyrate (PDBu), 4- α -PDBu, and okadaic acid were purchased from LC Services Corp. (Woburn, MA). Acridine orange was purchased from Eastman Kodak Co. (Rochester, NY).

Pulse-chase metabolic labeling and immunoprecipitation

Undifferentiated rat pheochromocytoma (PC12) cells were grown to confluence on three 10-cm diameter culture dishes in Dulbecco's modified Eagle's medium (DMEM) containing 10% (vol/vol) heat-inactivated fetal bovine serum (FBS), 5% (vol/vol) heat-inactivated horse serum, and antibiotic-antimycotic solution (Gibco BRL, Gaithersburg, MD) with 5% CO₂ at 37°C (all subsequent incubations up until cell lysis were performed at this temperature). Cells were washed twice with Hepes-buffered saline solution (HBS) (10 mM Hepes, pH 7.4, 110 mM NaCl, 5 mM KCl, 2 mM CaCl₂, 1 mM MgSO₄), suspended in HBS, and pelleted by brief centrifugation. The cells were resuspended in 1 ml of methionine-free Eagle's modified minimum essential medium (MEM) containing 25 mM Hepes (pH 7.4). After a 45-min preincubation, cells were pulse-labeled for 20 min by the addition of 1 mCi of [³⁵S]methionine (1000 mCi/mmol; NEN Research Products, Boston, MA). The chase period was initiated by the addition of 5 ml of MEM containing excess unlabeled methionine (200 μ M) and 25 mM Hepes (pH 7.4). Aliquots (200 μ l) of samples were incubated in microcentrifuge tubes.

When the effects of chloroquine (50 μ M), ammonium chloride (50 mM), phorbol esters (1 μ M), or okadaic acid (1 μ M) were examined, drug was added at the start of the chase period. When the

effects of monensin (10 μ M) or BFA (10 μ g/ml) were examined, drug was added at the start of the preincubation period and was present throughout the pulse-chase, or drug was present during the chase period only. Control cells were treated with drug vehicle alone. Cell viability remained unchanged throughout the chase period as determined by trypan blue exclusion.

At the end of the chase period (0 to 8 h), cells were rapidly pelleted and the medium removed. Cells and medium were treated with 1% (wt/vol) SDS, boiled 5 min, sonicated (cell lysates only), and centrifuged at 10,000 g for 10 min. After dilution with an equal volume of neutralization buffer [6% (vol/vol) Nonidet-P40, 200 mM Tris, pH 7.4, 300 mM NaCl, 10 mM EDTA, 4 mM NaN₃], supernatants were incubated at 4°C with antibody 22C11 overnight (medium) or with antibody 369A for 2 h (cell lysates), unless otherwise indicated. Immune complexes were precipitated with 200 μ l (vol/vol) of agarose-coupled anti-mouse or anti-rabbit antibody or with PAS, and the pellets washed three times with 1 ml of Tris-buffered saline solution (100 mM Tris, pH 7.4, 150 mM NaCl, 2 mM NaN₃).

Samples were boiled in 100 μ l of sample buffer [62.5 mM Tris, pH 6.8, 2% (wt/vol) SDS, 5% (vol/vol) 2-mercaptoethanol, 10% (wt/vol) sucrose] and separated by SDS-polyacrylamide gel electrophoresis (Laemmli, 1970) on 4-15% gradient gels (cell lysates) or 6% gels (medium). Gels were treated for fluorography with enhancer solution (Entensify; NEN Research Products), dried, and exposed to preflashed x-ray film at -70°C. Proteins were quantitated by scanning densitometry (since immature APP₇₅₁ and APP₇₇₀ isoforms could not be resolved by densitometry, they are reported

together as immature APP_{751/770}). Care was taken to work within the linear range of film sensitivity. Values were corrected for length of exposure time, signal decay, and the number of methionine residues in individual APP species, and normalized to the total amount of full-length APP present in untreated cells at the start of the chase period (100 relative units). It should be noted that synthesis of labeled protein continued after the start of the chase, and therefore, that the values for the recovery of mature APP, secreted APP, and the carboxyl-terminal APP fragment are overestimated in absolute terms but accurate in relative terms.

Preparation of clathrin-coated vesicles (CCVs)

CCVs were prepared from undifferentiated PC12 cells grown in suspension using a combination of protocols described earlier (Pearse, 1976; Nandi *et al.*, 1982; Campbell *et al.*, 1984). Pelleted cells were stored at -70°C prior to use. The cells (approximately 20 ml of packed cell volume) were homogenized at room temperature in 10 volumes of buffer A [0.1 M 2-(*N*-morpholino)ethanesulfonic acid, pH 6.5, 1 mM EGTA, 0.5 mM MgCl₂, 0.02% (wt/vol) NaN₃, 7 mM 2-mercaptoethanol, 6 units/ml aprotinin, 10 µg/ml leupeptin, 1 µg/ml antipain, 1 µg/ml pepstatin] with a steel Dounce-type homogenizer. The homogenate was centrifuged at 20,000 *g* for 30 min, and the supernatant was further centrifuged at 55,000 *g* for 1 h. The pellet was then homogenized with a loose-fitting glass-Teflon homogenizer in 10 volumes of buffer A and mixed with an equal volume of buffer A containing 12.5% (wt/vol) Ficoll 400 (Pharmacia LKB) and 12.5% (wt/vol) sucrose. This mixture was centrifuged at 38,000 *g* for 40

min. The supernatant was diluted with 5 volumes of buffer A and centrifuged at 100,000 g for 1 h. The pellet was homogenized in approximately 30 volumes of buffer A and centrifuged at 20,000 g for 20 min. The supernatant was layered over a cushion of buffer A made with 100% D₂O and containing 8% sucrose. The CCVs were pelleted by centrifugation at 80,000 g for 2 h. This centrifugation was performed at 20°C, whereas all other procedures were performed at 4°C. The purified CCVs were further fractionated either by density-equilibrium centrifugation on 10-ml linear 2/9%-20/90% Ficoll 400/D₂O gradients in buffer A (80,000 g for 15 h) as described (Turkewitz and Harrison, 1989) or by gel-filtration chromatography on a 1x50 cm Sephacryl S-1000 column (Pharmacia LKB) as described (Campbell *et al.*, 1984).

Protein determination and immunoblot analysis of CCVs

The protein content of CCV fractions obtained by gel-filtration chromatography was determined by spectrophotometric absorbance at a wavelength of 280 nm. The protein concentration of cell homogenates and of CCV fractions obtained by density-equilibrium centrifugation was determined by the method of Bradford (1976).

Proteins from cell homogenates and CCVs were separated on 4-15% SDS-polyacrylamide gradient gels under reducing conditions (Laemmli, 1970) and transferred to nitrocellulose membranes (Towbin *et al.*, 1979). The nitrocellulose blots were first blocked with Tris-buffered saline solution (150 mM NaCl, 50 mM Tris-HCl, pH 7.3) containing 0.05% (vol/vol) Tween-20 (TBST) and then with TBST containing 5% (wt/vol) nonfat milk ("Blotto"). Primary antibodies

were made up in Blotto with 0.02% (wt/vol) NaN_3 and stored at 4°C between experiments. After a 3-h incubation at room temperature with primary antibody, blots were washed several times with TBST. Blots were then incubated for 1 h with either horseradish peroxidase-conjugated donkey anti-rabbit or sheep anti-mouse secondary antibody prepared in Blotto. Following extensive washing with TBST, immunoreactivity was visualized with the enhanced chemiluminescence system (Amersham Corp.) according to the manufacturer's instructions, and blots were exposed to x-ray film. Total protein was visualized by staining the nitrocellulose blots with 0.1% (wt/vol) amido black (Towbin *et al.*, 1979).

Electron microscopy of CCVs

Peak fractions of APP immunoreactivity eluted from the S-1000 column were examined by electron microscopy. Small droplets of sample were placed on grids coated with a carbon-stabilized Formvar film and left for 30-60 s. After removal of excess liquid, the adsorbed material was negatively stained with unbuffered 1% (wt/vol) uranyl acetate for 1 min. Imaging was performed with a Jeol 100CX electron microscope. This procedure was performed by Helen Shio of the Rockefeller University electron microscopy services.

Cell cultures for immunofluorescence microscopy

Primary cultures of rat hippocampal neurons were prepared from 18-d-old fetal rats as described (Banker and Cowan, 1977; Bartlett and Banker, 1984). Cells were grown for 4 d on poly-L-lysine-treated glass coverslips in MEM without serum, containing 1%

HL1 supplement (Ventrex, Portland, ME), 2 mM glutamine, and 1 mg/ml bovine serum albumin.

Chinese hamster ovary (CHO) cells were grown in DMEM containing 10% heat-inactivated FBS, 34 μ g/ml proline, 100 units/ml penicillin, and 100 μ g/ml streptomycin. African green monkey kidney (COS) cells were grown in DMEM containing 10% heat-inactivated FBS, 20 mM Hepes (pH 7.4), and 1x antibiotic/antimycotic solution (Gibco BRL). Undifferentiated PC12 cells were grown in DMEM containing 10% heat-inactivated FBS, 5% heat-inactivated horse serum, and 1x antibiotic/antimycotic solution. Rat insulinoma (RINm5F) cells (Gazdar *et al.*, 1980) were grown in RPMI 1640 medium containing 10% fetal calf serum. Mouse insulinoma (β TC3) cells (Efrat *et al.*, 1988) were grown in Click medium (Irvine Scientific, Santa Ana, CA) containing 5% fetal calf serum. Primary cultures and all cell lines were grown in 5% CO₂ at 37°C.

Immunofluorescence labeling

Cells were grown for 2-3 days on poly-L-ornithine-coated glass coverslips. Following incubation in medium alone or in medium containing drugs, cells were washed once with 120 mM phosphate buffer (pH 7.4) and then fixed for 30 min at 37°C with 4% formaldehyde (freshly prepared from paraformaldehyde)/4% sucrose in 120 mM phosphate buffer. All subsequent steps were performed at room temperature. After a wash with high-salt phosphate-buffered saline solution (PBS) (500 mM NaCl, 20 mM phosphate buffer), cells were incubated for 30 min with "goat serum dilution buffer" (GSDB; 0.45 M NaCl, 20 mM phosphate buffer, 0.3%

Triton X-100, 17% goat serum) in order to permeabilize membranes and block non-specific secondary antibody binding sites. Cells were next incubated for 2-3 h with primary antibodies prepared in GSDB. Following washes with high-salt PBS, cells were incubated for 30-90 min with fluorescent secondary antibodies prepared in GSDB. Cells were washed with high-salt PBS, then briefly with 5 mM phosphate buffer before mounting the coverslips onto glass slides using freshly-prepared mounting solution [70% glycerol, 1 mg/ml *p*-phenylenediamine (Sigma Chemical Co.), 150 mM NaCl, 10 mM phosphate buffer]. Slides were viewed with a Zeiss Axiophot microscope equipped with epifluorescence optics and photographed with Kodak TMAX-100 film.

In other studies, the brains of adult Sprague-Dawley rats (150-200 g) were fixed by perfusion with 4% paraformaldehyde in 120 mM phosphate buffer and 7- μ m sections were prepared (De Camilli *et al.*, 1983a). Brain sections were labeled for immunofluorescence microscopy essentially as described above.

Immunoelectron microscopy of rat brain tissue fragments

Preparation of agarose-embedded rat brain tissue fragments and immunoelectron microscopy were performed as described previously (De Camilli *et al.*, 1983b; Takei *et al.*, 1992).

Immunoblot analysis of cultured cells

Cells were grown for 2-3 days on 6-cm culture dishes. Following drug treatment, the medium was removed and the cells were washed with 120 mM phosphate buffer or Hank's balanced

saline solution, scraped from the dishes in 400-600 μ l of 1% SDS, and the lysates were boiled and sonicated. Following centrifugation at 14,000 g for 10 min, supernatants were assayed for total protein using the BCA system (Pierce, Rockford, IL). Aliquots of cell lysates containing equal amounts of protein, or volumes of medium normalized for cell-lysate protein, were diluted and boiled in sample buffer, separated on SDS-polyacrylamide gels by electrophoresis under reducing conditions (Laemmli, 1970), and transferred to nitrocellulose membranes (Towbin *et al.*, 1979). The procedure for immunoblotting was identical to that described above (Protein determination and immunoblot analysis of CCVs).

Chapter 3

Separate Processing Pathways for APP Secretion and Proteolytic Degradation

Introduction

A convenient animal model for AD is not available. Aged non-human primates and dogs experience cognitive decline and develop AD pathology (Selkoe *et al.*, 1987), but routine study in such animals is impractical. Also, no transgenic mouse developed to date produces AD pathology (Quon *et al.*, 1991). Therefore, alternative systems for examining the role of APP in the pathogenesis of AD must be employed. Cultured mammalian cells provide a readily accessible and well-characterized system for studies of protein processing. Although the events in the metabolism of APP that lead to amyloidosis and plaque formation might not be reproducible in cell culture, elucidation of normal processing pathways may provide insights into the pathogenesis of AD.

In this section, the intracellular trafficking and processing of APP is examined by [³⁵S]methionine pulse-chase analysis of PC12 neuroendocrine cells in the presence of pharmacologic agents known to affect the function of specific intracellular organelles. Sharing a developmental origin with neurons, PC12 rat pheochromocytoma cells synthesize the catecholamines dopamine and norepinephrine, and have proven useful in studies of neuronal differentiation and function (Greene and Tischler, 1976; Greene *et al.*, 1991), as well as

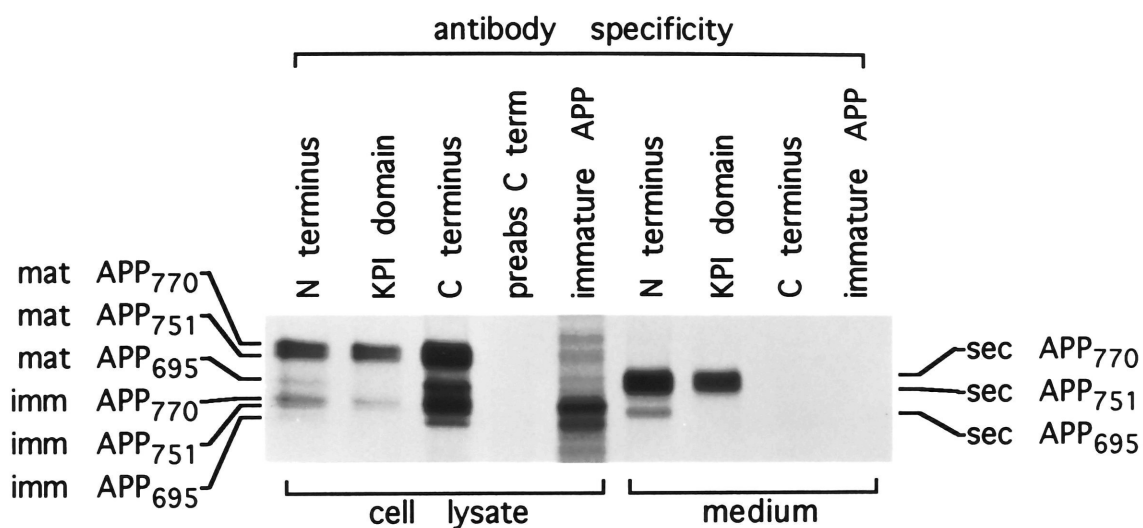
studies on the cellular trafficking of both neuronal and non-neuronal proteins (*e.g.*, see Régnier-Vigouroux *et al.*, 1991; Chanat and Huttner, 1991; Green and Kelly, 1992). In addition, PC12 cells have previously been shown to synthesize large amounts of APP endogenously--circumventing the need for transfection--and to process APP molecules from synthesis to degradation in a relatively short time (Weidemann *et al.*, 1989; Buxbaum *et al.*, 1990).

The contents of this section also appear in Caporaso *et al.* (1992a; 1992b).

Identification of APP species

Domain-specific antibodies were employed to identify the APP species present in cell lysates and cultured medium from [³⁵S]methionine metabolically-labeled PC12 cells. Antibodies directed against the amino terminus (22C11; Weidemann *et al.*, 1989) or against the carboxyl terminus (369A; Buxbaum *et al.*, 1990) of APP immunoprecipitated from cell lysates proteins with molecular masses of 106, 112, 116, 125, 139, and 146 kDa (Figure 6, *lanes 1* and *3*). The three lower bands have previously been designated as immature APP₆₉₅, APP₇₅₁, and APP₇₇₀ holoprotein, respectively, and the three higher bands as the corresponding mature APP isoforms, in which the proteins are fully *N*- and *O*-glycosylated and sulfated (Weidemann *et al.*, 1989; Buxbaum *et al.*, 1990). In support of this earlier identification, the 112-, 116-, 139-, and 146-kDa proteins were also immunoprecipitated with antibody 56.1 (Wunderlich *et al.*, 1992), which was raised against the KPI domain of APP₇₅₁ and APP₇₇₀ (Figure 6, *lane 2*). Further, an antibody raised against

Figure 6. Identification of APP species in PC12 cells by immunoprecipitation with domain-specific antibodies. APP species immunoprecipitated from cell lysates (*lanes 1-5*) or the cultured medium (*lanes 6-9*) of [^{35}S]methionine-labeled PC12 cells chased for 1 h in the absence of PDBu (*lanes 1-5*) or for 4 h in the presence of PDBu (see Chapter 4) (*lanes 6-9*) were separated on a 4-15% continuous gradient SDS-polyacrylamide gel and examined by fluorography. Four immunoprecipitating antibodies were used to identify the various APP species: (*lanes 1 and 6*) anti-amino-terminal monoclonal antibody 22C11; (*lanes 2 and 7*) anti-KPI domain monoclonal antibody 56.1; (*lanes 3 and 8*) anti-carboxyl-terminal affinity-purified polyclonal antibody 369A; (*lane 4*) antibody 369A preincubated with synthetic peptide corresponding to the cytoplasmic domain of APP (APP⁶⁴⁵⁻⁶⁹⁴); (*lanes 5 and 9*) whole serum from a guinea pig injected with unglycosylated APP₆₉₅ produced in *Escherichia coli*.



unglycosylated APP₆₉₅ produced in *Escherichia coli* (kindly provided by Triprayar Ramabhadran, our laboratory) was found to immunoprecipitate mainly the 106-, 112-, and 116-kDa proteins (Figure 6, lane 5).

In addition, antibody 369A, but not the other antibodies, immunoprecipitated a 16-kDa peptide[†] (Figure 9), which was found by radiosequence analysis to be the carboxyl-terminal fragment resulting from intra- β /A4 amyloid secretory cleavage of APP (Sisodia *et al.*, 1990; Esch *et al.*, 1990; Anderson *et al.*, 1991; Joseph Buxbaum, our laboratory, unpublished results). Preincubation of antibody 369A with a synthetic peptide corresponding to the cytoplasmic domain of APP abolished recovery of all cell-associated APP species (Figure 6, lane 4).

Proteins with molecular masses of 109, 123, and 129 kDa were immunoprecipitated from cultured medium using antibody 22C11 (Figure 6, lane 6), but no protein was recovered using antibody 369A or the antibody raised against the unglycosylated APP bacterial product (Figure 6, lanes 8 and 9), indicating that only mature, amino-terminal APP fragments were present in the medium. The 123- and 129-kDa species could also be immunoprecipitated using antibody 56.1 (Figure 6, lane 7). Based upon these results, and the fact that the difference in masses between the mature APP holoproteins (from which the secreted forms are believed to arise; see below) and the

[†] This APP species comigrated with the α -lactalbumin standard marker, which has a reported molecular mass of 14.2 kDa, in pulse-chase/immunoprecipitation experiments. However, when the molecular mass of the APP species was determined by linear regression analysis using a series of protein standards, as was done for the full-length or secreted APP molecules, the molecular mass was calculated to be 16 kDa. For consistency, the molecular mass is reported in this chapter and in Chapter 4 as 16 kDa.

carboxyl-terminal APP fragment closely agrees with the masses of the secreted forms, it is concluded that the 109-, 123-, and 129-kDa proteins are the secreted fragments of APP₆₉₅, APP₇₅₁, and APP₇₇₀, respectively.

No secreted forms were recovered from cell lysates when the supernatants from immunoprecipitations with antibody 369A were re-incubated with antibody 22C11. In addition, immunoprecipitations from cell lysates with antibody 369A and from cultured medium with antibody 22C11 were judged to be quantitative, since no further APP was recovered when samples were re-immunoprecipitated.

Effect of chloroquine on acidic organelles

Since some evidence for lysosomal APP processing was reported previously (Benowitz *et al.*, 1989; Cole *et al.*, 1989), the effects of chloroquine on APP metabolism were examined. Chloroquine is a weak base that is taken up by cells, where it is concentrated in and neutralizes acidic organelles such as lysosomes (de Duve *et al.*, 1974; Poole and Ohkuma, 1981) (Figure 7). The elevated pH of these organelles results in the inhibition of their acid-dependent hydrolases. Chloroquine neutralization of acidic organelles in the PC12 cells was confirmed by fluorescence microscopy after acridine orange treatment (Moriyama *et al.*, 1982; Niederau and Grendell, 1988) in the absence and presence of chloroquine (Figure 8).

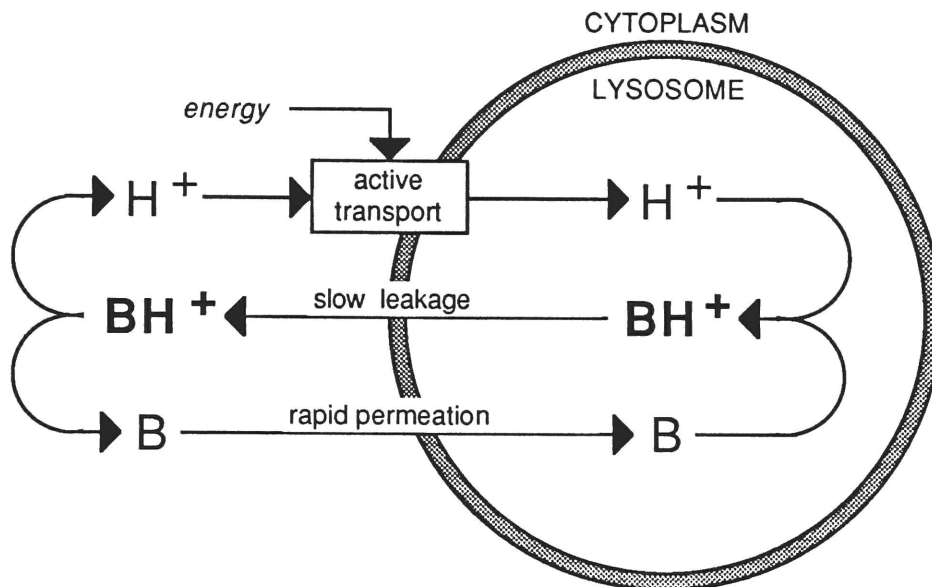
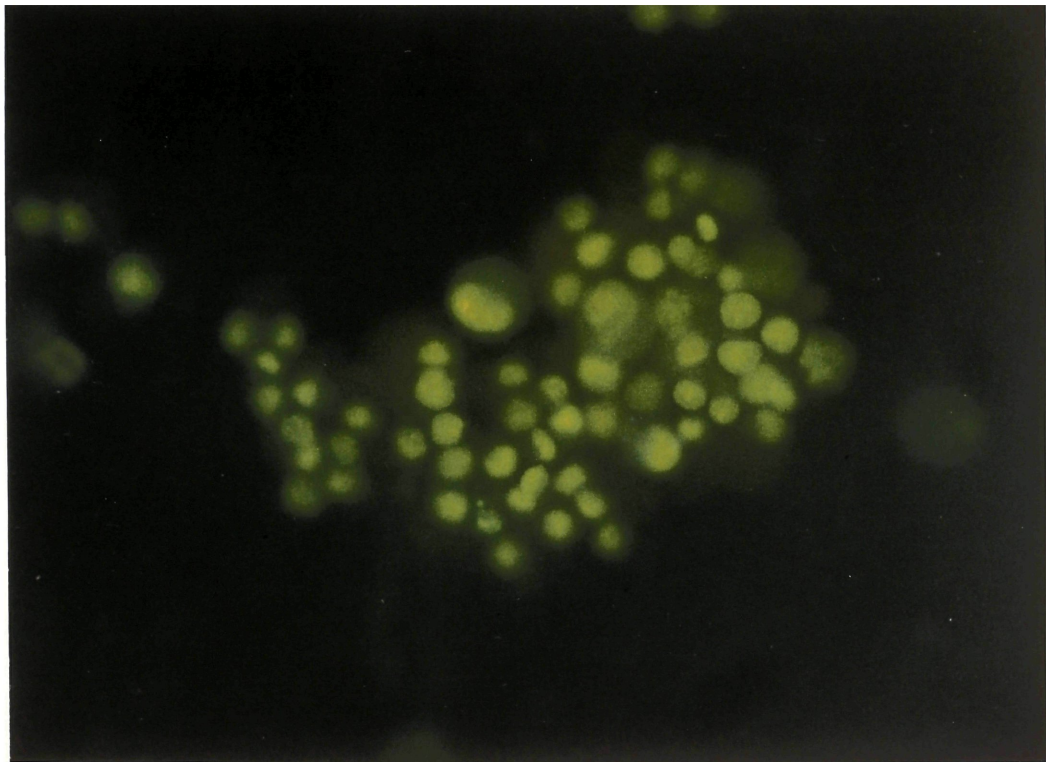
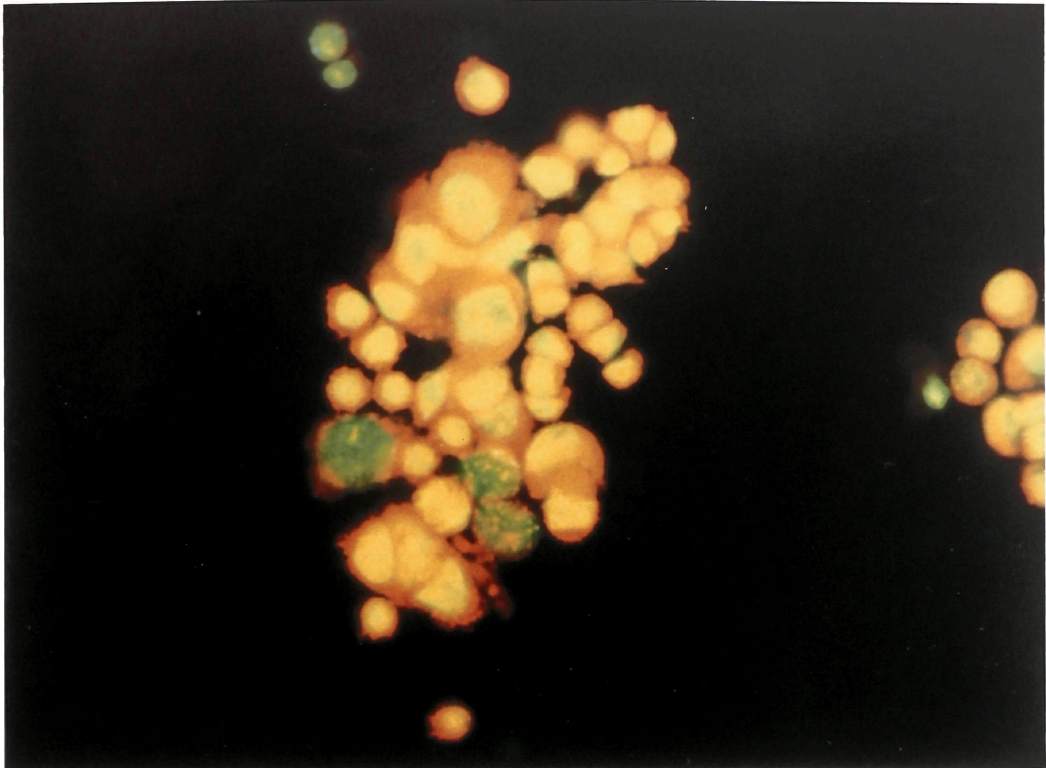


Figure 7. Model of lysosomal pH maintenance and the uptake of weak bases (from Poole and Ohkuma, 1981). An ATP-dependent ion pump establishes a proton (H^+) gradient across the lysosomal membrane, thereby acidifying the organelle. Weak bases (B) such as chloroquine readily permeate the lysosomal membrane, but upon protonation are trapped within the lysosome and raise the pH of this organelle. As the lysosomal concentration of protonated base (BH^+) increases, an osmotic influx of water from the cytoplasm results in a swelling, or "vacuolation," of the lysosome (Ohkuma and Poole, 1981). The process is limited by slow leakage of the protonated base down the steep concentration gradient that is formed. The leakage also serves to raise intralysosomal pH by transporting protons out of the organelle.

Figure 8. Neutralization of acidic compartments in chloroquine-treated cells. PC12 cells grown on microscope slide culture chambers were incubated in the absence (*top*) or presence (*bottom*) of 50 μ M chloroquine for 1 h prior to treatment with 50 μ M acridine orange for 5 min and viewing by fluorescence microscopy at a wavelength of 460-490 nm. A weak base that is concentrated in acidic compartments (see Figure 7), acridine orange undergoes a fluorescence shift from red-orange at acidic pH (*top*) to green at neutral or basic pH (*bottom*).



Effect of chloroquine on APP maturation

At the start of the chase period, nearly all of the labeled APP was in the form of immature holoprotein (Figure 9). Within approximately 15 min, half of the immature APP was converted to mature APP (Figure 10). No difference in the rate of maturation was found between APP₆₉₅ and APP_{751/770}. Chloroquine had virtually no effect on APP maturation (Figure 10).

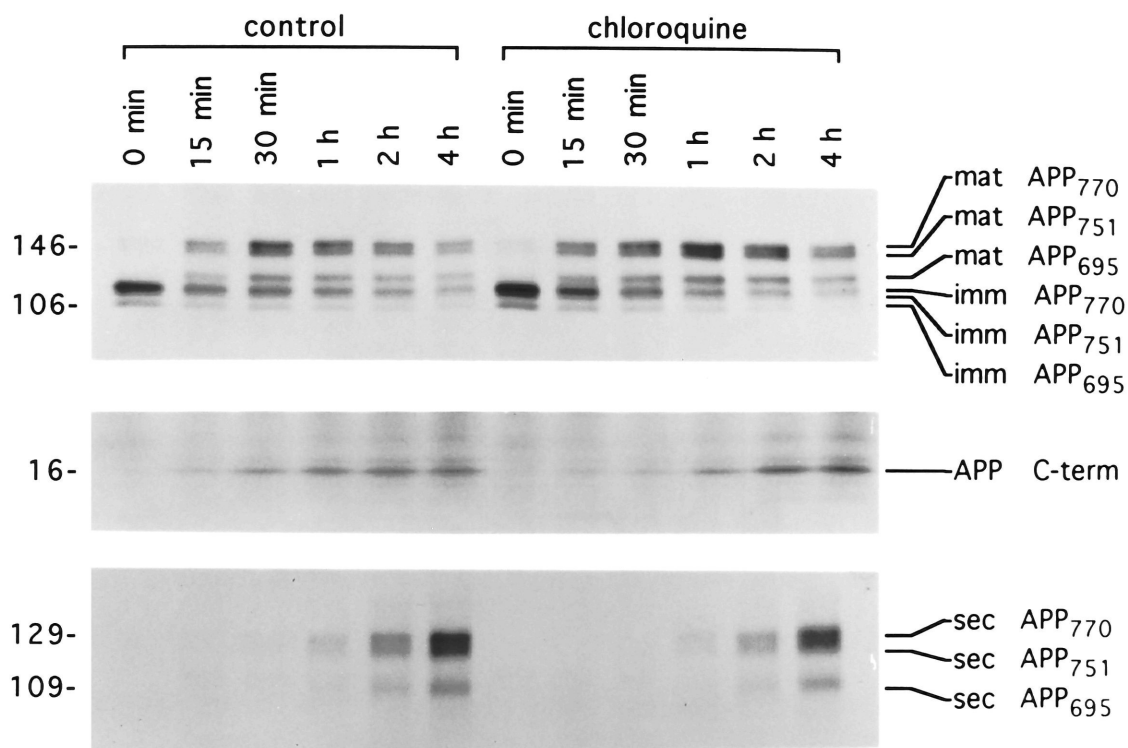
Effect of chloroquine on mature APP holoprotein

In untreated cells, the level of mature APP holoprotein rose to a maximum by 30 min, corresponding to conversion of immature APP to its fully glycosylated and sulfated forms (Figure 11, *a*) (Weidemann *et al.*, 1989). The amount of mature APP isoforms then decreased with a half-life of about 90 min. At 8 h of chase, the levels of mature APP isoforms had returned to their starting levels. The decrease of APP levels with time was attributed to conversion of mature APP to secreted forms, as well as to proteolytic degradation unassociated with secretion.

When cells were treated with chloroquine, a significant effect on turnover of mature APP was observed (Figure 11, *a*). The levels of mature APP holoprotein peaked 30 min later than in control samples. APP isoforms were present at approximately twice the levels found in untreated cells, from 1 to 8 h of chase. The magnitude of the chloroquine effect was the same for the different APP isoforms.

In order to better examine whether chloroquine was affecting the rate of mature APP turnover, the amount of mature APP

Figure 9. Effects of chloroquine on APP processing. APP species immunoprecipitated from cell lysates and the cultured medium of [³⁵S]methionine-labeled PC12 cells that were incubated during the chase period for 0, 15, 30 min, 1, 2, or 4 h in the absence (*left*) or presence (*right*) of chloroquine were examined by fluorography. (*Top*) APP holoproteins of 106, 112, 116, 125, 139, and 146 kDa representing immature APP₆₉₅, APP₇₅₁, and APP₇₇₀ and mature APP₆₉₅, APP₇₅₁, and APP₇₇₀, respectively, in cell lysates. (*Middle*) 16-kDa peptide in cell lysates representing the carboxyl-terminal APP fragment resulting from intra- β /A4 amyloid secretory cleavage. (*Bottom*) APP amino-terminal peptides of 109, 123, and 129 kDa representing the secreted fragments of APP₆₉₅, APP₇₅₁, and APP₇₇₀, respectively, in cultured medium. Autoradiograms are from a single experiment analyzed either on a 4-15% continuous gradient SDS-polyacrylamide gel (*top*, top portion of film; *middle*, bottom portion of film) or on a 6% SDS-polyacrylamide gel (*bottom*). Fluorograms were exposed for different lengths of time to optimize signal clarity. Molecular masses (kDa) are indicated at left.



recovered with time was replotted semi-logarithmically (Figure 11, *b*). It was evident that data points from 30 min to 8 h for untreated cells could be fitted best by two lines. From 30 min to 2 h, mature APP decreased with a half-life of approximately 90 min; from 4 to 8 h, the half-life of mature APP was about 3 h. These data suggested a biphasic pathway for mature APP processing. In cells treated with chloroquine, a single line could be fitted to the data points, indicating that the half-life of mature APP was now approximately 3 h throughout the chase period.

Effect of chloroquine on APP secretion

In untreated cells, after a brief lag, levels of secreted APP isoforms rose linearly from 0 to 4 h of chase (Figure 12). Little or no further increase in APP secretion was observed up to 8 h of chase. Maximal levels of secreted APP represented about 14% of total APP present at the start of chase.

When cells were treated with chloroquine, virtually no change in the rate of APP secretion was found for any APP isoform (Figure 12). The maximal level of APP secretion was approximately the same for control and chloroquine-treated samples at 4 h. At 6 and 8 h of chase there tended to be a small decrease in recovery of secreted APP. This decrease was attributable to proteolytic degradation in the medium, since recovery of secreted APP in 4-h chase medium incubated in the absence of cells decreased with time. Chloroquine was found to promote the proteolysis in the medium to an extent comparable to that shown in Figure 12 (not shown).

Figure 10. Effect of chloroquine on APP maturation. Recovery of immature APP from cells incubated in the absence (*open circles*) or presence (*filled diamonds*) of chloroquine was quantitated by densitometry of fluorograms, normalized, and plotted as a function of time. (*Top*) Immature APP₆₉₅. (*Bottom*) Immature APP_{751/770}. Results are the means \pm SEM of seven experiments; n = 3 to 7 for individual time points. There was no statistically significant difference between untreated and treated samples (Student's unpaired t-test).

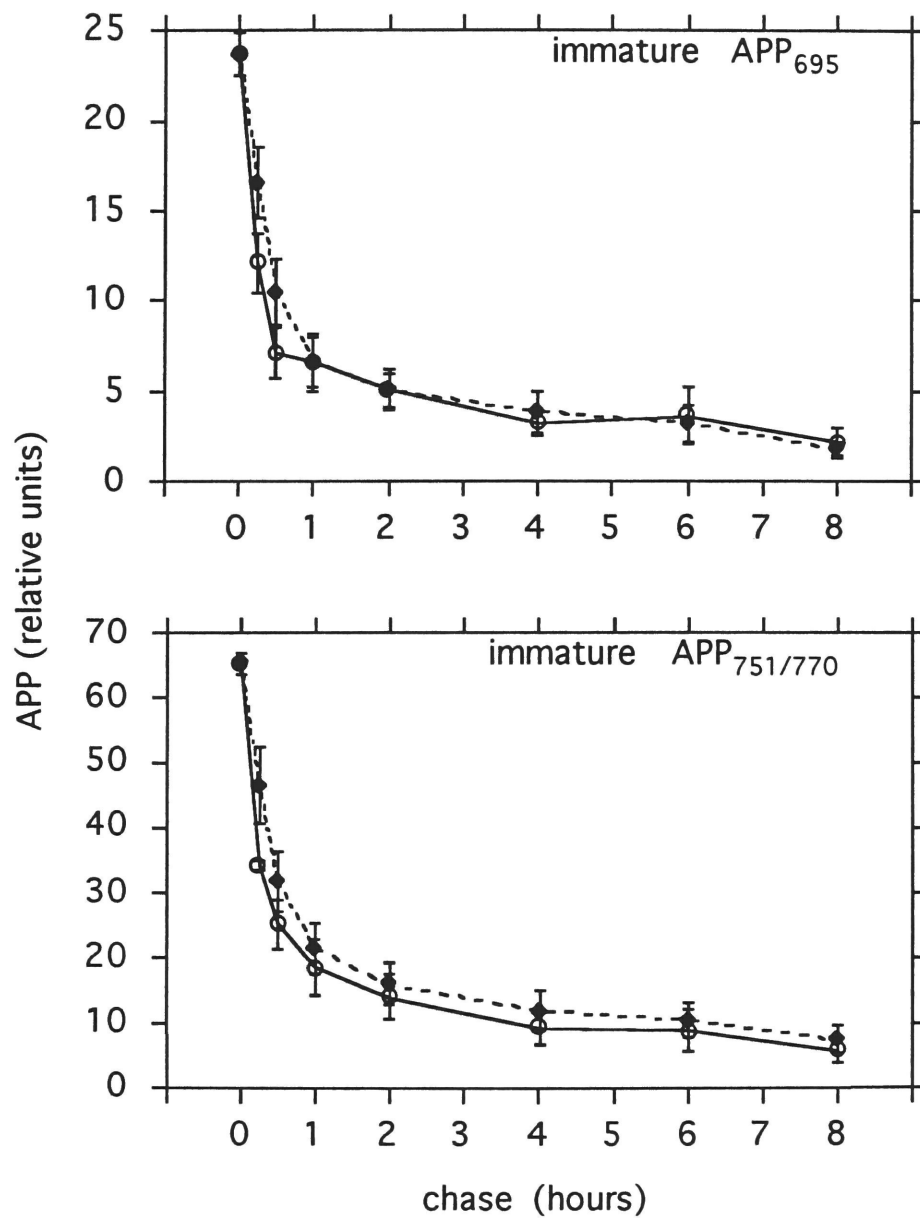


Figure 11. Effect of chloroquine on the turnover of mature APP. Recovery of mature APP from cells incubated in the absence (*open circles*) or presence (*filled diamonds*) of chloroquine was quantitated by densitometry of fluorograms, normalized, and plotted either linearly (*a*) or logarithmically (*b*) as a function of time. (*Top*) Mature APP₆₉₅. (*Middle*) Mature APP₇₅₁. (*Bottom*) Mature APP₇₇₀. Results are the means \pm SEM of seven experiments; $n = 3$ to 7 for individual time points. Statistical significance between untreated and treated samples for individual time points was determined by Student's unpaired t-test (*, $p < 0.05$).

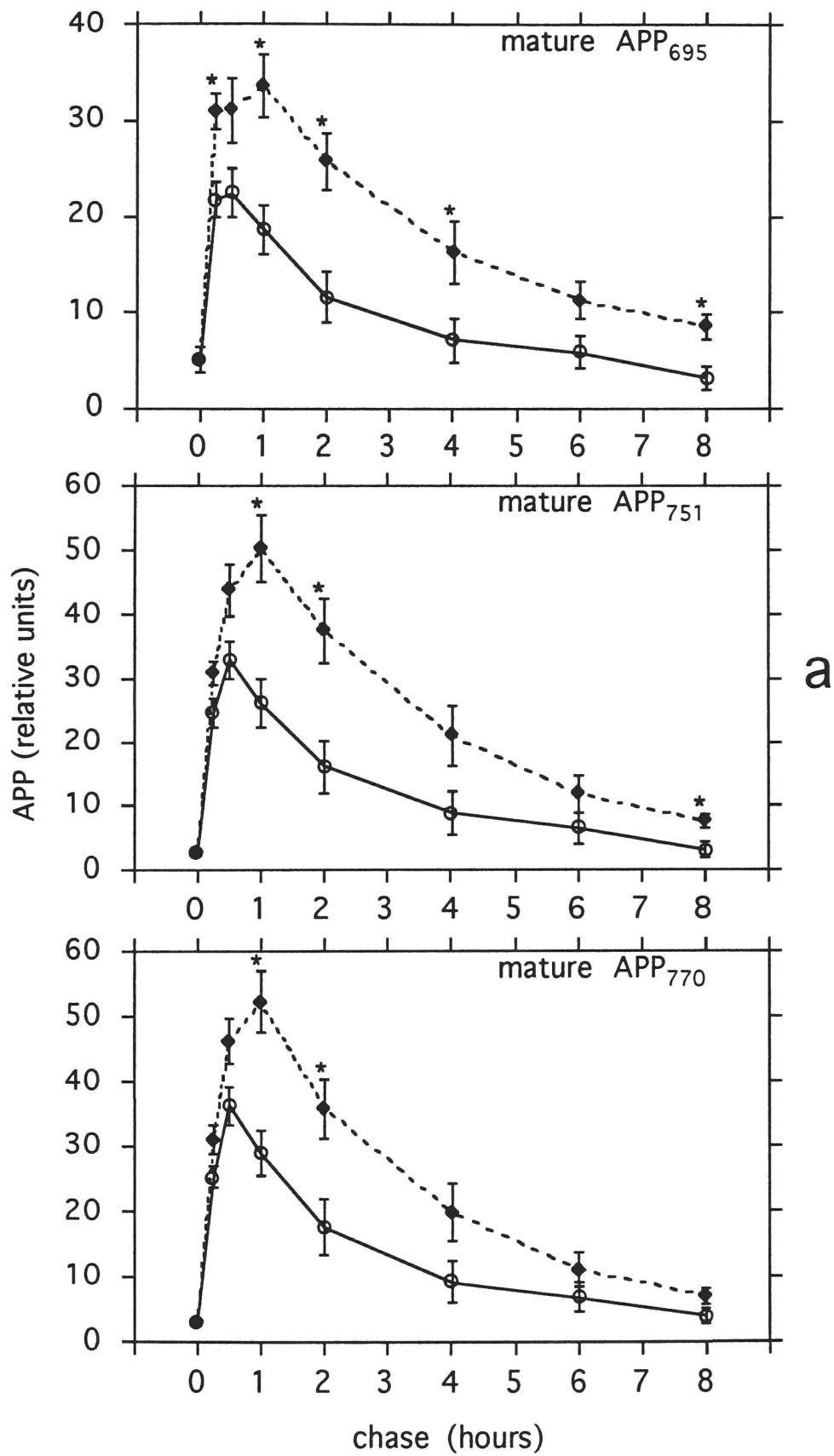


Figure 11. Effect of chloroquine on the turnover of mature APP
(continued).

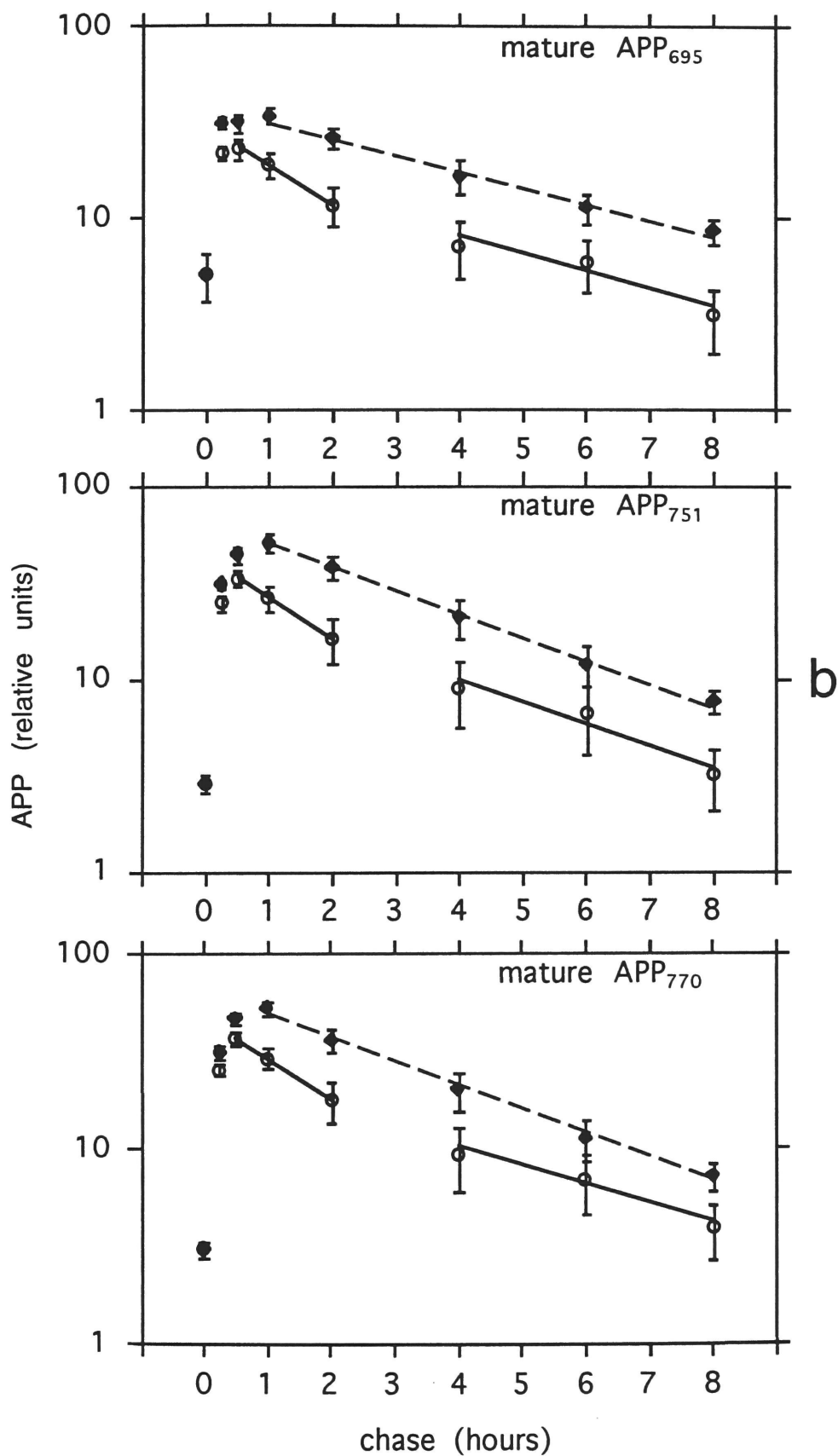
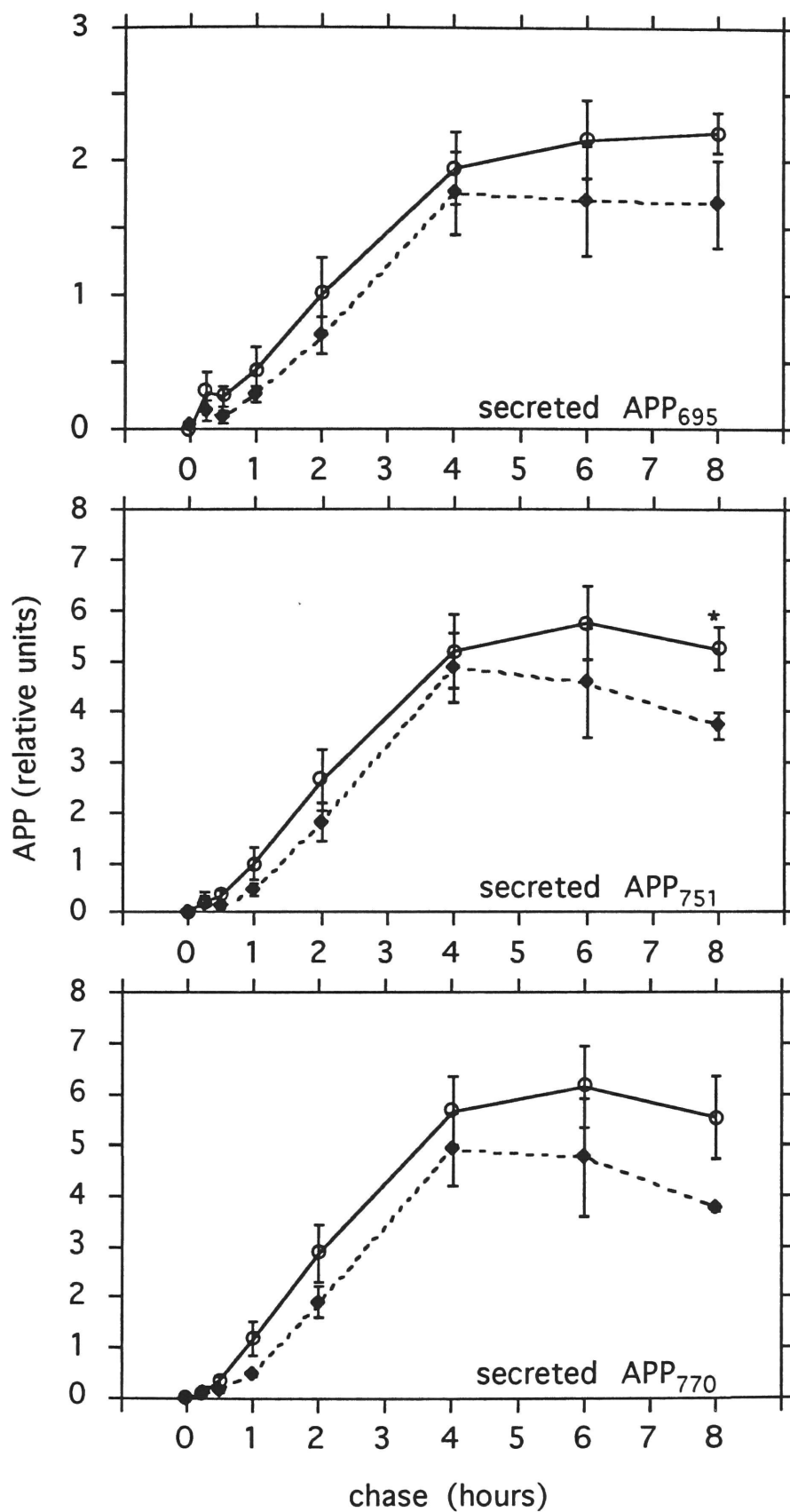


Figure 12. Effect of chloroquine on APP secretion. Recovery of secreted APP fragments from the cultured medium of cells incubated in the absence (*open circles*) or presence (*filled diamonds*) of chloroquine was quantitated by densitometry of fluorograms, normalized, and plotted as a function of time. (*Top*) Secreted APP₆₉₅. (*Middle*) Secreted APP₇₅₁. (*Bottom*) Secreted APP₇₇₀. Results are the means \pm SEM of seven experiments; n = 3 to 7 for individual time points. Statistical significance between untreated and treated samples for individual time points was determined by Student's unpaired t-test (*, $p < 0.05$).



Effect of chloroquine on the carboxyl-terminal APP fragment

In untreated cells, the level of the carboxyl-terminal APP fragment reached a maximum at 1 h of chase and decreased slowly thereafter (Figure 13). Since mature APP holoprotein was still being degraded, and secreted APP was still being produced at this time, one could conclude that the carboxyl-terminal APP fragment is subject to further proteolytic degradation.

Chloroquine had a marked effect on recovery of the carboxyl-terminal fragment. At all time points from 2 to 8 h, recovery of the 16-kDa APP fragment was significantly greater from chloroquine-treated than from untreated cells. These data are consistent with the idea that the carboxyl-terminal APP fragment is further degraded in an acidic organelle following its formation by APP secretory cleavage.

The maximal level of APP fragment was equivalent to approximately 9% of APP holoprotein present at the start of chase and 60% of total secreted APP. In the presence of chloroquine, these values were 13% and 92%, respectively.

Effects of ammonium chloride, monensin, and brefeldin A on APP processing

In addition to chloroquine, the effect of the lysosomotropic agent ammonium chloride on APP processing was examined. Ammonium chloride exhibited effects on APP turnover similar to those of chloroquine. However, it also had a strong inhibitory effect on APP maturation. Because of these multiple effects, ammonium chloride was not further examined.

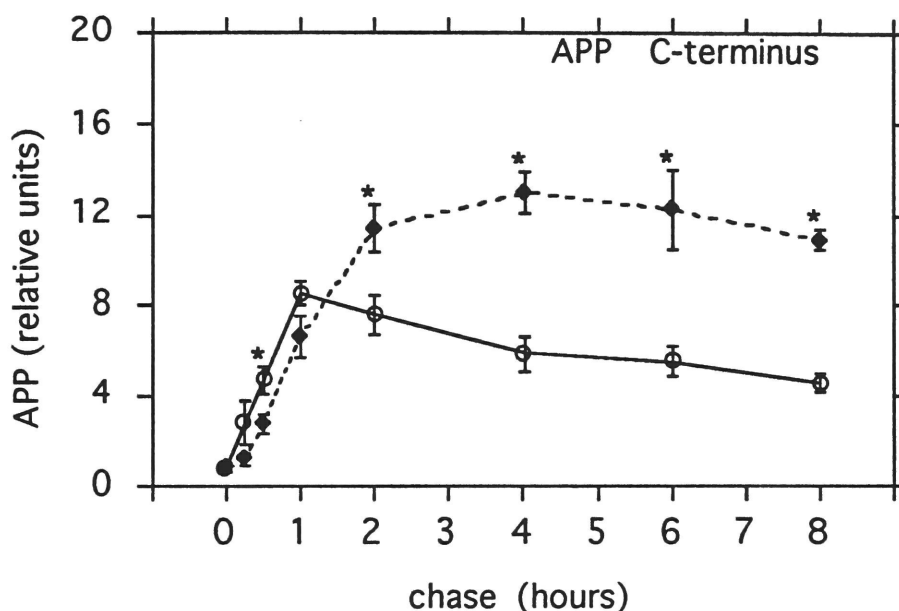
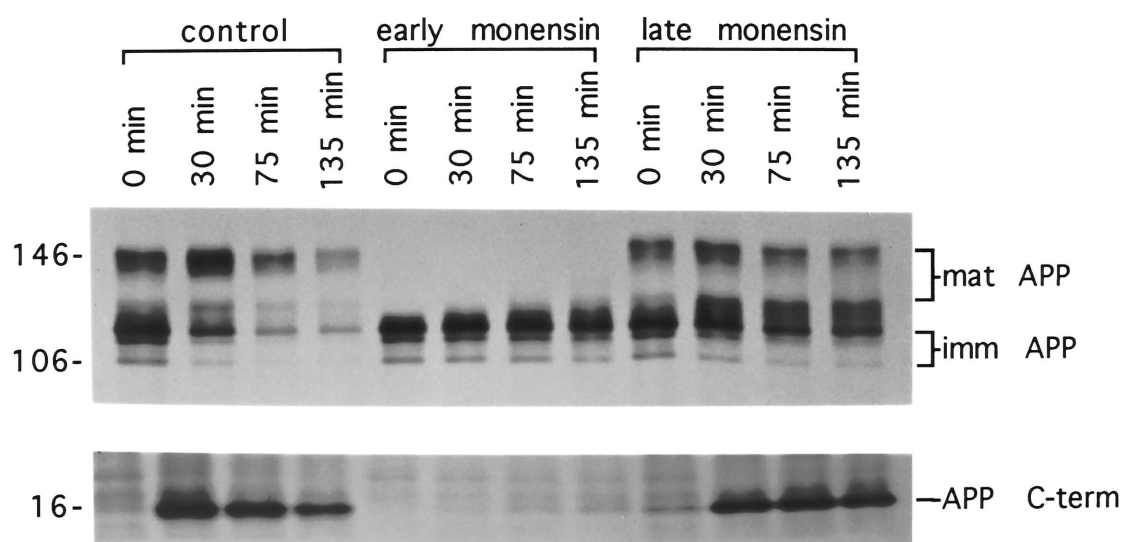


Figure 13. Effect of chloroquine on the turnover of the carboxyl-terminal APP fragment. Recovery of the 16-kDa carboxyl-terminal APP fragment from cells incubated in the absence (*open circles*) or presence (*filled diamonds*) of chloroquine was quantitated by densitometry of fluorograms, normalized, and plotted as a function of time. Results are the means \pm SEM of seven experiments; $n = 3$ to 7 for individual time points. Statistical significance between untreated and treated samples for individual time points was determined by Student's unpaired t-test (*, $p < 0.05$).

The monovalent cation ionophore monensin abolishes Na^+ , K^+ , and H^+ gradients and thereby disrupts the function of lysosomes and distal Golgi cisternae (Tartakoff, 1983). When monensin was added at the start of chase, it inhibited APP turnover to an extent similar to that observed with chloroquine and ammonium chloride (Figure 14). When monensin was present from the beginning of the preincubation period and throughout the pulse-chase period, it completely inhibited APP maturation (Figures 14 and 15). Furthermore, no secreted APP fragment (Figure 15) or 16-kDa APP fragment (Figure 14) was recovered.

The fungal product brefeldin A (BFA) produces an apparent dissolution of the Golgi complex by causing resorption of Golgi components into the endoplasmic reticulum (ER) and fusion of the *trans*-Golgi network (TGN) with the early endosomal system (Pelham, 1991; Klausner *et al.*, 1992; see Chapter 6 for a detailed discussion on the cellular effects of BFA). When cells were treated with BFA from the start of the preincubation period, normal APP maturation was inhibited (Figure 15). Instead, a broad protein band of molecular mass greater than that of immature APP, but less than that of mature APP, was observed. As Golgi enzymes, though relocated to the ER, can still function in the presence of BFA (Doms *et al.*, 1989), it seems that APP underwent aberrant glycosylation. BFA also prevented secretion of APP fragments (Figure 15) and production of the carboxyl-terminal fragment (not shown). (Full-length APP was slowly metabolized in the presence of either monensin or BFA, but no discrete proteolytic products were recovered with the APP antibodies employed.)

Figure 14. Effects of monensin on APP maturation and secretory processing. APP species were immunoprecipitated from cell lysates of [^{35}S]methionine-labeled PC12 cells that were chased for the indicated times and examined by fluorography. Monensin was absent (*left*), present during the preincubation, pulse-label, and chase periods (*center*), or present during the chase period only (*right*). (*Top*) APP holoproteins of 106, 112, 116, 125, 139, and 146 kDa representing immature APP₆₉₅, APP₇₅₁, and APP₇₇₀ and mature APP₆₉₅, APP₇₅₁, and APP₇₇₀, respectively. (*Bottom*) 16-kDa carboxyl-terminal APP fragment. Molecular masses (kDa) are indicated at left.

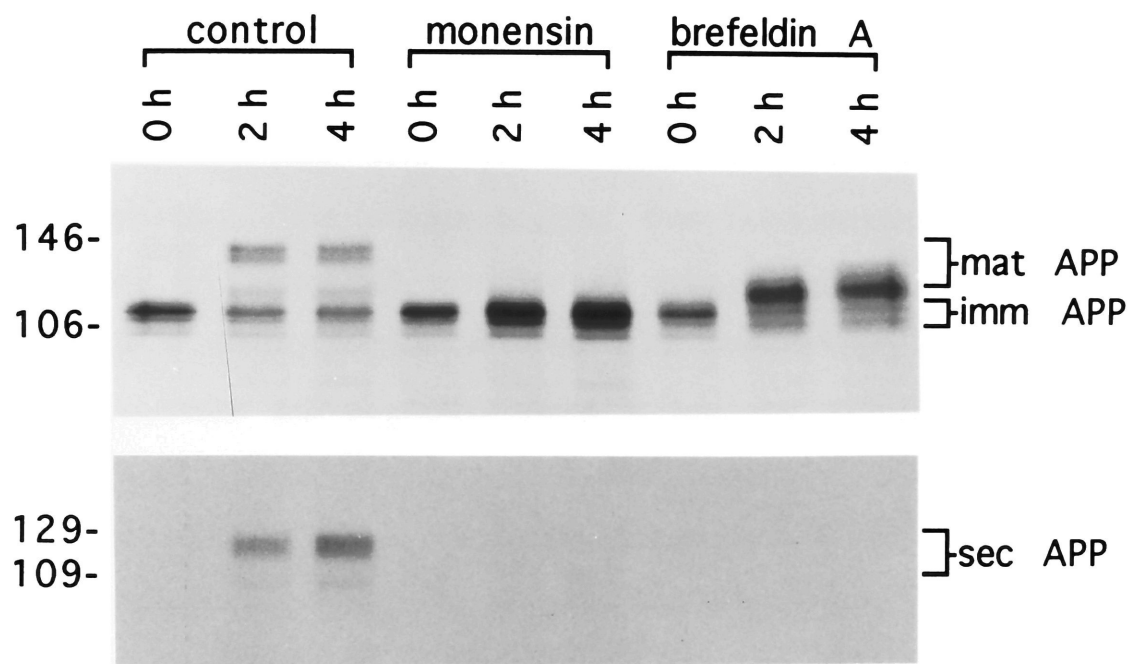


The data obtained with monensin and brefeldin A suggest that full maturation does not occur until APP reaches the distal Golgi complex, where final glycosylation (Farquhar, 1985) and sulfation (Baeuerle and Huttner, 1987) are believed to occur. Both monensin and BFA inhibited complete APP maturation and prevented APP proteolysis and secretion. This indicates that proteolysis and secretory cleavage occur in the distal Golgi or a subsequent compartment, since monensin inhibits middle- to *trans*-Golgi transport (Griffiths *et al.*, 1983) and BFA inhibits *trans*-Golgi to TGN transport (Chege and Pfeffer, 1990). These results exclude earlier APP proteolysis, for example, as might occur in the ER (Lippincott-Schwartz *et al.*, 1988; Klausner and Sitia, 1990).

Conclusions

The lysosomotropic agent chloroquine was demonstrated to significantly affect the metabolism of mature APP and a carboxyl-terminal APP fragment, with virtually no effect on APP maturation or secretion. In this study, the APP fragments released into the medium represented about 14% of the APP holoprotein present at the start of the chase. Recovery of the carboxyl-terminal APP fragment in the presence of chloroquine represented approximately 13% of total APP holoprotein, but 92% of total secreted APP. The quantitative agreement between the production of secreted APP fragments and the carboxyl-terminal APP fragment suggests that the 16-kDa fragment arising by intra-amyloid cleavage results almost entirely from the secretory pathway. This fragment would then be sorted for further proteolysis in acidic organelles such as lysosomes.

Figure 15. Comparative effects of monensin and brefeldin A on APP maturation and secretion. APP species were immunoprecipitated from cell lysates (*top*) and the cultured medium (*bottom*) of [³⁵S]methionine-labeled PC12 cells that were incubated during preincubation, pulse, and chase periods of 0, 2, or 4 h in the absence (*left*) or presence of monensin (*center*) or BFA (*right*), and then examined by fluorography. (*Top*) APP holoproteins of 106, 112, 116, 125, 139, and 146 kDa representing immature APP₆₉₅, APP₇₅₁, and APP₇₇₀ and mature APP₆₉₅, APP₇₅₁, and APP₇₇₀, respectively. (*Bottom*) APP amino-terminal peptides of 109, 123, and 129 kDa representing secreted fragments of APP₆₉₅, APP₇₅₁, and APP₇₇₀, respectively. Molecular masses (kDa) are indicated at left.



In support of this possibility, chloroquine caused increased recovery of the 16-kDa peptide; since secretion was unchanged by chloroquine, the increased recovery of the carboxyl-terminal fragment is unlikely to be due to enhanced production, but rather to decreased degradation.

The chloroquine-sensitive proteolytic turnover of APP presumably takes place in an acidic compartment such as endosomes or lysosomes. The specific cleavage of APP to produce a secreted species, on the other hand, was not sensitive to chloroquine, suggesting that this event occurs at a different cellular location. Quantitatively, these results suggest that intra-amyloid cleavage of APP and the associated secretion of amino-terminal APP fragments represent a minor portion of total APP metabolism, and that most APP molecules are degraded along a separate subcellular route of trafficking.

The analysis of the effects of chloroquine on the rate of mature APP turnover (Figure 11, *b*) suggest that chloroquine was selectively affecting an early, rather than a late, step in APP processing. In control cells, the turnover of mature APP appeared to be a biphasic process, with a fast early phase ($t_{1/2} = 90$ min) and a slow later phase ($t_{1/2} = 3$ h). The rate of mature APP turnover in chloroquine-treated cells was virtually identical to the rate of turnover in untreated cells during the slow later phase, but it was half that of the fast early phase. This suggests that the effects of chloroquine were primarily on the early stage of mature APP proteolysis.

One interpretation of these results is that most proteolysis of mature APP occurs in endosomes, while the remainder of mature

APP would be degraded in lysosomes. According to this model, the endosomal APP proteases would be more sensitive to the effects on intraluminal pH by chloroquine than would be APP proteases in lysosomes. An alternative explanation might be that chloroquine is affecting endosomal-lysosomal transport. The effects of chloroquine could involve either the shunting of APP into lysosomes (presumably the location of the slow APP proteolysis) or the drug-induced fusion of membranes delimiting the fast and slow degradative compartments, resulting in the earlier arrival of mature APP to the latter compartment.

Chapter 4

Regulation of APP Secretion by Protein Phosphorylation

Introduction

The reversible covalent attachment of phosphate groups to proteins (addition of a phosphate group being catalyzed by protein kinases and the removal by protein phosphatases) is an important regulatory mechanism in the nervous system, modulating such activities as neurotransmitter biosynthesis, neurotransmitter release, synaptic plasticity (receptor and ion channel activity, and receptor desensitization), and gene expression (Nestler and Greengard, 1984). Although the role of protein phosphorylation in non-neurologic tissues is well established (*e.g.*, the regulation of glycogen metabolism in the liver), the brain is especially enriched in protein kinases activated by second messengers, such as cyclic AMP-, cyclic GMP-, and Ca^{2+} -dependent protein kinases, and in phosphoproteins such as synapsin and DARPP-32 (Nestler *et al.*, 1984; Nairn *et al.*, 1985). That careful regulation of protein phosphorylation states is necessary for physiological balance is evident in several diseases (*e.g.*, cystic fibrosis, diabetes mellitus, and cancer) in which abnormalities in protein phosphorylation have been implicated (Gandy *et al.*, 1991). In AD, aberrant phosphorylation of the microtubule-associated protein tau has been suggested to be an etiologic factor in the formation of neurofibrillary tangles (Lee *et al.*,

1991; see Chapter 1, "Neurofibrillary tangles"). An underlying defect in some aspect of protein phosphorylation might also contribute to the generation of senile plaques. With this in mind, a regulatory function for protein phosphorylation in the metabolism of APP was examined.

Noting that the cytoplasmic domain of APP contains consensus sequences for several protein kinases, Gandy *et al.* (1988) synthesized peptides corresponding to these different regions of the APP molecule and measured their ability to serve as substrates for purified kinases. Protein kinase C (PKC; Ca^{2+} /phospholipid-dependent protein kinase) (Kikkawa and Nishizuka, 1986) was found to phosphorylate an APP peptide on serine⁶⁵⁵, and Ca^{2+} /calmodulin-dependent protein kinase II phosphorylated residues threonine⁶⁵⁴ and serine⁶⁵⁵ (Figure 5). A role for APP phosphorylation was suggested by comparison with integral membrane proteins known to serve as PKC substrates (Gandy *et al.*, 1988). The receptors for epidermal growth factor (EGF) and interleukin 2 (IL-2) contain PKC phosphorylation sites within ten residues of the plasma membrane, as does APP (Figure 16) (Hunter *et al.*, 1984; Gallis *et al.*, 1986). PKC phosphorylation of the EGF and IL-2 receptors has been shown to regulate internalization and downregulation of these proteins (Beguinet *et al.*, 1985; Lin *et al.*, 1986; Gallis *et al.*, 1986; Shackelford and Trowbridge, 1986), though at least in the case of the EGF receptor the effects of PKC can be strikingly different among cell types (Lund *et al.*, 1990). It was therefore hypothesized that PKC phosphorylation of APP might likewise modulate its cellular trafficking (Gandy *et al.*, 1988).

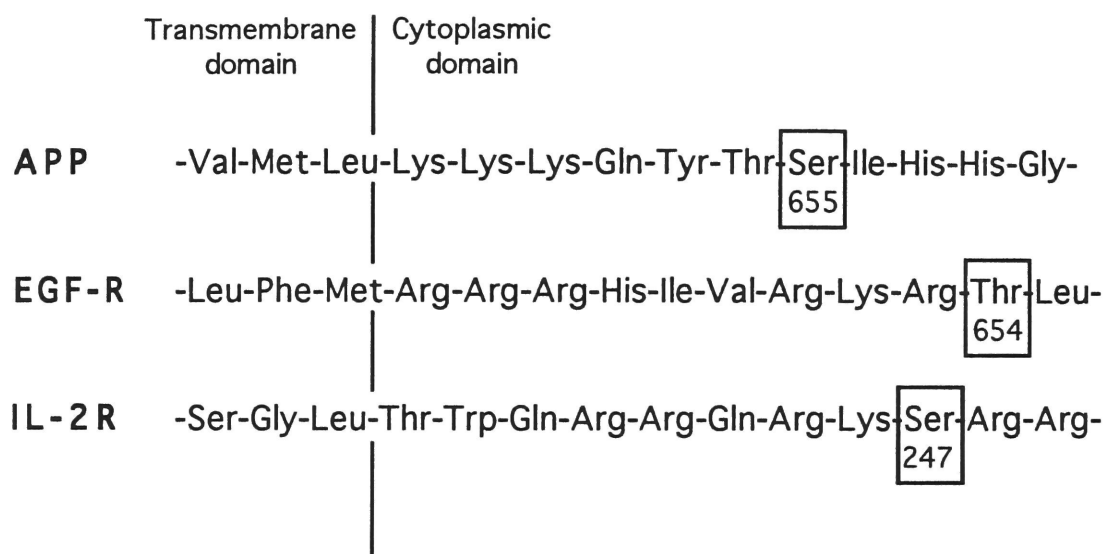


Figure 16. Comparison of the protein kinase C phosphorylation sites of APP and the receptors for EGF and IL-2 (from Gandy *et al.*, 1988). Amino acid residues are indicated by their three-letter codes. Residues that can undergo phosphorylation by PKC are boxed.

To test this possibility, the proteolytic turnover of APP was assayed in PC12 cells treated with phorbol esters (Buxbaum *et al.*, 1990). Phorbol esters are tumor promoters that directly activate PKC by mimicking the role of diacylglycerol, its physiological activator (Castagna *et al.*, 1982). The recovery of full-length APP was significantly diminished in cells treated with phorbol esters, whereas increased levels of carboxyl-terminal APP fragments were found, suggesting that PKC activation resulted in enhanced APP proteolysis (Buxbaum *et al.*, 1990). In support of this idea, the effect could be reproduced by treatment with okadaic acid, an inhibitor of protein phosphatases 1 and 2A (Cohen *et al.*, 1990), and recovery of full-length APP was increased when inhibitors of protein kinases were applied.

In pursuing the role of protein phosphorylation in APP processing, the effects of phorbol esters and okadaic acid on APP secretion are investigated in this chapter.

The contents of this section also appear in Caporaso *et al.* (1992b).

Effects of phorbol ester on maturation and turnover of APP holoprotein and on recovery of the carboxyl-terminal APP fragment

It was demonstrated previously (Buxbaum *et al.*, 1990) that treatment of PC12 cells with the phorbol ester PDBu has no effect on APP maturation, but results in more rapid turnover of mature APP as well as increased production of a carboxyl-terminal APP fragment. Those results were extended to differentiate among APP isoforms in

the present study. PDBu had no effect on APP maturation, as indicated by nearly identical rates for the disappearance of immature APP₆₉₅ and APP_{751/770} (Figure 17). Recovery of mature APP in intact cells was maximal at 30 min of chase and decreased thereafter (Figure 18). The recovery of mature APP in the presence of PDBu at 30 min of chase represented approximately 75% of that seen in control cells. By 8 h of the chase period, the amounts of labeled mature APP isoforms had returned to the levels present at the start of chase. Maximal recovery of the 16-kDa carboxyl-terminal APP fragment occurred at 1 h of chase and was increased 90% over basal levels when cells were treated with PDBu (Figure 19).

Effect of phorbol ester on APP secretion

As phorbol ester was found to cause an increase in mature APP turnover, it was examined whether this effect was associated with an alteration in the rate and/or amount of APP secretion. Indeed, PDBu treatment caused a dramatic increase in APP secretion (Figure 20). When the amounts of secreted APP were quantitated, the relative phorbol ester effects were approximately the same among APP isoforms (Figure 21). In both untreated and treated cells, APP secretion continued up to 4 h of the chase period. From 4 to 8 h, the amount of secreted APP fragments recovered from the medium remained unchanged or decreased slightly. The amount of secreted APP in the medium decreased with time when the 4-h conditioned medium was incubated in the absence of cells (not shown), indicating that the disappearance was attributable to proteolysis.

There was a three-fold accumulation of secreted APP in the

Figure 17. Effect of phorbol ester on APP maturation. Recovery of immature APP from cells incubated in the absence (*open circles*) or presence (*filled diamonds*) of PDBu was quantitated by densitometry of fluorograms, normalized, and plotted as a function of time. (*Top*) Immature APP₆₉₅. (*Bottom*) Immature APP_{751/770}. Results are the means \pm SEM of seven experiments; n = 3 to 7 for individual time points. There was no statistically significant difference between untreated and treated samples (Student's unpaired t-test).

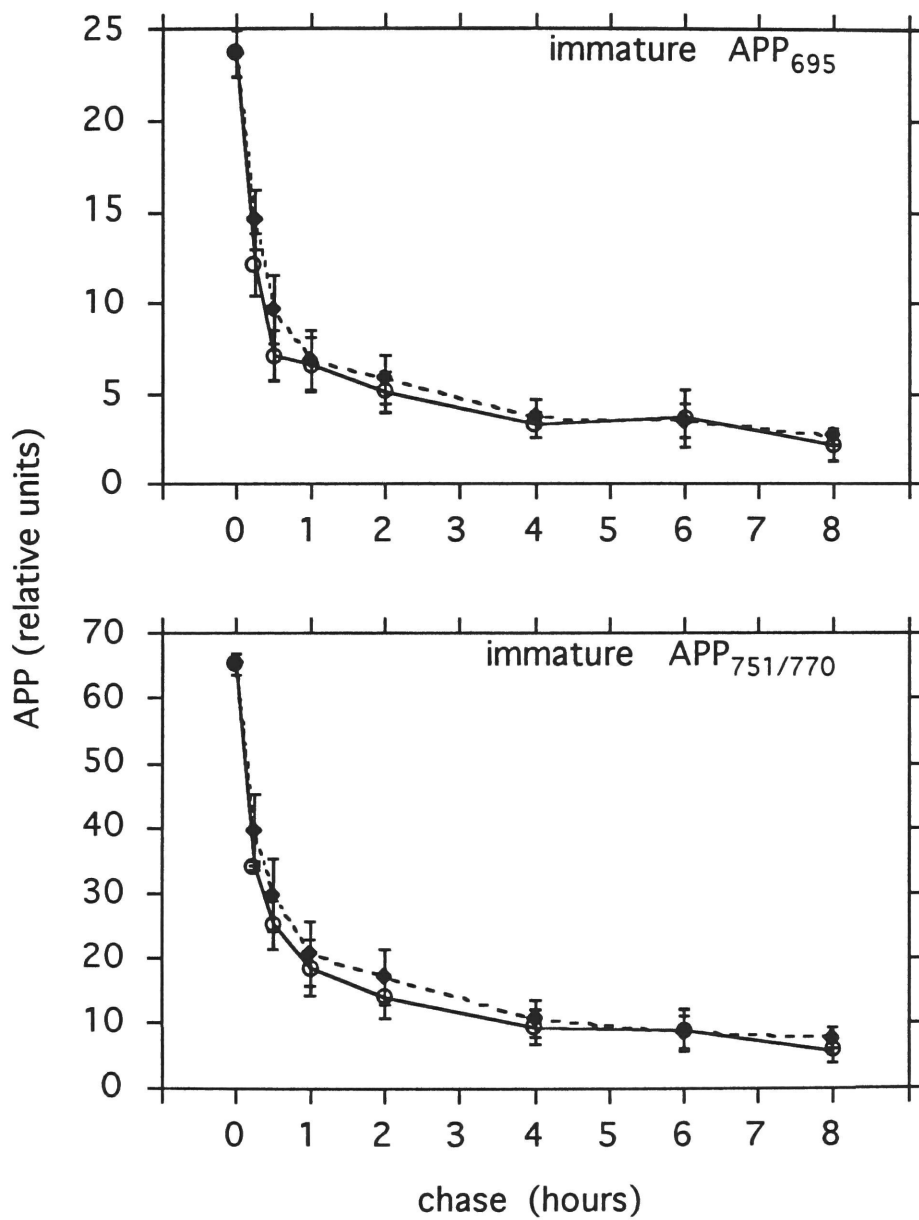
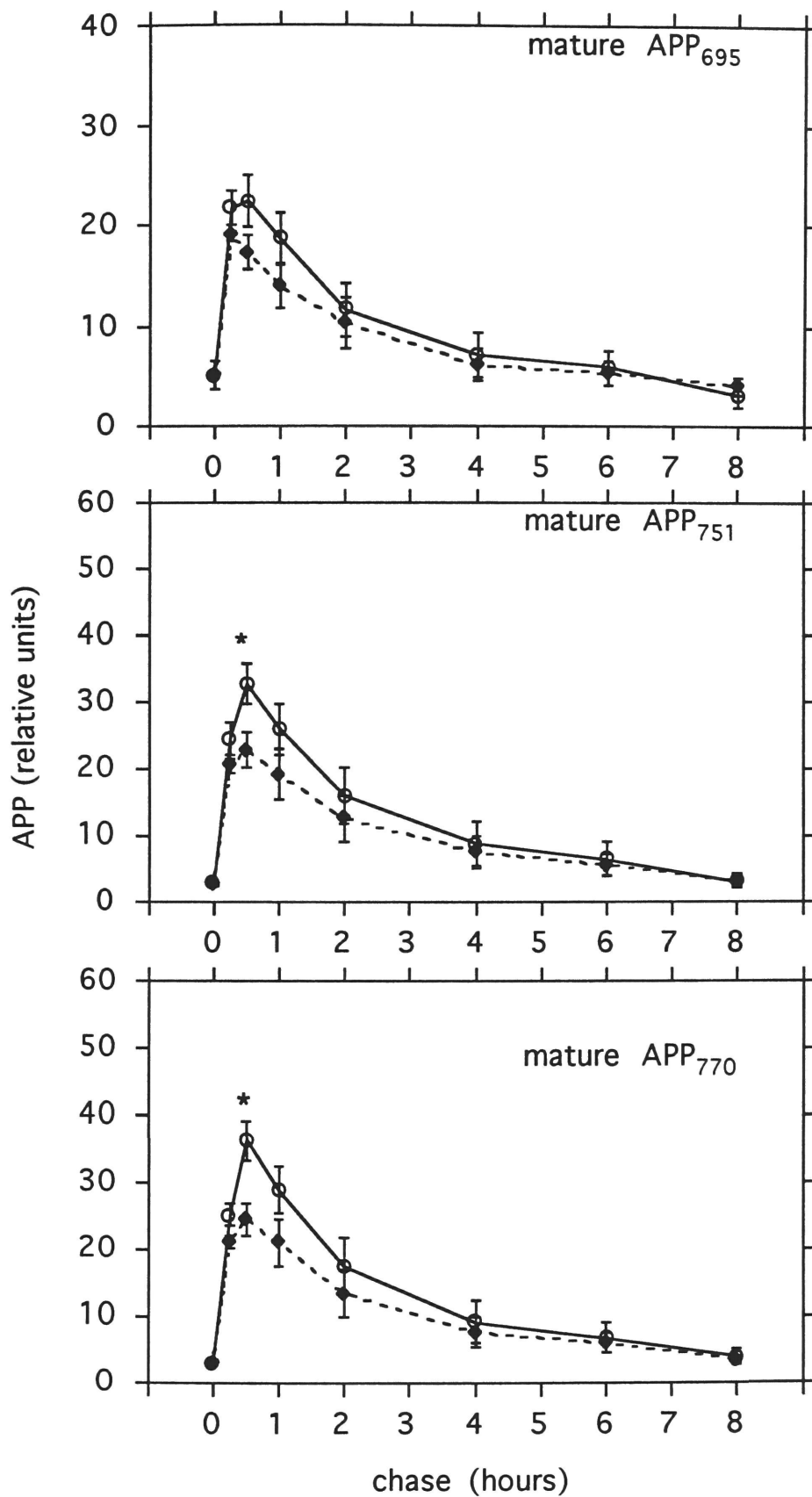


Figure 18. Effect of phorbol ester on the turnover of mature APP. Recovery of mature APP from cells incubated in the absence (*open circles*) or presence (*filled diamonds*) of PDBu was quantitated by densitometry of fluorograms, normalized, and plotted as a function of time. (*Top*) Mature APP₆₉₅. (*Middle*) Mature APP₇₅₁. (*Bottom*) Mature APP₇₇₀. Results are the means \pm SEM of seven experiments; $n = 3$ to 7 for individual time points. Statistical significance between untreated and treated samples for individual time points was determined by Student's unpaired t-test (*, $p < 0.05$).



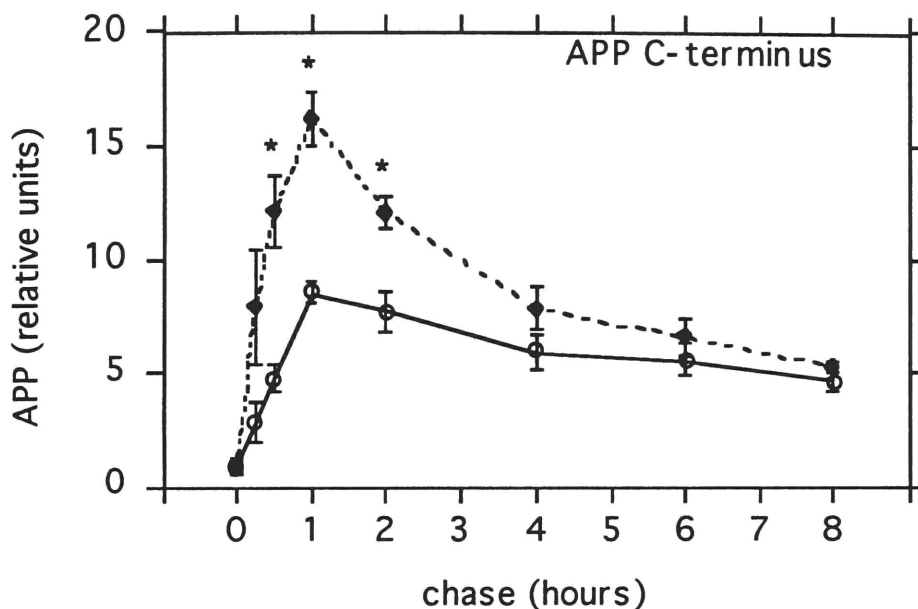
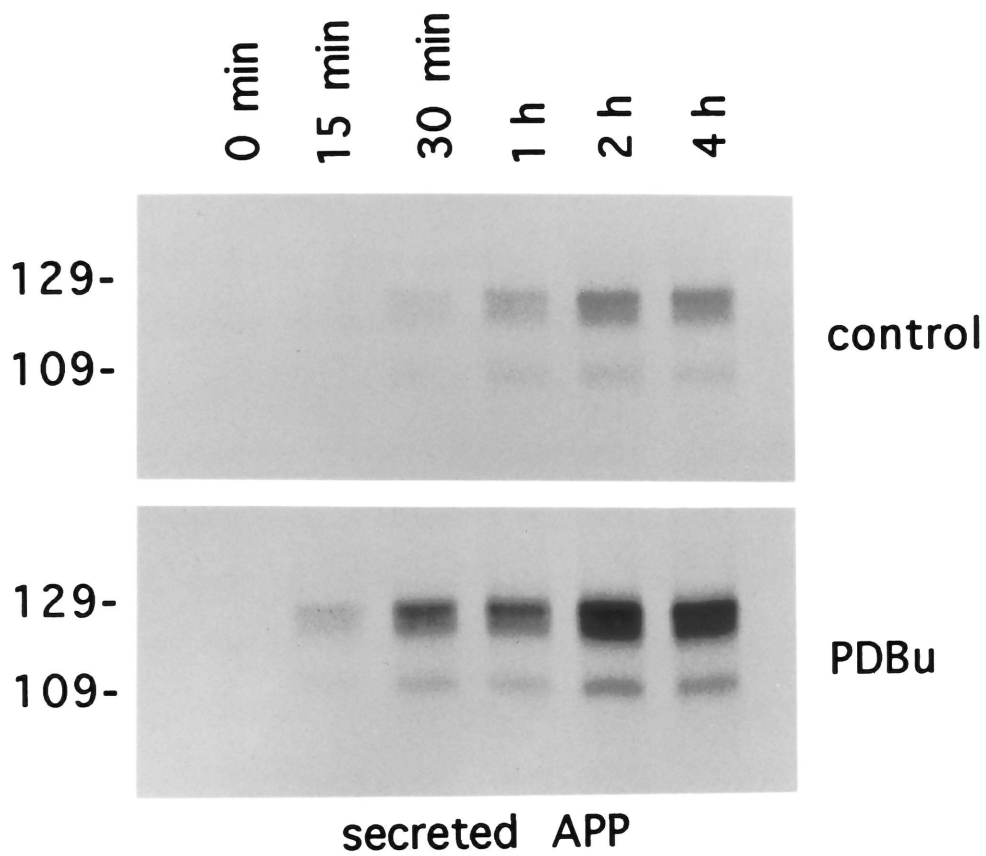


Figure 19. Effect of phorbol ester on the turnover of the carboxyl-terminal APP fragment. Recovery of the 16-kDa carboxyl-terminal APP fragment from cells incubated in the absence (*open circles*) or presence (*filled diamonds*) of PDBu was quantitated by densitometry of fluorograms, normalized, and plotted as a function of time. Results are the means \pm SEM of seven experiments; $n = 3$ to 7 for individual time points. Statistical significance between untreated and treated samples for individual time points was determined by Student's unpaired t-test (*, $p < 0.05$).

Figure 20. Effect of phorbol ester on APP secretion. APP species were immunoprecipitated from the cultured medium of [³⁵S]methionine-labeled PC12 cells incubated during the chase period for the indicated times in the absence (*top*) or presence (*bottom*) of PDBu, and examined by fluorography with 6% SDS-polyacrylamide gels. Molecular masses (kDa) are indicated at left.



medium of PDBu-treated cells relative to control levels. Phorbol ester caused an increase both in the rate of accumulation as well as in the absolute amount of secreted APP. At 4 h of chase, approximately 15% of the labeled APP present at the start of chase was recovered as secreted amino-terminal APP fragments from the medium of control cells, whereas approximately 45% was recovered from the medium of PDBu-treated cells. This indicates that under control conditions, a relatively small pool of APP was cleaved within the β /A4 amyloid domain to produce secreted APP. The majority of APP molecules were presumably degraded via an intracellular proteolytic pathway unassociated with secretion (Caporaso *et al.*, 1992a; Chapter 3).

When the difference between mature APP holoprotein recovered from PDBu-treated and untreated cells (at 30 min of chase) was compared to the difference between secreted APP fragments recovered from the medium of PDBu-treated and untreated cells (at 4 h of chase), a close correlation was found (27 ± 6 versus 31 ± 3 relative units, respectively). Thus, the phorbol ester-stimulated turnover of mature APP holoprotein could be quantitatively accounted for by enhanced APP secretion.

Absence of effect of inactive phorbol ester on APP secretion

As a control for the specificity of PDBu activation of PKC, cells were also treated with the inactive analogue, 4- α -PDBu (Castagna *et al.*, 1982). There was virtually no effect on APP maturation or holoprotein turnover (not shown) or on APP secretion (Figure 22) in

Figure 21. Effect of phorbol ester on APP secretion. Recovery of secreted amino-terminal APP fragments from the cultured medium of cells incubated in the absence (*open circles*) or presence (*filled diamonds*) of PDBu was quantitated by densitometry of fluorograms, normalized, and plotted as a function of time (see Figure 20). (*Top*) Secreted APP₆₉₅. (*Middle*) Secreted APP₇₅₁. (*Bottom*) Secreted APP₇₇₀. Results are the means \pm SEM of seven experiments; n = 3 to 7 for individual time points. Statistical significance between untreated and treated samples for individual time points was determined by Student's unpaired t-test (*, p < 0.05).

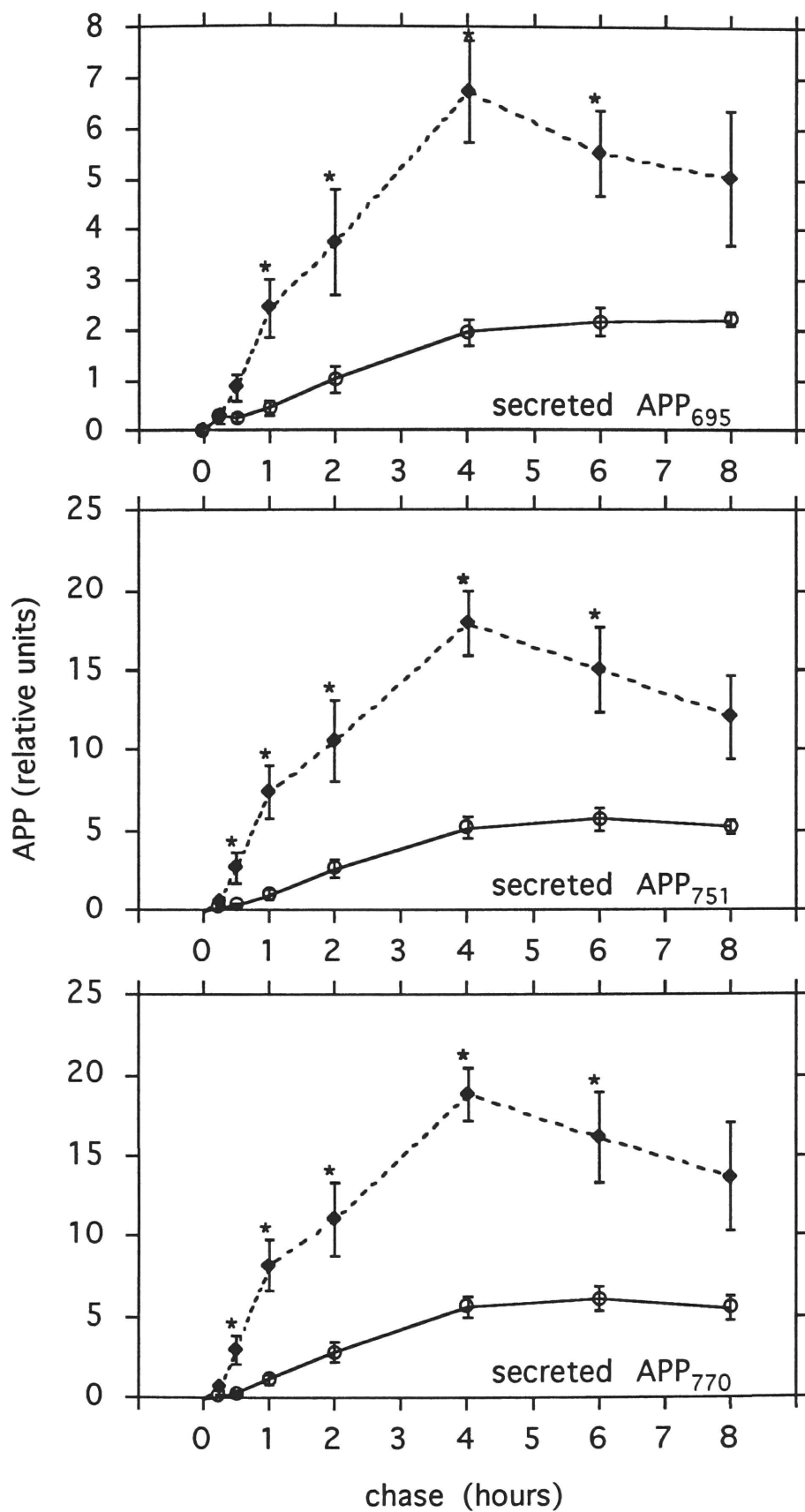
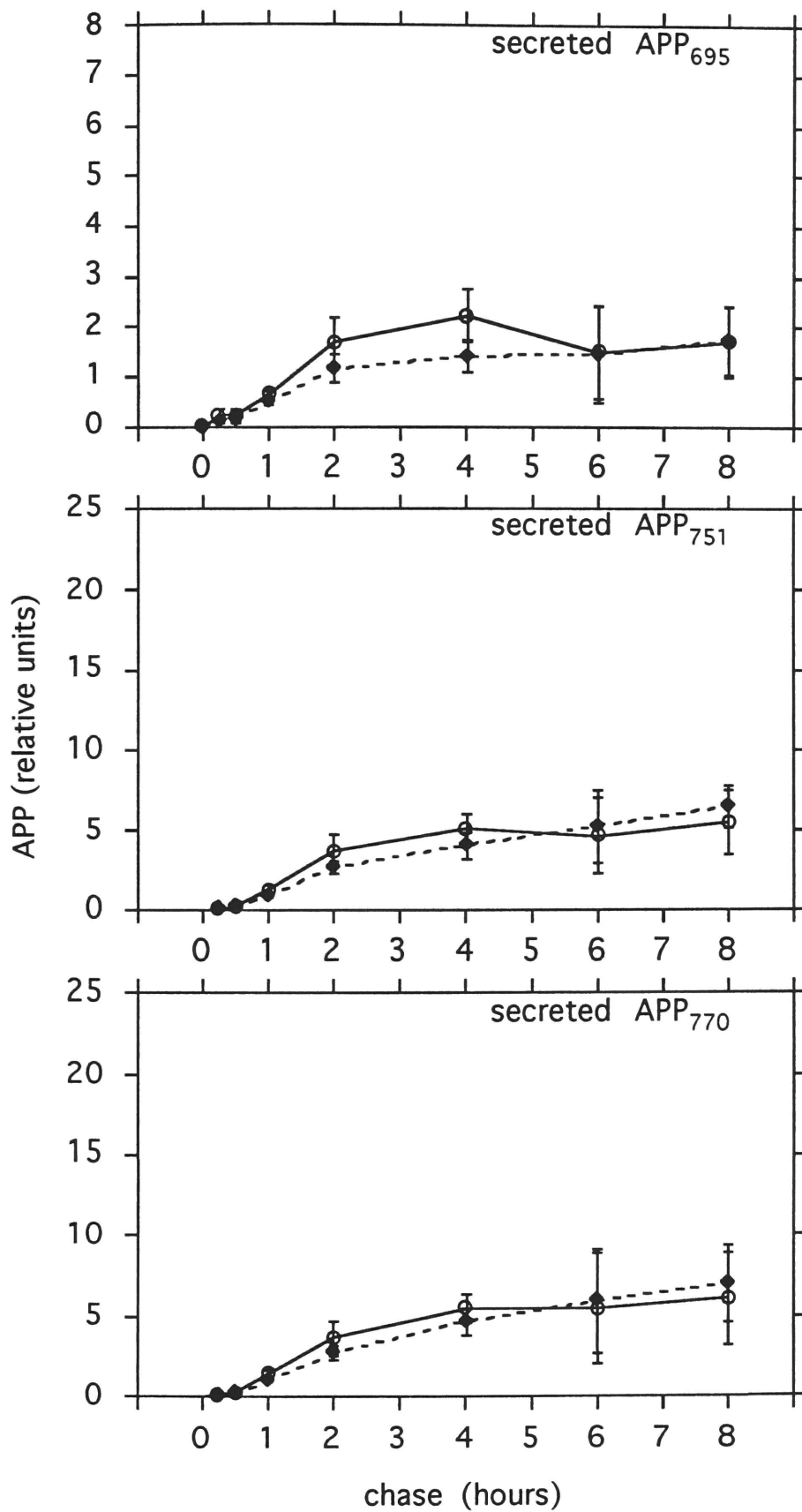


Figure 22. Effect of an inactive phorbol ester on APP secretion. Recovery of secreted amino-terminal APP fragments from the cultured medium of cells incubated in the absence (*open circles*) or presence (*filled diamonds*) of 4- α -PDBu was quantitated by densitometry of fluorograms, normalized, and plotted as a function of time. (*Top*) Secreted APP₆₉₅. (*Middle*) Secreted APP₇₅₁. (*Bottom*) Secreted APP₇₇₀. Results are the means \pm SEM of four experiments; n = 2 to 4 for individual time points. There was no statistical significance between untreated and treated samples for any time points as determined by Student's unpaired t-test.



the presence of 4- α -PDBu relative to cells treated with vehicle alone.

Effect of combined treatment with phorbol ester and okadaic acid on APP secretion

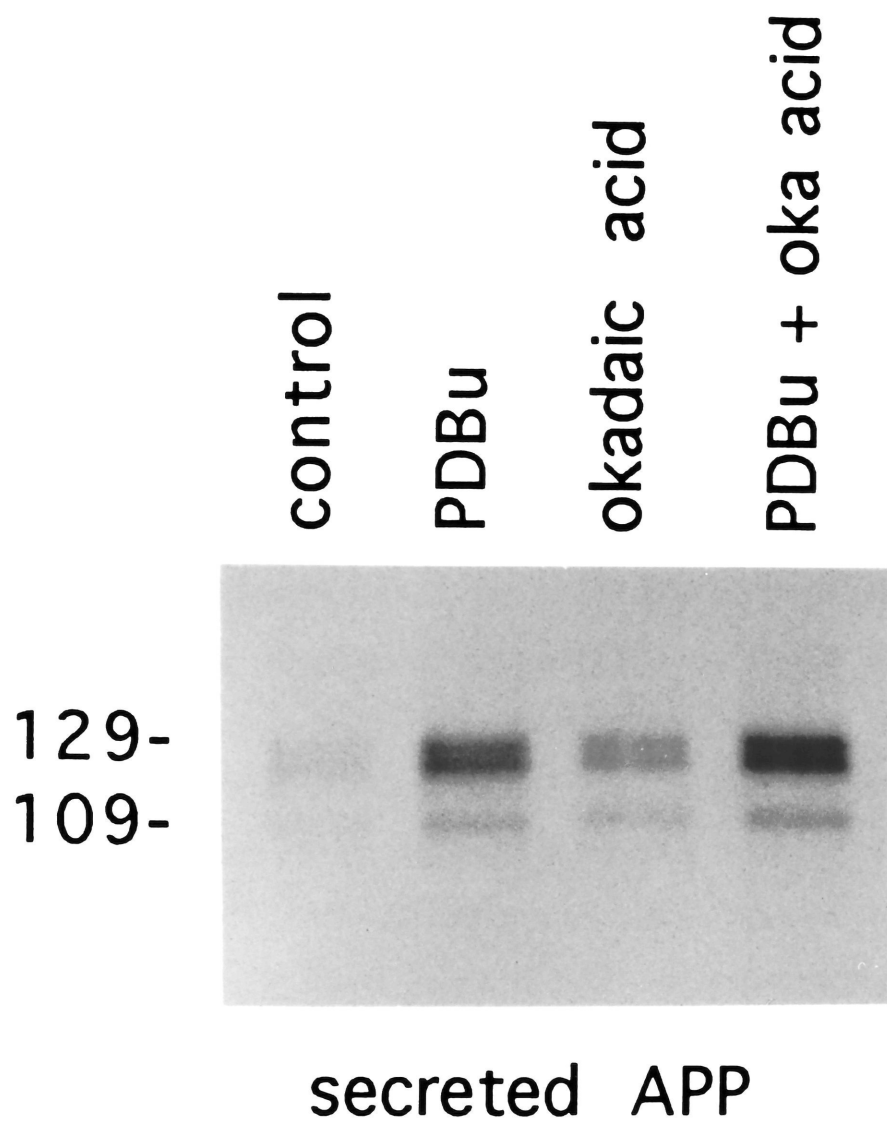
Combined treatment with PDBu and okadaic acid, an inhibitor of protein phosphatases 1 and 2A (Cohen *et al.*, 1990), was previously found to produce a more rapid turnover of mature APP as well as increased recovery of carboxyl-terminal APP fragments than treatment with either phorbol ester or okadaic acid alone (Buxbaum *et al.*, 1990). Therefore, the effect of combined treatment on APP secretion was examined (Figure 23). Cells treated for 1 h with okadaic acid alone secreted more APP than untreated cells, but less than those treated with PDBu. When cells were treated with both PDBu and okadaic acid, APP secretion at 1 h was greater than in cells treated with PDBu or okadaic acid alone.

Although combined treatment with PDBu and okadaic acid produces a carboxyl-terminal fragment that migrates on SDS-polyacrylamide gels more slowly than the 16-kDa species (Buxbaum *et al.*, 1990), no evidence of truncated secreted APP fragments was found. Furthermore, with no treatments nor combinations of treatments were secreted APP fragments detected in cell lysates.

Conclusions

In this and the previous chapter, it was demonstrated in PC12 cells that, under basal conditions, a relatively small pool of APP was cleaved within the β /A4 amyloid domain to produce secreted APP, indicating that the majority of APP molecules were degraded via a

Figure 23. Comparative effects of phorbol ester and okadaic acid on APP secretion. APP species were immunoprecipitated from the cultured medium of [³⁵S]methionine-labeled PC12 cells incubated during the chase period for 1 h in the absence or presence of agents that regulate protein phosphorylation: (*lane 1*) vehicle alone; (*lane 2*) PDBu; (*lane 3*) okadaic acid; (*lane 4*) PDBu plus okadaic acid. Samples were examined by fluorography of a 6% SDS-polyacrylamide gel. Molecular masses (kDa) are indicated at left.



proteolytic pathway unassociated with secretion. The intra- β /A4 amyloid cleavage and secretion of amino-terminal APP fragments were stimulated several-fold by PDBu treatment, presumably by the activation of PKC (see Table 4). These data provide a possible mechanism for regulation of APP function.

Regulation by PKC of the conversion of integral proteins from membrane-bound to soluble forms with a subsequent alteration in their function has been reported for tumor necrosis factor receptor (Lantz *et al.*, 1990), colony-stimulating factor 1 (CSF-1) receptor (Downing *et al.*, 1989; Stein and Rettenmier, 1991), murine neutrophil MEL-14 antigen (Kishimoto *et al.*, 1989), plasminogen activator (Jaken and Black, 1981; Eaton and Baker, 1983), and the precursor for transforming growth factor α (TGF- α) (Pandiella and Massagué, 1991). On the basis of the resemblance of APP's structure to that of certain cell-surface receptors, APP was postulated to function as a cell-surface binding protein for an as yet unidentified ligand (Kang *et al.*, 1987), an interpretation supported by the localization of some APP molecules to the plasma membrane (Weidemann *et al.*, 1989; Haass *et al.*, 1992a; Sisodia, 1992).

Regulated proteolytic cleavage and secretion of APP by activation of PKC could serve two purposes: down-regulation of APP from the cell surface, and release of a functional APP fragment into the surrounding environment (Ehlers and Riordan, 1991). Functional modulation of a plasma membrane protein is exemplified by TGF- α ; in addition to its well-known role as a soluble mitogen that binds to and activates the receptor for EGF (Derynck, 1988), the cell-surface precursor for TGF- α can effect signal transduction by binding to EGF

Table 4. Summary of drug effects on the recovery of APP species.

Drug	Immature APP	Mature APP	Secreted APP	C-terminal APP fragment
monensin	+	-	-	-
brefeldin A	+	-	-	-
chloroquine	0	+	0	+
PDBu	0	-	+	+
okad. acid	(+)	(-)	+	(+)

Key: +, more recovered; -, less recovered; 0, no change. The effects of okadaic acid indicated in parentheses were reported in Buxbaum *et al.*, 1990.

receptors on adjacent cells (Wong *et al.*, 1989; Brachmann *et al.*, 1989). Although the physiological function of APP is not known, secreted amino-terminal fragments of APP₇₅₁ and APP₇₇₀ have been identified as protease nexin-II (PN-II) (Oltersdorf *et al.*, 1989; Van Nostrand *et al.*, 1989), a soluble protein that forms complexes with EGF-binding protein, γ -subunit of nerve growth factor, and trypsin (Van Nostrand and Cunningham, 1987). Protease nexins are believed to regulate the function of extracellular serine proteases by irreversibly binding to them and mediating their internalization and degradation (Low *et al.*, 1981). The specific physiological significance of these interactions is not understood, but PN-II released from platelets has been found to be a potent inhibitor of coagulation factor XI_a (Smith *et al.*, 1990).

It has not yet been determined whether the phorbol ester-induced effects on APP secretion are due to phosphorylation of APP by PKC ("substrate activation"), activation of an APP "secretase" ("enzyme activation"), or redirected cellular trafficking that brings APP in contact with its protease(s). Support for the "substrate activation" model comes from studies in our laboratory demonstrating that PKC can phosphorylate synthetic APP carboxyl-terminal peptides (Gandy *et al.*, 1988) and full-length APP in semi-intact cells (Suzuki *et al.*, 1992), as well as from other studies which demonstrate that mature APP is phosphorylated in cultures of intact cells (Oltersdorf *et al.*, 1990). A proline-directed kinase that phosphorylates the microtubule-associated protein tau (Roder and Ingram, 1991; see Chapter 1, "Neurofibrillary tangles," for details) has also been demonstrated *in vitro* to phosphorylate APP on

threonine⁶⁶⁸ (Figure 5) (T. Suzuki *et al.*, manuscript in preparation). In a system that might be analogous, phosphorylation of the polymeric immunoglobulin receptor results in acceleration of its transcytosis and proteolytic cleavage to produce secretory component (Casanova *et al.*, 1990). The "enzyme activation" model is supported by studies on the CSF-1 receptor, in which PKC has been suggested to act on the protease responsible for the release of soluble receptor, rather than on the membrane-bound receptor itself (Downing *et al.*, 1989). Appearance of the transferrin receptor (Tf-R) at the surface of some cell types is increased by treatment with phorbol esters by a mechanism that is independent of Tf-R phosphorylation (McGraw *et al.*, 1988). In contrast, in other cell types PKC-mediated Tf-R phosphorylation results in the internalization and downregulation of the receptor (May *et al.*, 1984; May *et al.*, 1985). It should be added that PKC might exert its effects through activation of another signal transduction system, such as cyclic AMP or cyclic GMP systems (Kikkawa and Nishizuka, 1986).

The majority of APP molecules are degraded in unstimulated PC12 cells via a chloroquine-sensitive endosomal/lysosomal proteolytic pathway; a small fraction undergoes intra- β /A4 amyloid cleavage via a chloroquine-insensitive pathway to produce secreted amino-terminal APP fragments and the 16-kDa carboxyl-terminal APP fragment (Caporaso *et al.*, 1992a; Chapter 3). These earlier observations, combined with the results of the present study, suggest a scheme for the cellular trafficking and proteolytic processing of APP (Figure 24). These results indicate that PKC stimulates the non-amyloidogenic secretory pathway of APP. At present, the possibility

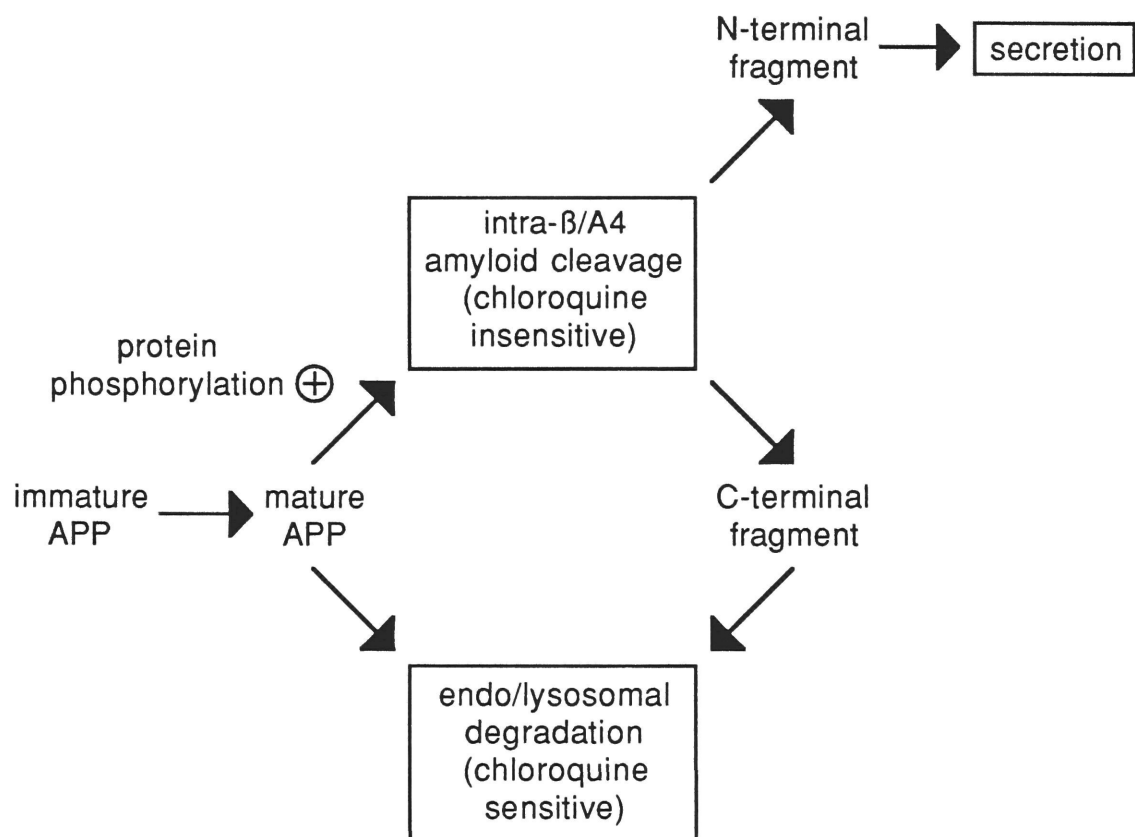


Figure 24. Proposed scheme for the cellular trafficking and proteolytic processing of APP.

cannot be excluded that PKC also regulates the alternative, and possibly amyloidogenic, APP degradative (endosomal/lysosomal) pathway. The existence of distinct physiological and amyloidogenic pathways could facilitate the development of anti-amyloidogenic drugs.

Chapter 5

Cellular Transport of APP via Clathrin-coated Vesicles

Introduction

The secretory route of APP proteolytic processing seemingly represents a quantitatively minor metabolic pathway (though its functional significance might not be minor), since in unstimulated rat neuroendocrine PC12 cells only a small fraction of APP molecules is targeted for secretion. The bulk of APP is degraded in a separate chloroquine-sensitive compartment, presumably endosomes and lysosomes (Caporaso *et al.*, 1992a; Chapter 3). In addition, there is evidence that the endosomal/lysosomal system might be the site for generation of APP proteolytic fragments that preserve intact β /A4 and thus contribute to the pathology of Alzheimer disease (Golde *et al.*, 1992; Haass *et al.*, 1992a). These studies, though, did not directly demonstrate the cellular trafficking of APP to the endosomal/lysosomal system.

In this section, the presence of APP in clathrin-coated vesicles (CCVs) is investigated. CCVs are responsible for the trafficking of many proteins to the endosomal compartment, including the transport of plasma membrane receptors to early endosomes and of proteins destined for lysosomes from the *trans*-Golgi network (TGN) to late endosomes/prelysosomes (Goldstein *et al.*, 1985; Brodsky, 1988; Kornfeld and Mellman, 1989). While little is known about the

mechanism(s) whereby integral membrane proteins are targeted to the population of CCVs that exit the TGN (*e.g.*, see Harter and Mellman, 1992), specific signals have been identified that are responsible for targeting cell-surface proteins to the CCVs that bud off the plasma membrane. Both the influenza virus hemagglutinin molecule and the cation-independent mannose 6-phosphate receptor are efficiently endocytosed only if a tyrosine residue is present at specific locations in their cytoplasmic domains (Lazarovits and Roth, 1988; Lobel *et al.*, 1989). Endocytosis of the low density lipoprotein receptor requires an asparagine-proline-X-tyrosine (NPXY, where X represents any amino acid) motif in its cytoplasmic domain (Chen *et al.*, 1990), perhaps enabling its interaction with the assembly/adaptor proteins that are believed to mediate the interactions between internalized proteins and the clathrin cage of the CCV (Pearse, 1988). APP is among the numerous cell-surface proteins possessing an NPXY motif in their cytoplasmic domains, suggesting that it too might be targeted to and internalized via clathrin-coated pits (Table 5) (Chen *et al.*, 1990; Gandy *et al.*, 1991). The identification of APP in CCVs would provide direct evidence for the trafficking of APP to the endosomal/lysosomal system.

This chapter describes the purification of CCVs from PC12 cells by using a combination of protocols developed for the isolation of CCVs from mammalian organs. The CCV preparation was characterized by SDS-polyacrylamide gel electrophoresis, electron microscopy, and immunoblot analysis using as a marker the transferrin receptor (Tf-R), an internalized protein known to be present in CCVs (Turkewitz and Harrison, 1989). It is shown that

Table 5. Cell surface proteins whose cytoplasmic domains contain the consensus sequence NPXY (Chen *et al.*, 1990).

Protein	Amino acid sequence ^a	No. of residues from plasma membrane ^b
LDL receptor	NPVY	15
Insulin receptor	NPEY	17
IGF-1 receptor	NPEY	18
EGF receptor	NPVY	439
	NPEY	467
	NPDY	501
<i>c-erbB-2 (neu)</i>	NPEY	518
	NPEY	570
Fibronectin receptor (β subunit)	NPIY	29
	NPKY	41
Glycoprotein IIIa	NPLY	23
APP	NPTY	36

^aHuman sequence. ^bPosition of the asparagine residue (N).

full-length mature (fully post-translationally modified) APP and the carboxyl-terminal fragment resulting from APP secretory cleavage are enriched in CCVs.

The contents of this section also appear in Nordstedt *et al.* (1993).

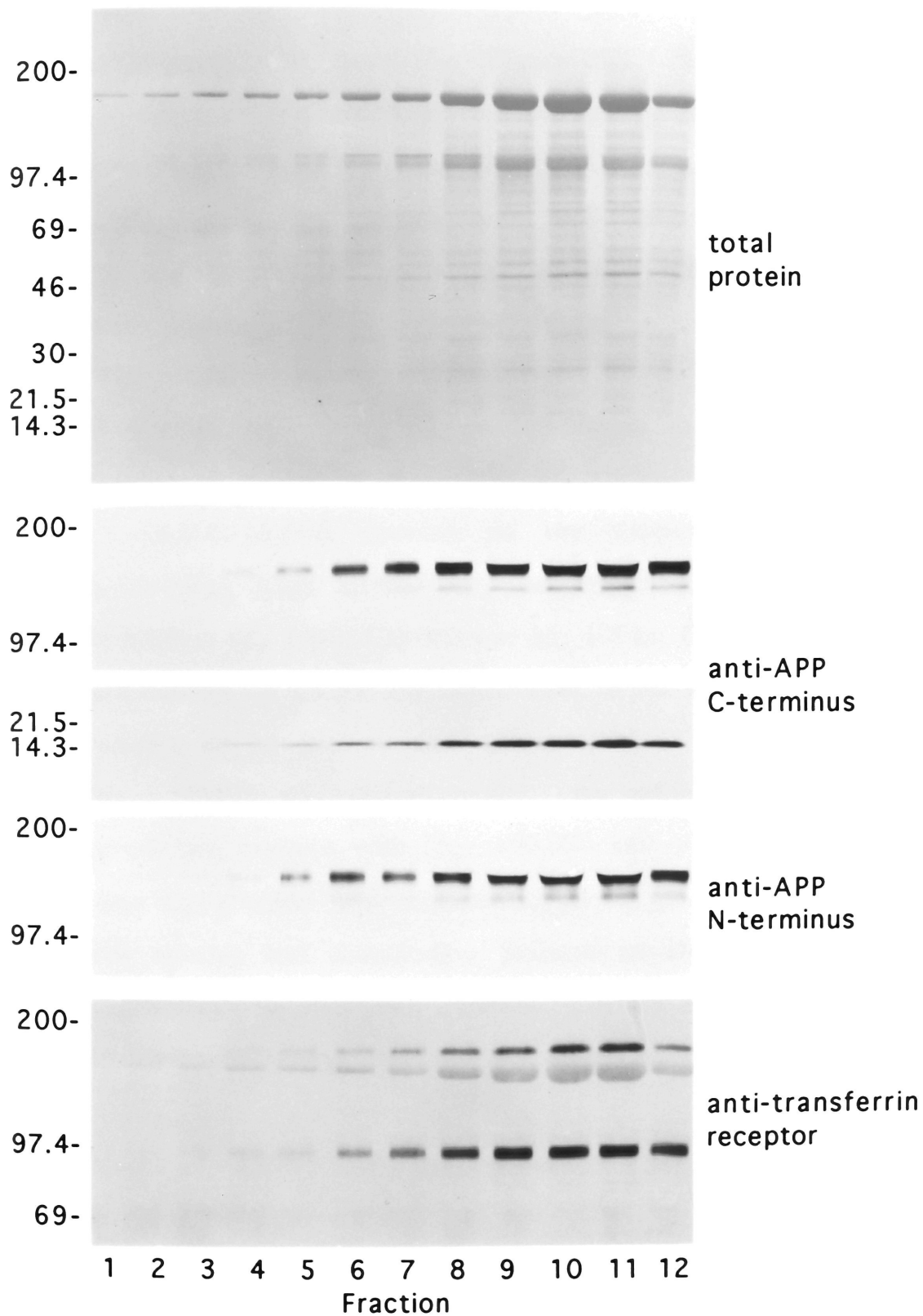
Separation of CCVs by density gradient centrifugation

Highly purified CCVs were prepared from PC12 cells by differential centrifugation according to established methods (see Chapter 2, "Preparation of clathrin-coated vesicles"). The CCVs were then fractionated according to differences in density or size, and examined for possible co-distribution of clathrin and APP. This procedure allowed for the separation of minor contaminating structures from CCVs.

In these experiments, CCVs were separated according to density on a 10-ml linear density-equilibrium gradient consisting of 2/9%-20/90% Ficoll 400/D₂O. Twelve fractions of approximately 0.8 ml each were collected from the gradient. Equal volumes of these fractions were separated on 4-15% SDS-polyacrylamide gradient gels followed by transfer of the proteins to nitrocellulose membranes. The total protein was visualized by amido black staining of the nitrocellulose membranes (Figure 25). Fractions 8-12 contained a protein pattern typical of CCV preparations: a large quantity of clathrin heavy chain (M_r ~180,000) and smaller quantities of clathrin light chains (M_r ~32,000) and assembly/adaptor proteins (M_r ~100,000, ~50,000, and ~17,000) (Ahle *et al.*, 1988).

When the fractions were analyzed by immunoblotting using an

Figure 25. Co-purification of APP and transferrin receptor with clathrin-coated vesicles fractionated by density-equilibrium centrifugation. CCVs prepared from PC12 cells by differential centrifugation (see Chapter 2, "Preparation of clathrin-coated vesicles") were loaded on a linear 2/9%-20/90% Ficoll 400/D₂O gradient and centrifuged at 80,000 g for 15 h. Proteins from equal volumes of each fraction (1 = top, 12 = bottom of gradient) were separated on 4-15% SDS-polyacrylamide gels and transferred to nitrocellulose membranes. Total protein was visualized by amido black staining, and revealed a large quantity of clathrin heavy chain ($M_r \sim 180,000$) and smaller quantities of clathrin light chains ($M_r \sim 32,000$) and assembly/adaptor proteins ($M_r \sim 100,000$, $\sim 50,000$, and $\sim 17,000$). Immunoblotting with an antibody against the carboxyl terminus of APP (369A) revealed proteins of $M_r \sim 140,000$, $\sim 120,000$, and $\sim 14,000$ - $15,000$ corresponding to full-length mature APP_{751/770} and APP₆₉₅, and the carboxyl-terminal APP fragment resulting from secretory processing, respectively. Antibody against the amino terminus of APP (22C11) recognized only the $M_r \sim 140,000$ and $\sim 120,000$ proteins. Antibody against rat Tf-R revealed proteins of $M_r \sim 190,000$ and $\sim 95,000$, corresponding to the dimeric and monomeric forms of the molecule, respectively (the weaker protein band below the dimeric Tf-R might represent antibody cross-reactivity with clathrin heavy chain). Approximate M_r ($\times 10^3$) values are indicated at left.



antibody against the carboxyl terminus of APP (369A), three distinct APP species with M_r ~140,000, ~120,000, and ~14,000-15,000 were shown to co-purify with the CCVs (Figure 25). An antibody against the amino-terminal end of APP (22C11) recognized only the two higher molecular mass APP species (Figure 25). Based on comparison of the APP immunoblot pattern seen with cell homogenates (see Figure 28 and below) and previously reported identification of the APP species present in PC12 cells (Weidemann *et al.*, 1989; Buxbaum *et al.*, 1990; Caporaso *et al.*, 1992b; Chapter 3), the M_r ~140,000 and ~120,000 species were assigned as full-length mature (fully post-translationally modified) APP_{751/770} and APP₆₉₅, respectively, and the M_r ~14,000-15,000 species as the carboxyl-terminal APP fragment resulting from normal APP secretory cleavage (Sisodia *et al.*, 1990; Esch *et al.*, 1990; Caporaso *et al.*, 1992a; Chapter 3).

As a marker for CCVs, the distribution in the fractions of Tf-R, a protein known to be present and concentrated in CCVs (Turkewitz and Harrison, 1989), was also examined. An antibody against rat Tf-R recognized two proteins with M_r ~190,000 and ~95,000 (Figure 25), representing the dimeric and monomeric forms of Tf-R, respectively. Both Tf-R species had distribution patterns in the density gradient virtually identical to those of clathrin, clathrin-associated proteins, and APP immunoreactivity.

Separation of CCVs by gel-filtration chromatography

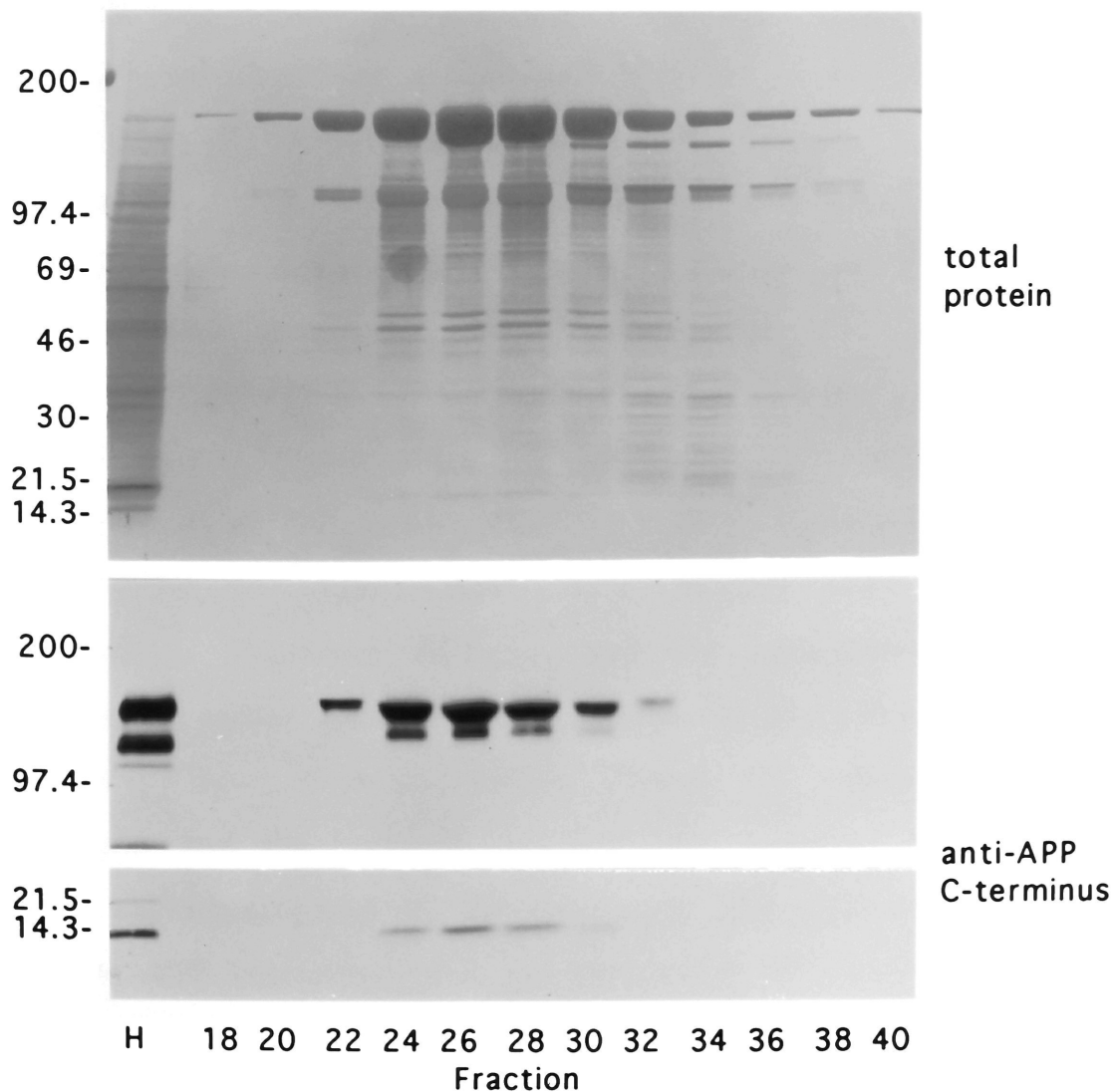
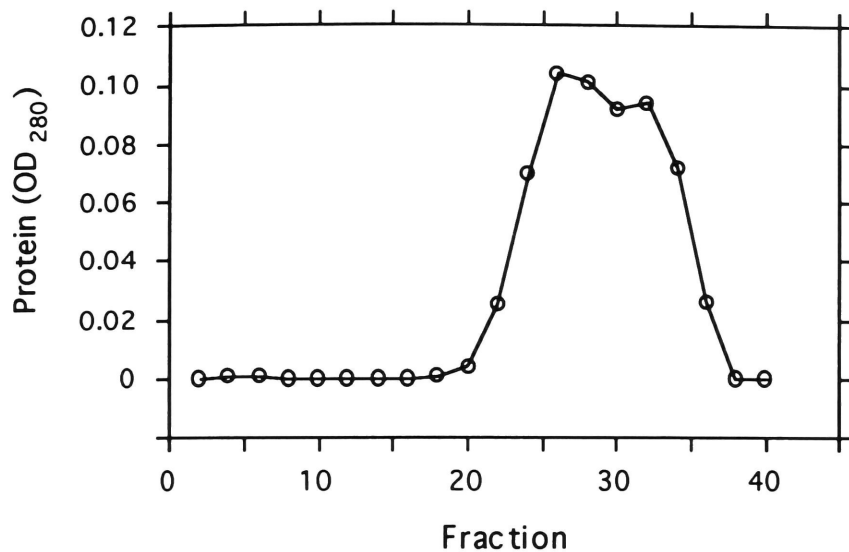
In order to demonstrate that the APP immunoreactivity was indeed present in CCVs, and not in contaminating structures with a density similar to that of CCVs, the CCVs were also subjected to gel-

filtration chromatography on an S-1000 column, in which structures were separated according to size rather than density (Figure 26). Measurement of protein content by spectrophotometric absorbance at a wavelength of 280 nm of the column eluate produced a broad peak centered at fractions 26 and 28, with a "shoulder" at fraction 32. The protein pattern in the fractions was virtually identical to the protein pattern obtained when CCVs were separated according to density (compare Figure 26 with Figure 25). However, a protein with $M_r \sim 150,000$ and some smaller proteins that peaked in fraction 32 were clearly separated from the clathrin peak, and probably represent a smaller-diameter contaminating structure (Figure 26). The APP species with $M_r \sim 140,000$, $\sim 120,000$, and $\sim 14,000$ - $15,000$ that co-purified with CCVs in the density gradient also co-purified with CCVs on the S-1000 column (Figure 26), supporting the conclusion that APP was present in CCVs.

Electron microscopy of CCVs

To determine the purity of the CCV preparation, CCV fractions eluted from the S-1000 column were examined by electron microscopy (Figure 27). The morphology of the purified structures was identical to that of CCVs prepared from other sources (*e.g.*, see Brodsky, 1988). The preparation was found almost exclusively to contain CCVs with well-defined membrane vesicles (Figure 27, *closed arrows*) and vesicle-free clathrin cages (Figure 27, *open arrows*). Very few contaminating structures were seen, with approximately 99% of the structures (as determined by manual counting) representing CCVs or clathrin cages. The fine granular pattern seen

Figure 26. Co-purification of APP with clathrin-coated vesicles fractionated by gel-filtration chromatography. CCVs prepared from PC12 cells by differential centrifugation (see Chapter 2, "Preparation of clathrin-coated vesicles") were eluted from an S-1000 column and the protein content of each fraction was monitored by spectrophotometric absorbance at a wavelength of 280 nm. Fractions corresponding to the absorbance peak (*fractions 18-40*) were concentrated by centrifugation at 100,000 g for 90 min. Proteins from a total cell homogenate (*lane H*) or from equal volumes of each fraction were separated on 4-15% SDS-polyacrylamide gels and transferred to nitrocellulose membranes. Total protein was visualized by amido black staining, and revealed a protein pattern very similar to that seen in CCVs separated by density-equilibrium centrifugation (see Figure 25), with CCVs being most concentrated in fractions 26 and 28. However, proteins of $M_r \sim 150,000$ and $M_r \sim 110,000$ (along with several lower molecular mass proteins) that peaked in fraction 32 probably represent a smaller-diameter contaminating structure. Immunoblotting with an antibody against the carboxyl terminus of APP (369A) indicated that APP immunoreactivity was concentrated in the structures centered at fractions 24-28. Approximate M_r ($\times 10^3$) values are indicated at left.

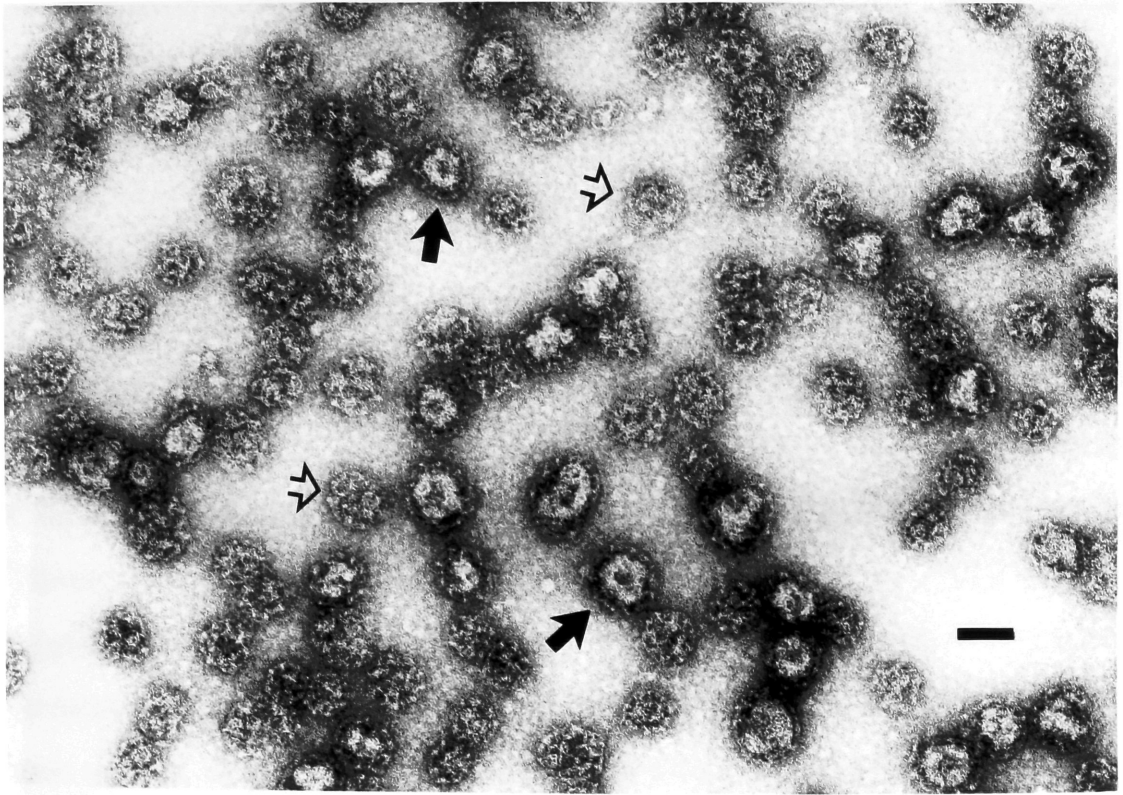


in the background of the electron micrograph in Figure 27 is a staining artifact that also is obtained with buffer alone (not shown). Due to the presence of Ficoll 400 in the fractions from the density-equilibrium gradient, these CCVs could not be examined by electron microscopy.

Enrichment of APP in CCVs

To assess whether APP was enriched in CCVs compared to the total cell homogenates, the APP content in equal amounts of protein from cell homogenates and CCVs was compared (Figure 28). Equal amounts of protein from a total cell homogenate and from the peak fractions of CCVs purified on density-equilibrium gradients were separated on 4-15% SDS-polyacrylamide gradient gels, transferred to nitrocellulose membranes, and analyzed by amido black total protein staining and by immunoblotting with antibodies 369A or 22C11 and antibody against Tf-R. Immunoblot analysis with antibody 369A revealed in cell homogenates immunoreactive protein bands of M_r ~140,000, ~120,000, ~115,000, ~105,000, and ~14,000-15,000 corresponding to mature APP_{751/770}, mature APP₆₉₅, immature APP_{751/770}, immature APP₆₉₅, and the carboxyl-terminal APP fragment as earlier identified (Weidemann *et al.*, 1989; Buxbaum *et al.*, 1990; Caporaso *et al.*, 1992b; Chapter 3). Both mature APP holoprotein and the carboxyl-terminal APP fragment were enriched in the CCVs compared to the total cell homogenate (Figure 28). Immature APP holoprotein was not detected in CCVs (Figures 26 and 28) as might be expected, since CCVs are formed only at post-Golgi locations, distal to the site where APP maturation is believed to occur

Figure 27. Electron micrograph of clathrin-coated vesicles fractionated by gel-filtration chromatography. CCVs eluted in fraction 25 from an S-1000 column (see Figure 26) were negatively stained and viewed by electron microscopy. Both CCVs with membrane vesicles (*closed arrows*) and vesicle-free clathrin cages (*open arrows*) can be seen. Scale bar represents 100 nm.

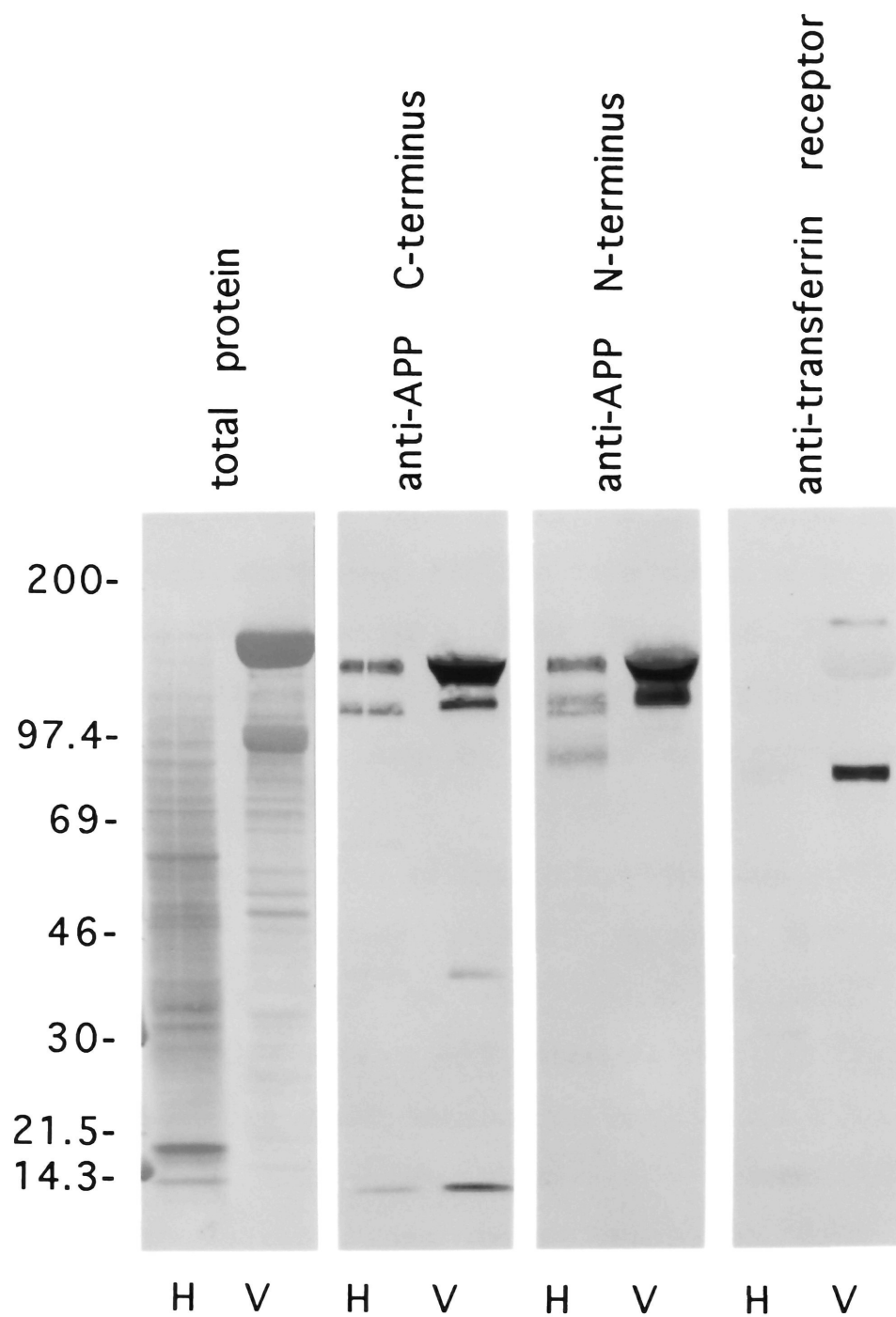


(Caporaso *et al.*, 1992a; Chapter 3). Immunoblotting with antibody 22C11 confirmed that mature APP holoprotein was enriched in CCVs. However, small amounts of proteins with M_r ~125,000 and ~110,000, corresponding to secreted APP_{751/770} (*i.e.*, protease nexin-II; see Chapter 4, Conclusions) and APP₆₉₅ (Caporaso *et al.*, 1992b; Chapter 3), were also detectable in CCVs. The much greater quantity of Tf-R in the CCVs compared to the total cell homogenate was consistent with enrichment of Tf-R in CCVs as previously reported (Turkewitz and Harrison, 1989).

Conclusions

In this section, it was shown that CCVs prepared from PC12 cells are enriched in both full-length mature APP and the carboxyl-terminal fragment generated by APP secretory cleavage, indicating that these proteins are targeted to the endosomal compartment. These data are consistent with the earlier findings in PC12 cells that degradation of mature full-length APP molecules and the carboxyl-terminal fragment can be inhibited by chloroquine, which implies that acidic organelles such as endosomes or lysosomes are involved in their metabolism (Caporaso *et al.*, 1992a; Chapter 3). In addition, other groups have found evidence suggesting that APP is present in lysosomes (Benowitz *et al.*, 1989), that APP metabolic processing occurs in endosomes or lysosomes (Cole *et al.*, 1989), and that generation of amyloidogenic APP fragments might occur in endosomes or lysosomes (Golde *et al.*, 1992). It was also recently demonstrated that APP is present in a subcellular fraction enriched in lysosomes (Haass *et al.*, 1992a) and that lysosomotropic agents can

Figure 28. Enrichment of APP in clathrin-coated vesicles. Total protein, APP immunoreactivity, and Tf-R immunoreactivity were compared in cell homogenates (*H*) and CCVs fractionated by density-equilibrium centrifugation (*V*). Equal amounts of protein (20 μ g/lane) were separated by 4-15% SDS-polyacrylamide gradient gels, transferred to nitrocellulose membranes, and either stained with amido black (*total protein*) or immunoblotted with antibodies against the carboxyl terminus of APP (369A), the amino terminus of APP (22C11), or rat Tf-R. The predominant APP species in cell homogenates are the immature and mature APP_{751/770} isoforms (M_r ~115,000 and ~140,000, respectively) as well as the carboxyl-terminal APP fragment resulting from secretory cleavage (M_r ~14,000-15,000). Immature APP₆₉₅ is barely visible (M_r ~105,000) in this film exposure, but mature APP₆₉₅ can be seen as a faintly staining band (M_r ~120,000) above immature APP_{751/770}. CCVs are enriched in mature APP isoforms and the carboxyl-terminal APP fragment, with mature APP_{751/770} being the major species. Due to the large amount of clathrin heavy chains present, the APP bands have been pushed slightly downward. Nonetheless, it can be seen that both of the full-length APP species in CCVs migrate more slowly than either immature APP species in cell homogenates (also seen in Figure 26). The M_r ~40,000 protein seen by immunoblotting with antibody 369A is a non-specific cross-reacting protein. The M_r ~97,000 protein seen with antibody 22C11 probably represents a truncated form of APP_{751/770}, as it is also recognized with an antibody against the KPI domain specific for APP_{751/770} (56.1). Approximate M_r ($\times 10^3$) values are indicated at left.



affect the production of intact B/A4 peptide that is secreted from cells (Shoji *et al.*, 1992). The present study provides direct evidence that APP utilizes a specific intracellular route that targets proteins to the endosomal/lysosomal system.

It was not possible, with the procedures used, to distinguish between the two known populations of CCVs; *i.e.*, those that transport proteins to early endosomes from the cell surface and those that transport proteins to late endosomes/prelysosomes from the TGN. Therefore, it was not possible to determine whether APP is targeted to the endosomal system from the plasma membrane or from the TGN. A plasma membrane origin for APP in CCVs seems more likely at present, though, since some APP has been shown to be present on the cell surface (Weidemann *et al.*, 1989; Haass *et al.*, 1992a; Sisodia, 1992) and since APP contains in its cytoplasmic domain an NPXY motif, suggesting that it may be targeted to clathrin-coated pits (Chen *et al.*, 1990).

The presence in CCVs of the carboxyl-terminal APP fragment produced in the secretory pathway suggests that secretory processing occurs prior to the arrival of APP at the endosomal/lysosomal system. APP secretory cleavage might occur within constitutive secretory vesicles *en route* to the cell surface or while resident at the plasma membrane. Alternatively, such cleavage might occur during transit from the TGN to late endosomes/prelysosomes. Although one cannot exclude secretory processing within the TGN, processing in the Golgi complex seems unlikely since secretory cleavage of APP is completely inhibited by treatment of PC12 cells with brefeldin A (Caporaso *et al.*, 1992a;

Chapter 3), a drug that prevents transport of proteins from the *trans*-Golgi to the TGN (Chege and Pfeffer, 1990). Finally, if secretory cleavage occurred within CCVs, one would expect to find an enrichment of amino-terminal APP fragments in CCVs. However, only a negligible amount of amino-terminal APP secretory products was detected in CCVs, and it is possible that these fragments actually represent secreted APP fragments that were endocytosed from the medium. While these results limit the number of cellular sites where secretory cleavage could occur, precise localization of the site of APP secretory processing awaits further study.

Chapter 6

Correlation Between the Subcellular Localization of APP and Its Biochemical Processing

Introduction

Current evidence suggests the existence of multiple processing pathways for APP. One pool of APP molecules is cleaved within the β /A4 region, with the APP ectodomain secreted into cerebrospinal fluid and into the medium of cultured cells (Weidemann *et al.*, 1989; Palmert *et al.*, 1989; Oltersdorf *et al.*, 1990). Since the proteolytic event that results in APP secretion occurs within the β /A4 domain of APP, it precludes a contribution of this population of molecules to amyloid deposits (Sisodia *et al.*, 1990; Esch *et al.*, 1990). The principal cellular site of APP secretory cleavage has not been determined, but recently it has been shown that at least some molecules may be cleaved at the cell surface (Sisodia, 1992). Although the kinetics of APP ectodomain secretion indicate that APP does not follow the standard regulated secretory pathway (Overly *et al.*, 1991), APP secretion can be stimulated either by direct activation of protein kinase C (PKC) with phorbol ester (Caporaso *et al.*, 1992b; Chapter 4; Gillespie *et al.*, 1992; S. Sinha, personal communication) or by application of first messengers that act through PKC (Nitsch *et al.*, 1992; Buxbaum *et al.*, 1992), suggesting a regulatory mechanism for this processing pathway. The mechanism by which PKC modulates secretion of the APP ectodomain has not been determined, although

PKC can phosphorylate APP *in vitro* (Gandy *et al.*, 1988; Suzuki *et al.*, 1992).

In most cell types that have been studied, the secretory pathway accounts for only a small fraction of total APP processing (Weidemann *et al.*, 1989; Haass *et al.*, 1991; Caporaso *et al.*, 1992a; Chapter 3; Knops *et al.*, 1992). In rat neuroendocrine PC12 cells, the majority of APP molecules are proteolytically degraded in a chloroquine-sensitive intracellular compartment, presumably endosomes and/or lysosomes (Caporaso *et al.*, 1992a; Chapter 3). It has also been shown that full-length APP and APP degradative fragments are present in a lysosome-enriched subcellular fraction (Haass *et al.*, 1992a), that potentially amyloidogenic APP fragments are probably processed in endosomes and lysosomes (Golde *et al.*, 1992; Knops *et al.*, 1992), and that APP immunoreactivity is found in neuronal structures identified as secondary lysosomes (Benowitz *et al.*, 1989). Furthermore, full-length APP and the carboxyl-terminal APP fragment resulting from secretory cleavage are enriched in clathrin-coated vesicles (CCVs), suggesting that these protein species are targeted to the endosomal system after endocytosis from the plasma membrane or directly from the *trans*-Golgi network (TGN) (Nordstedt *et al.*, 1993; Chapter 5). It was demonstrated recently that intact β /A4 peptide is released from cultured cells and is present in plasma and cerebrospinal fluid (Haass *et al.*, 1992b; Seubert *et al.*, 1992), and that production of secreted β /A4 might occur in the endosomal/lysosomal system (Shoji *et al.*, 1992), additionally stressing the importance of this compartment in APP metabolism.

In this chapter, the subcellular distribution of APP is examined in a variety of cell types in an attempt to further elucidate APP trafficking. Employing markers specific for individual cellular compartments and pharmacological agents known to affect organelle function or signal transduction, the localization of APP is correlated with the biochemical processing of the molecule.

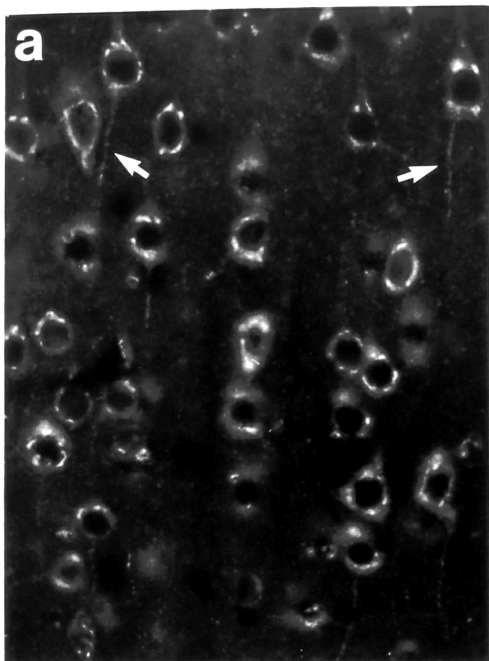
The contents of this section also appear in Caporaso *et al.* (1993).

Concentration of APP in the Golgi complex of neurons and in vesicular structures of dendrites and axons

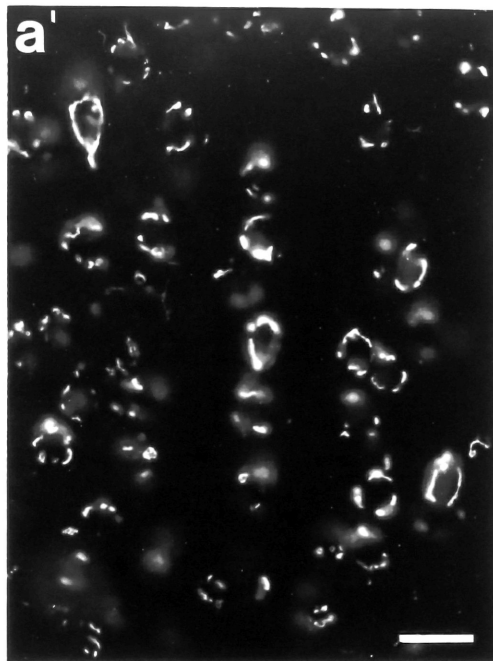
To examine the subcellular localization of APP, rat brains were fixed by perfusion with formaldehyde, cryosectioned, and 7- μ m slices were examined by immunofluorescence microscopy (De Camilli *et al.*, 1983a) with an antibody against the carboxyl terminus of APP (369A; Buxbaum *et al.*, 1990). In the brain regions studied--forebrain, hippocampus, brainstem, and cerebellum--most neurons were intensely APP immunoreactive (Figure 29). Some APP immunoreactivity was also detected in a variety of supporting cells, including glial cells. APP was observed predominantly in perinuclear structures in all cell types. In neurons, this intense immunoreactivity extended into the proximal portions of cell processes.

This distribution was suggestive of a concentration of APP in the region of the neuronal Golgi complex (De Camilli *et al.*, 1986). Brain sections were therefore double-labeled with an antibody directed against GIMP_t, an integral membrane protein localized to the *trans*-Golgi and TGN (Yuan *et al.*, 1987). Cellular areas of the greatest

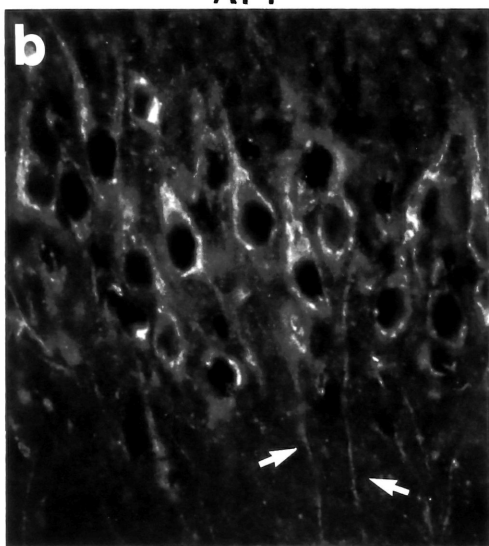
Figure 29. Comparison of the subcellular localization of APP and GIMP_t in rat brain by immunofluorescence microscopy. Rat brain sections were double-labeled for APP (antibody 369A) (*a, b, c, d*) and GIMP_t (*a', b', c', d'*). The following populations of cells are shown: (*a, a'*) cortical forebrain pyramidal cells, (*b, b'*) hippocampal pyramidal cells, (*c, c'*) brainstem neurons, and (*d, d'*) cerebellar Purkinje cells. APP immunoreactivity in the proximal segment of axons is indicated (*arrows*). Bars represent 20 μm .



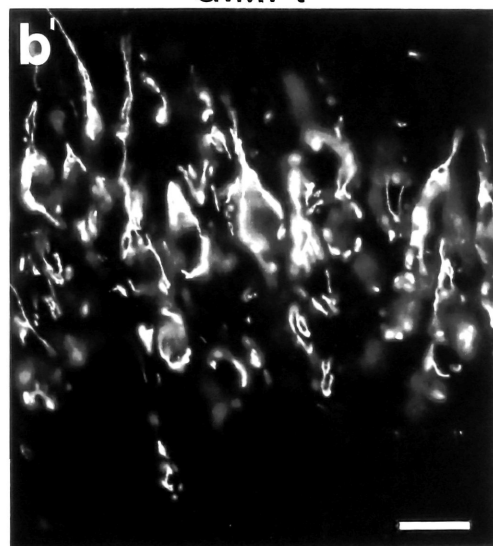
APP



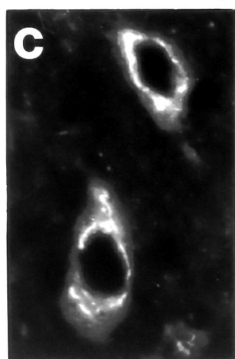
GIMPt



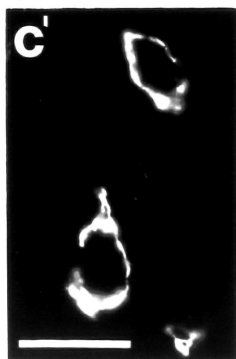
APP



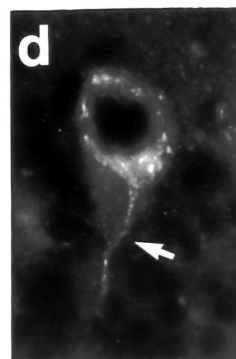
GIMPt



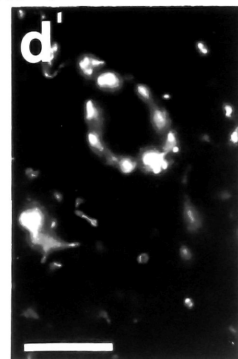
APP



GIMPt



APP



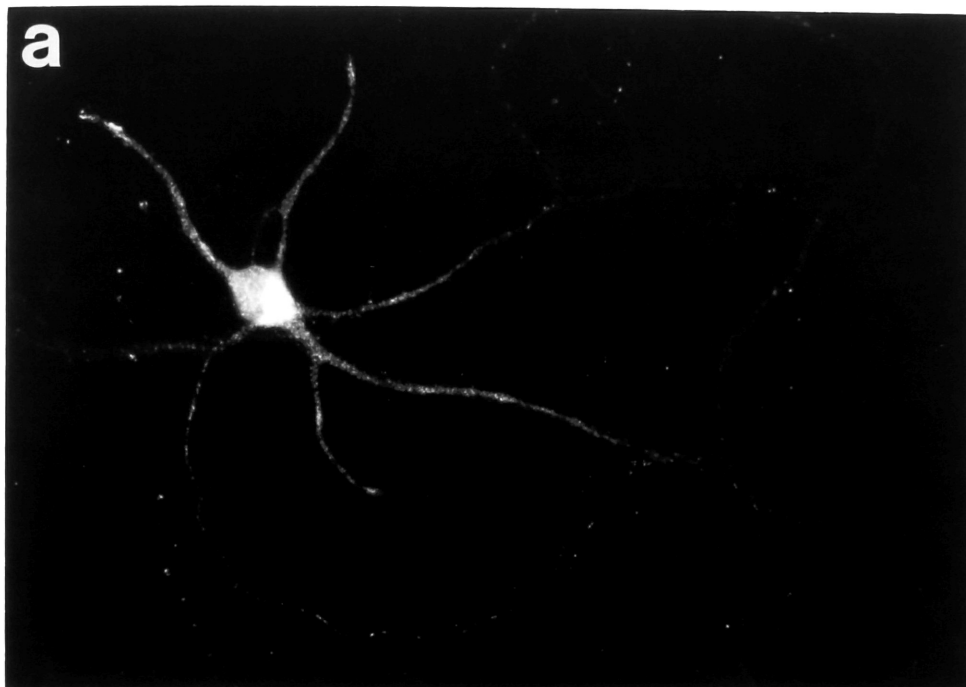
GIMPt

APP immunoreactivity coincided with GIMP_t-immunoreactive areas in perikarya and dendrites (Figure 29). In addition, high levels of APP staining were found in the proximal portion of axons, which do not contain elements of the Golgi complex (De Camilli *et al.*, 1986) and which were accordingly negative for GIMP_t immunoreactivity (Figure 29, *a*, *a'*, *b*, and *b'*). A high power view of a cerebellar Purkinje cell with its initial axonal segment is shown in Figure 29, *d* and *d'*. APP immunoreactivity extended along the axon into the granule cell layer (Figure 29, *d*). This staining became weaker with increasing distance from the perikaryon. Diffuse punctate APP immunofluorescence was present throughout the neuropil (compare the background immunofluorescence of *a*, *b*, *c*, and *d* with that of *a'*, *b'*, *c'*, and *d'*), but no accumulation of APP was seen at synapses.

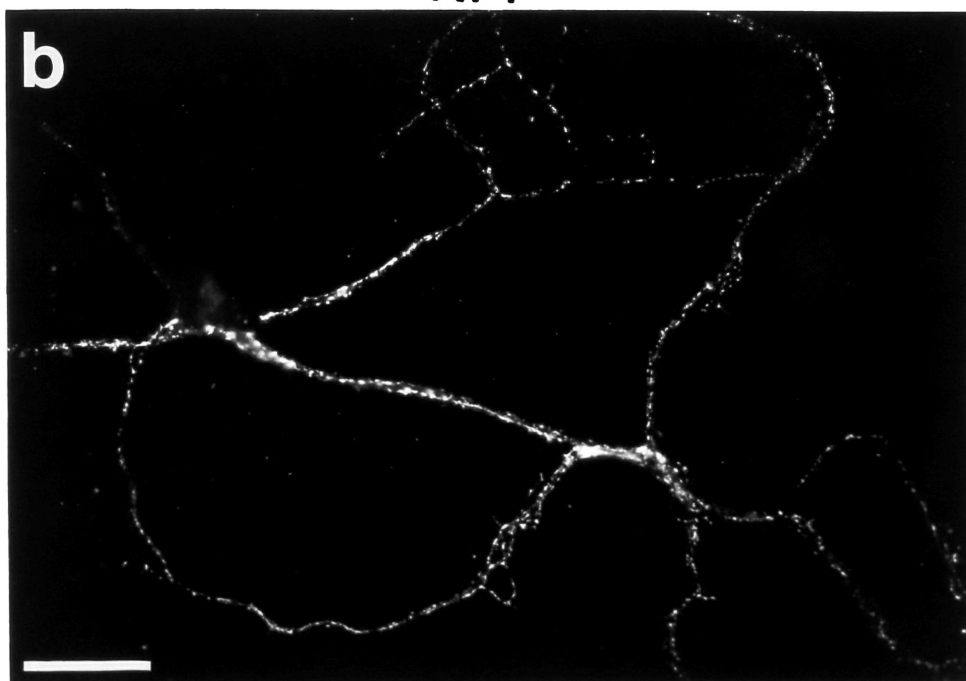
A predominant localization of APP in the region of the Golgi complex was also observed in neurons in culture (Banker and Cowan, 1977; Bartlett and Banker, 1984) (Figure 30, *a*). In addition, in these cells a moderate to intense APP immunoreactivity was present as fine puncta in neuronal processes. APP was not concentrated at synaptic vesicles, however, as indicated by double-labeling for the synaptic vesicle protein SV2 (Buckley and Kelly, 1985) (Figure 30, *b*).

To confirm the Golgi localization of APP and to examine the nature of the APP immunoreactivity seen in neuronal processes, fragments of brain tissue were obtained by coarse homogenization, embedded in agarose, immunogold-labeled for APP, and finally epon-embedded (De Camilli *et al.*, 1983b; Takei *et al.*, 1992). In fragments of the Golgi complex, the presence of gold particles on cisternae was visible (Figure 31, *a*). This labeling of the Golgi

Figure 30. Localization of APP and SV2 in primary cultures of rat hippocampal neurons by immunofluorescence microscopy. Hippocampal neurons were grown in culture for 4 days before fixation and double-labeled for APP (antibody 369A) (*a*) and SV2 (*b*). Bar represents 20 μm .



APP



SV2

complex was not seen in control preparations reacted with pre-immune serum.

In microscopic fields containing fragments of cell processes and synapses, APP immunoreactivity was found to be associated with medium-sized vesicles, many of which were characterized by outer and inner membranes, the latter appearing to arise by the invagination of the outer membrane (Figure 31, *b-f*). Gold particles were found at the cytoplasmic face of the outer membrane of these structures. The vesicles decorated with gold particles were seen both in myelinated (Figure 31, *b* and *c*) and in unmyelinated (Figure 31, *d*) axons as well as in pre- and post-synaptic compartments (Figure 31, *e* and *f*). No other dendritic or axonal structures were labeled, nor were the majority of synaptic vesicles (Figure 31, *e* and *f*).

Golgi localization of APP in cultured non-neuronal cells

Since it would be informative to determine the effects of experimental manipulations on the subcellular distribution of APP, several mammalian cell lines were examined to select a cell type appropriate for immunofluorescence microscopy of APP. Mouse insulinoma (β TC3), rat insulinoma (RINm5F), rat pheochromocytoma (PC12), African green monkey kidney (COS), and Chinese hamster ovary (CHO) cells all exhibited a predominant concentration of APP at a juxtannuclear location, with fine punctate staining seen in the cytoplasm (Figure 32). The juxtannuclear staining coincided with the localization of the Golgi complex and primarily with that of the TGN (see below). Another carboxyl-terminal APP antibody, C7 (Podlisy *et al.*, 1991), presented an identical pattern of APP immunoreactivity

Figure 31. Localization of APP in rat brain tissue fragments by immunoelectron microscopy. Rat brain tissue fragments from forebrain (*a, b, d*) or from cerebellum plus brain stem (*c, e, f*) were embedded in agarose and probed with antibody 369A and colloidal gold-conjugated protein A prior to plastic embedding. APP immunoreactivity, as revealed by gold particle accumulation, is visible on Golgi membranes (*small arrows*) (*a*) and on medium-sized vesicles (*large arrows; inset of b*) in cell processes (*b, c, d*), including myelinated (*b, c*) axons, and in pre- (*e*) and post-synaptic compartments (*f*). Some of these vesicles contain an internal membrane that appears to originate by an invagination of the outer membrane. A mitochondrion is indicated (*M*). Bars represent 200 nm.

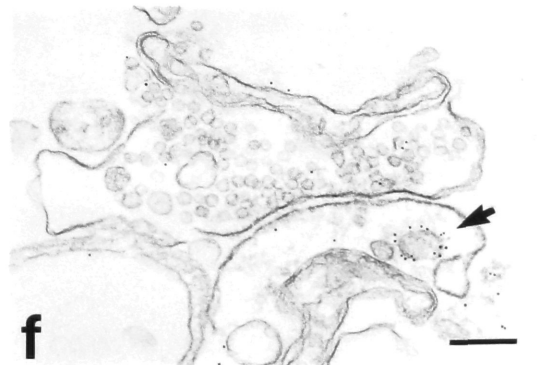
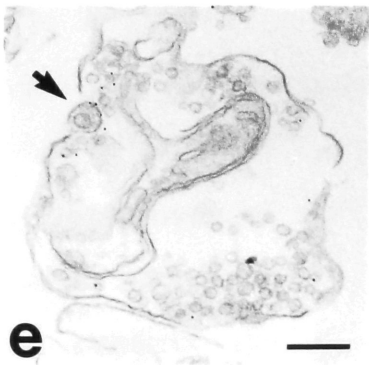
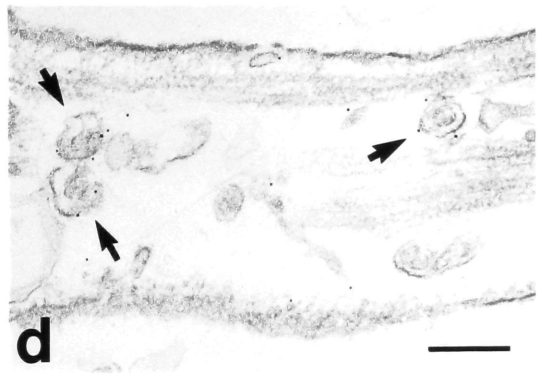
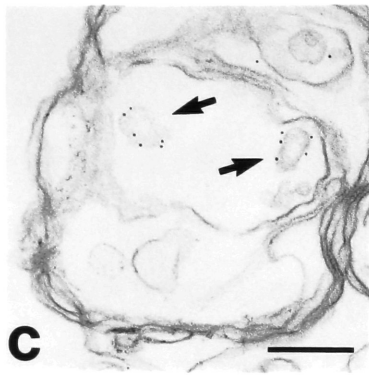
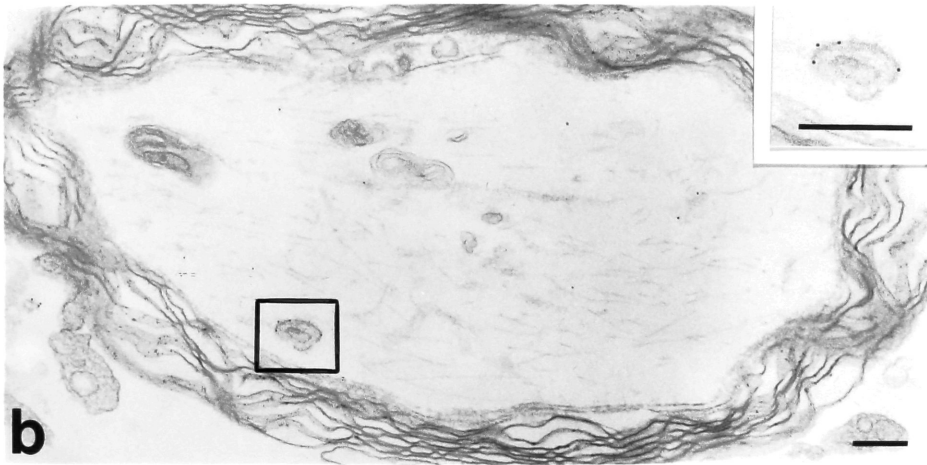
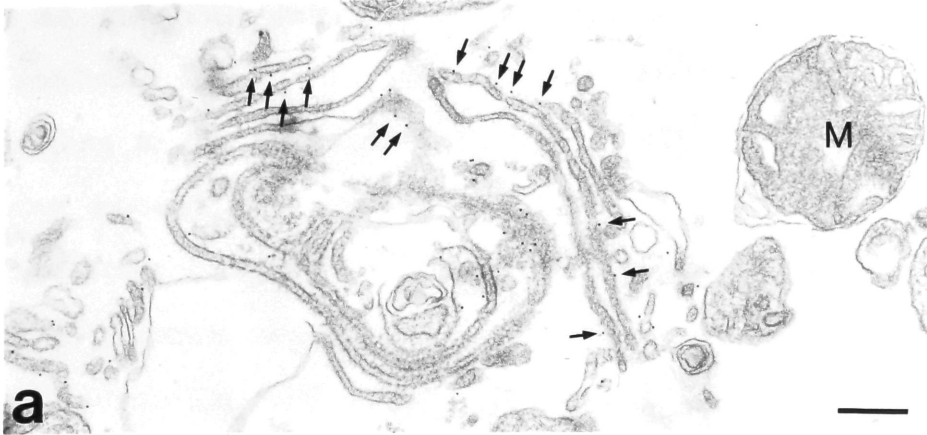
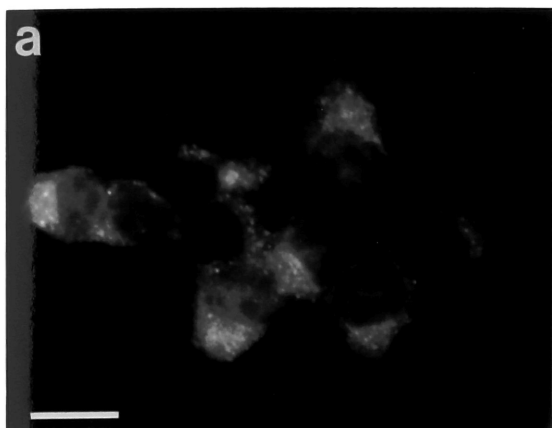


(Figure 32, *f*). This pattern was not seen with preimmune serum or when antibody 369A was preincubated with a synthetic peptide corresponding to the cytoplasmic domain of APP (APP⁶⁴⁵⁻⁶⁹⁴; APP₆₉₅ numbering system) (not shown).

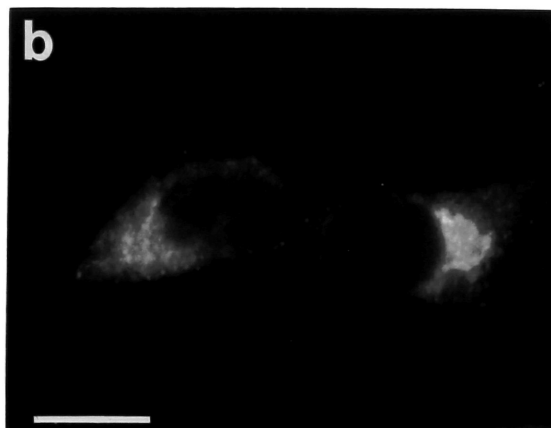
On immunoblots of these cell types (Figure 33), antibody 369A recognized proteins corresponding in apparent molecular mass to previously identified APP species (Weidemann *et al.*, 1989; Buxbaum *et al.*, 1990; Caporaso *et al.*, 1992b; Chapter 3). There were differences between cell types, though, in the relative intensities of specific APP bands. For example, PC12 cells contained abundant amounts of mature (completely glycosylated) full-length APP (Caporaso *et al.*, 1992b; Chapter 3), whereas both CHO and COS cells contained mostly APP species that co-migrated with the protein bands corresponding to immature full-length APP in PC12 cells. Much lower levels of mature full-length APP were present in these cells. CHO and COS cells were also found to produce almost exclusively the 751/770-amino acid isoforms of APP, as indicated by an antibody specific for these species (56.1) (not shown). CHO and COS cells also contained relatively high levels of an approximately 14-kDa APP immunoreactive protein that co-migrated with an immunoreactive band in PC12 cells, which was previously identified (Caporaso *et al.*, 1992a; Chapter 3) as the carboxyl-terminal fragment resulting from APP secretory cleavage (Sisodia *et al.*, 1990; Esch *et al.*, 1990). Because of the large size of CHO and COS cells, and their relative abundance of APP, these cells were selected for further microscopic study.

To confirm the Golgi localization of APP, several well-

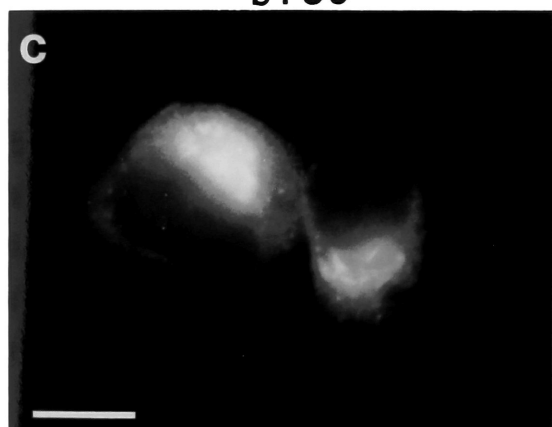
Figure 32. Immunofluorescence microscopy of various mammalian cell lines showing the juxtannuclear localization of APP. β TC3 (*a*), RINm5F (*b*), PC12 (*c*), and COS (*d*) cells were labeled with antibody 369A, and CHO cells were labeled with antibodies 369A (*e*) or C7 (*f*). Bars represent 10 μ m.



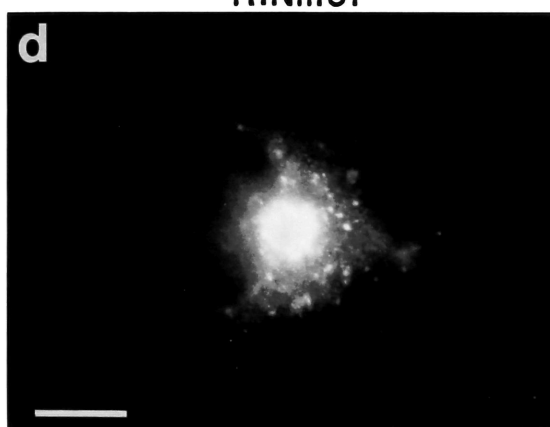
BTC3



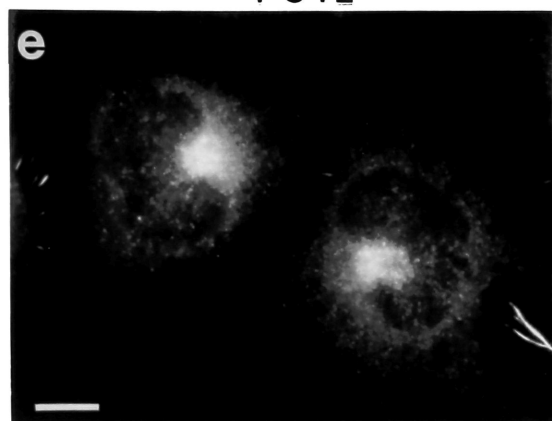
RINm5F



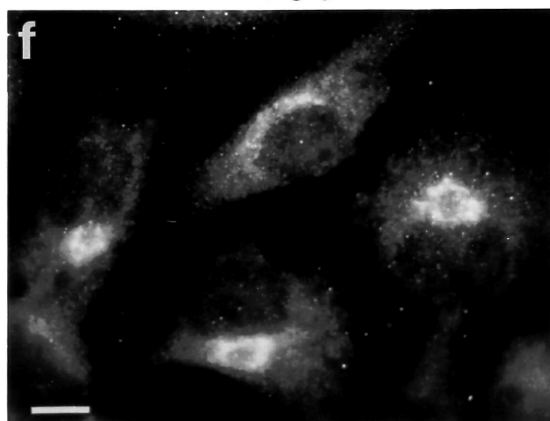
PC12



COS



CHO (Ab 369A)



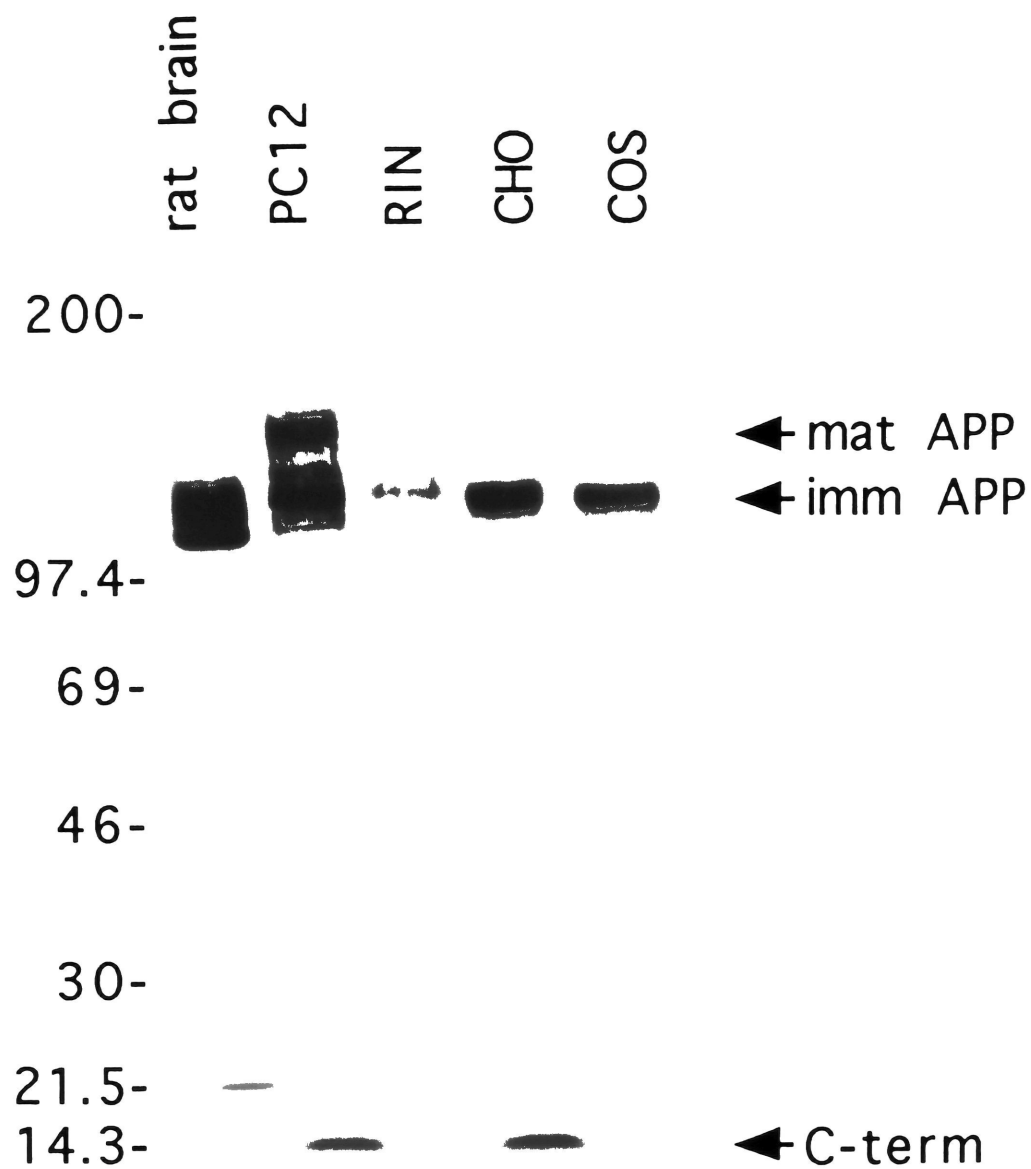
CHO (Ab C7)

characterized markers of the Golgi complex were used (the antibody recognizing GIMP_t did not react with CHO or COS cells). In CHO cells, APP was found to be concentrated in the region of the cell that stained most intensely for wheat germ agglutinin, a lectin which binds with high affinity, although not selectively, to the Golgi complex (Virtanen *et al.*, 1980; Tartakoff and Vassalli, 1983) (Figure 34, *a* and *a'*). The most intense APP immunoreactivity closely coincided with the distribution of lentil (*Lens culinaris*) lectin, which specifically labels glycoproteins of the Golgi complex (Ridgway *et al.*, 1992) (Fig. 34, *b* and *b'*), as shown by its co-localization with the Golgi-specific enzyme mannosidase II (Novikoff *et al.*, 1983; Moremen and Touster, 1985) (Fig. 34, *c* and *c'*). Similar results were obtained in COS cells (not shown).

Brefeldin A-induced redistribution of APP from a Golgi to an ER localization

To examine further the Golgi localization of APP, brefeldin A (BFA)--a fungal metabolite that induces disappearance of the Golgi complex and a relocation of its components into pre- and post-Golgi compartments (Pelham, 1991; Klausner *et al.*, 1992)--was used. Treatment of cells with BFA results in a functional and spatial dissection of the *trans*-Golgi from the TGN (Chege and Pfeffer, 1990; Reaves and Banting, 1992). Specifically, BFA causes a resorption of *cis*-, middle-, and *trans*-Golgi proteins and membranes to the endoplasmic reticulum (ER) (Lippincott-Schwartz *et al.*, 1989; Doms *et al.*, 1989). At the same time, BFA has also been shown to produce fusion of the TGN and early endosomes into a tubular network (Wood

Figure 33. Immunoblot analysis of APP in rat brain and mammalian cell lines. Proteins (50 μ g) from a rat cerebellar homogenate and from cell lysates of PC12, RINm5F, CHO, and COS cells were separated on a 4-15% continuous gradient SDS-polyacrylamide gel, then transferred to nitrocellulose membrane and probed with antibody 369A. The identities of immature and mature full-length APP and the carboxyl-terminal APP fragment resulting from secretory processing are indicated for the cell lines. Relative molecular masses (kDa) are indicated at left.

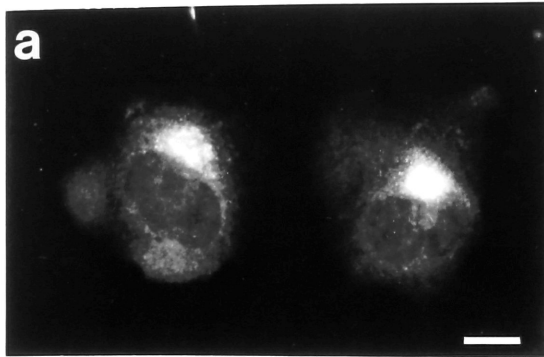


et al., 1991; Lippincott-Schwartz *et al.*, 1991).

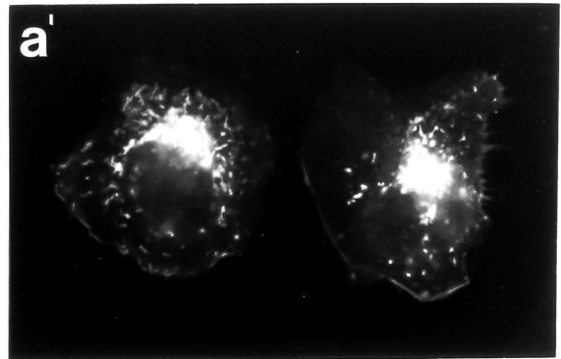
It was previously demonstrated in PC12 cells that BFA interferes with normal post-translational modification of APP and completely abolishes secretion and proteolytic turnover of APP (Caporaso *et al.*, 1992a; Chapter 3). Similar results were obtained in CHO cells treated with BFA and analyzed by immunoblotting (Figure 35). In untreated cells, most detectable APP consisted of the immature full-length molecule, with mature full-length APP and the carboxyl-terminal APP fragment representing minor species. After 30 min of BFA treatment, the protein band corresponding to immature APP was slightly shifted to a higher molecular mass; by 2 h of BFA treatment, APP immunoreactivity comprised a broad band spanning the positions of immature and mature APP (Figure 35). At the peak of BFA treatment, the intensity of the full-length APP band was greater than that in control cells, suggesting an overall accumulation of APP inside the cells. In addition, the carboxyl-terminal APP fragment was scarcely visible, indicating that secretory cleavage had been inhibited. The effects of BFA on APP metabolism were reversible; two hours after removal of BFA, all APP species had returned to their pre-treatment states (Figure 35).

The effects of BFA on the subcellular localization of APP was next examined. Assuming that APP is not a resident Golgi protein (see "Conclusions"), there are two plausible explanations for the intense APP immunoreactivity seen in the region of the Golgi complex. First, the abundance of APP in the Golgi complex might reflect its concentration in the distal Golgi as the protein travels through the central vacuolar system and is sorted in the TGN

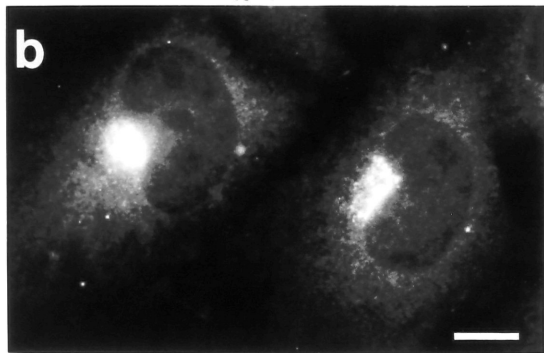
Figure 34. Comparison of the distributions of APP and several Golgi complex markers by fluorescence microscopy in CHO cells. Cells were double-labeled for APP (antibody 369A) (*a*) and wheat germ agglutinin (*a'*), for APP (*b*) and lentil lectin (*b'*), or for mannosidase II (*c*) and lentil lectin (*c'*).



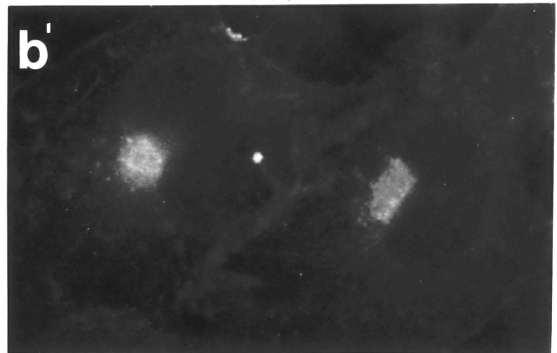
APP



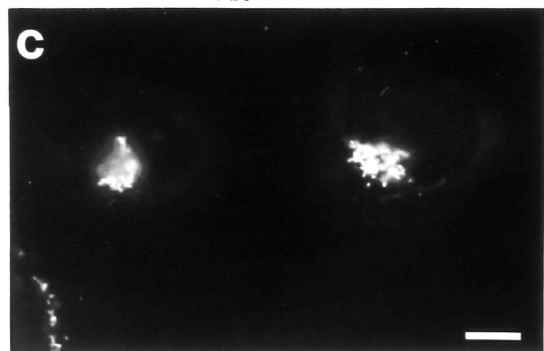
WGA



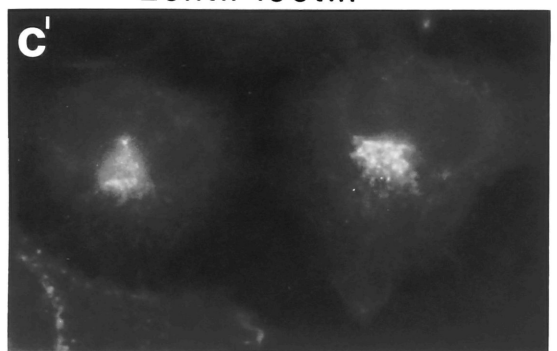
APP



Lentil lectin



Mann II

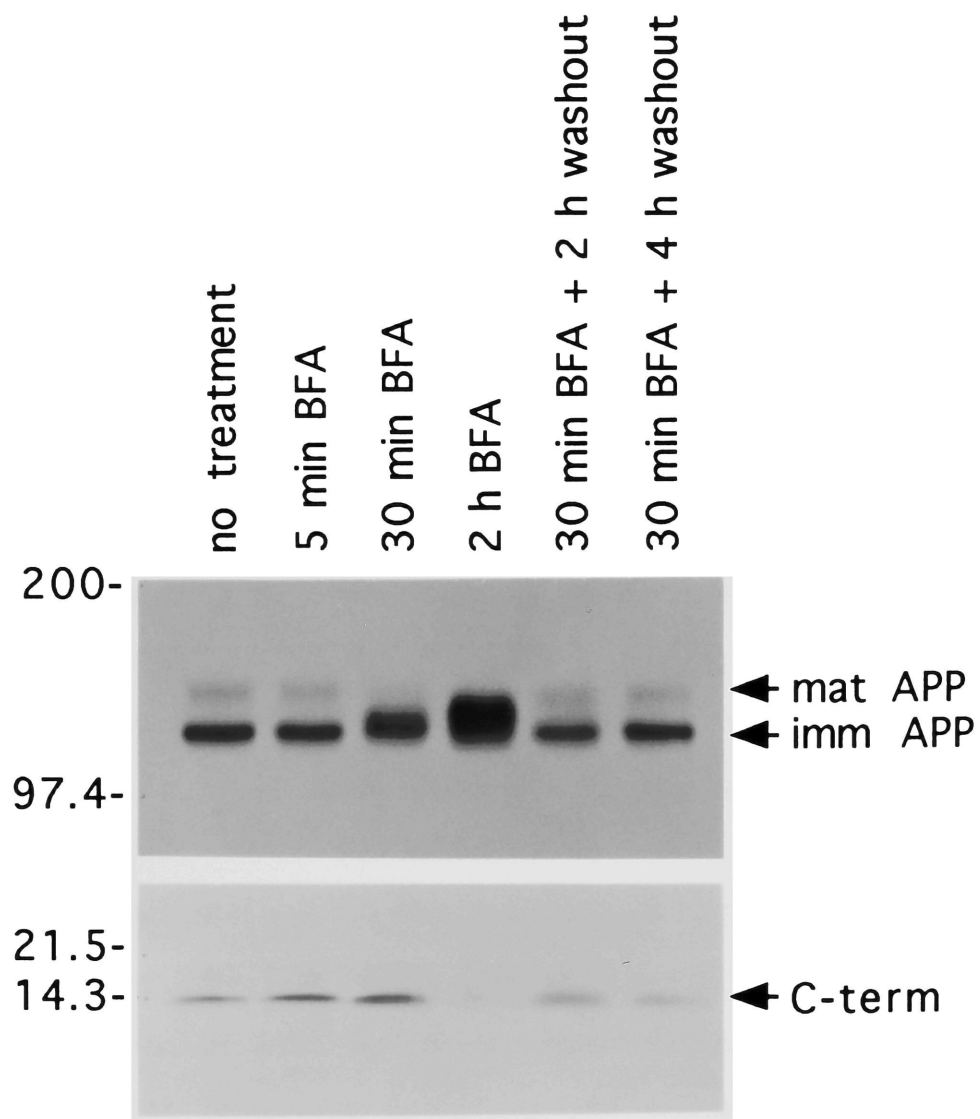


Lentil lectin

(Griffiths and Simons, 1986). In this case, upon BFA treatment one might expect a change in the distribution of APP immunoreactivity, resulting both from the rapid dispersal and clearance of APP molecules in the TGN to their post-Golgi destinations (*e.g.*, constitutive secretory vesicles), and from the accumulation of newly-synthesized APP in the ER-Golgi hybrid compartment (Lippincott-Schwartz *et al.*, 1989; Doms *et al.*, 1989; Chege and Pfeffer, 1990). Such a result would be consistent with the accumulation of full-length APP seen with the immunoblots of BFA-treated cells (Figure 35). Alternatively, the pattern of APP staining might represent a population of molecules in the TGN that is involved in recycling amongst the TGN, early endosomes, and the plasma membrane. In this case, APP should be present in the tubular reticulum resulting from the BFA-induced fusion of these compartments (Wood *et al.*, 1991; Lippincott-Schwartz *et al.*, 1991).

CHO cells were double-labeled for APP and transferrin receptor (Tf-R), a protein known to recycle between the TGN and endosomes (Stoorvogel *et al.*, 1988; Cameron *et al.*, 1991), and which can be used as a marker of the BFA-induced reticulum formed from these two compartments (Lippincott-Schwartz *et al.*, 1991). In untreated cells, both APP and Tf-R staining were most concentrated in the region of the Golgi complex, but intense punctate Tf-R immunoreactivity extended from the centrosomal region to the cell periphery (Figure 36, *a* and *a'*). Upon treatment with 10 μ g/ml BFA for 30 min, a network of tubules emanating from the Golgi region was stained for Tf-R (Figure 36, *b'*) (Lippincott-Schwartz *et al.*, 1991). In contrast, BFA treatment resulted in a more diffuse APP staining (Figure 36, *b*).

Figure 35. Immunoblot analysis of CHO cells treated with BFA. CHO cells were untreated or incubated with 10 μ g/ml BFA for 5 min, 30 min, or 2 h, or for 30 min followed by incubation in the absence of BFA for 2 or 4 h, then lysed with 1% SDS. Proteins (50 μ g) were separated on a 4-15% SDS-polyacrylamide gel, transferred to nitrocellulose, and probed with antibody 369A. The major APP immunoreactive protein band of approximately 128 kDa seen at 0 min represents immature full-length APP. Mature full-length APP appears as a faint band at approximately 145 kDa. The protein band of approximately 14 kDa represents the carboxyl-terminal fragment resulting from APP secretory cleavage. Two-hour BFA treatment results in abnormal APP post-translational processing and inhibits APP secretory processing as demonstrated by the virtual absence of the 14-kDa fragment. Relative molecular masses (kDa) are indicated at left.



There was no apparent co-localization of APP with the tubular network identified by Tf-R. After 4 h in the presence of BFA, cells exhibited a fine meshwork of APP immunostaining throughout the cytoplasm that resembled the structure of the ER (Figure 36, *c* and *d*) (see below).

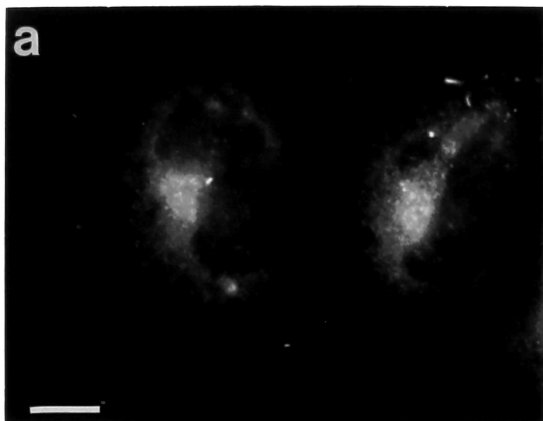
Similar results were obtained in COS cells double-labeled for APP and Tf-R before and after BFA treatment (Figure 37, *a*, *a'*, *b*, and *b'*). In these cells, the tubular network positive for Tf-R (Figure 37, *b'*) was not as well defined as that seen in CHO cells (Figure 36, *b'*).

Since the cellular distribution of APP after BFA treatment was suggestive of an ER localization, COS cells were double-labeled for APP and BiP, an ER-resident protein (Bole *et al.*, 1986). The distribution of BiP was the same in both untreated and BFA-treated cells, and consisted of a fine network of staining extending to the cell periphery (Figure 37, *c'* and *d'*). When cells were treated with BFA, the immunolocalization of APP was very similar to that of BiP (Figure 37, *d* and *d'*), although some difference in fine details was observed.

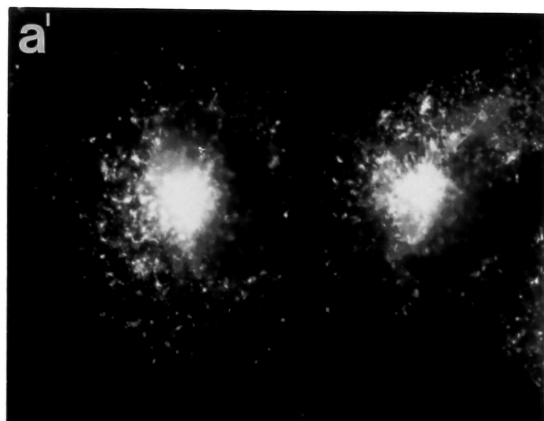
Lack of an obvious redistribution of APP immunoreactivity upon phorbol ester-stimulated APP secretion

Activation of PKC by phorbol ester has been shown previously to stimulate the proteolytic processing and secretion of APP in PC12, human embryonic kidney (293), and human mononuclear leukemia (K562) cells (Buxbaum *et al.*, 1990; Caporaso *et al.*, 1992b; Chapter 4; Gillespie *et al.*, 1992; S. Sinha, personal communication). To determine whether phorbol ester would stimulate APP secretion from CHO cells, cells were incubated with PDBu and both the medium

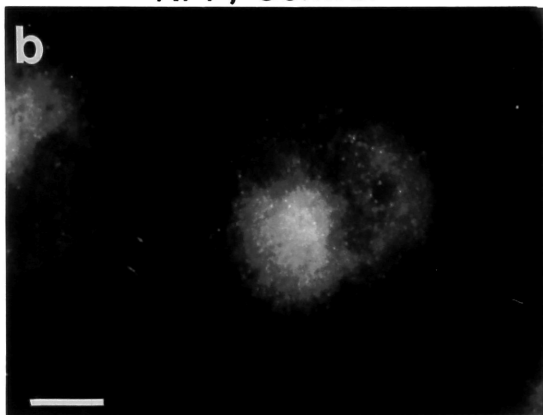
Figure 36. Comparison of the distributions of APP and Tf-R by immunofluorescence microscopy in control CHO cells and in CHO cells treated with BFA. Cells were untreated (*a, a'*) or treated with 10 $\mu\text{g/ml}$ BFA for 30 min (*b, b'*) or 4 h (*c, d*), fixed, and double-labeled for APP (antibody 369A) (*a, b*) and Tf-R (*a', b'*) or labeled for APP alone (*c, d*). Bars represent 10 μm .



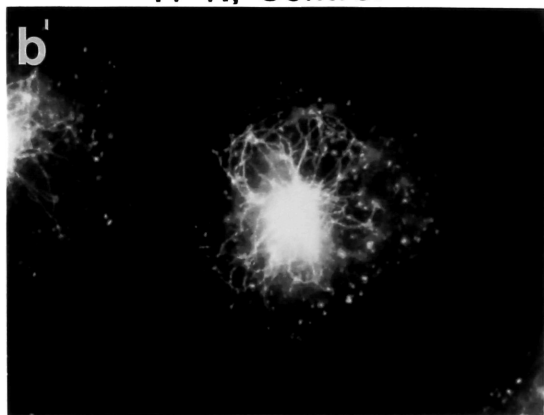
APP, Control



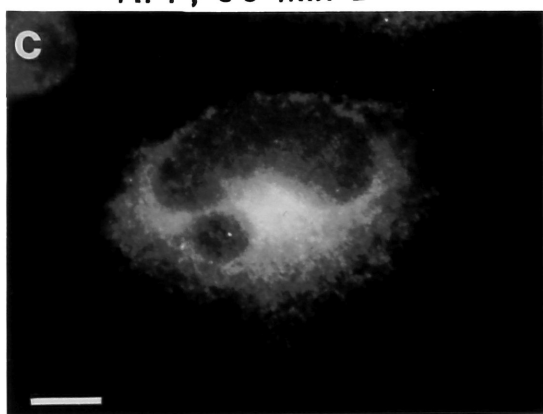
Tf-R, Control



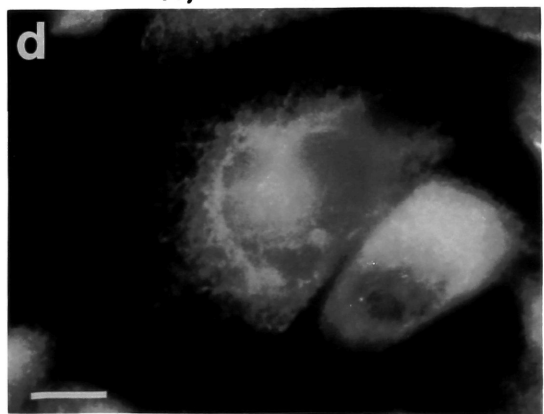
APP, 30 min BFA



Tf-R, 30 min BFA



APP, 4 h BFA



APP, 4 h BFA

and cell lysates were analyzed by immunoblotting with an antibody directed against the amino terminus of APP (22C11; Weidemann *et al.*, 1989) (Figure 38). PDBu produced a several-fold increase in APP secretion that was apparent as early as 15 min following initiation of treatment and that continued for at least 2 h (Figure 38, *bottom*).

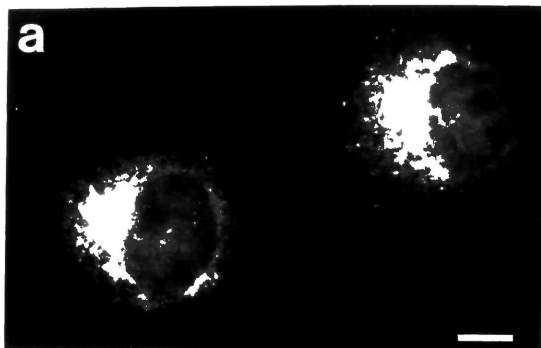
Concomitant with the increase in secretion, there was a decrease in levels of mature full-length APP observed between 15 min and 1 h of PDBu treatment (Figure 38, *middle*). (The increase in levels of mature APP seen at 2 h might reflect the PKC-mediated up-regulation of APP gene expression; Goldgaber *et al.*, 1989). This suggests that the secreted form of APP from CHO cells arises by proteolytic cleavage of mature full-length APP. Consistent with this model, PDBu had no detectable effects on the steady-state level of immature full-length APP (Figure 38, *top*)

Despite the dramatic effects that phorbol ester produced on APP secretion, no changes in the immunofluorescent pattern produced by multiple antibodies directed against the carboxyl terminus of APP were observed in CHO cells after PDBu treatment (not shown).

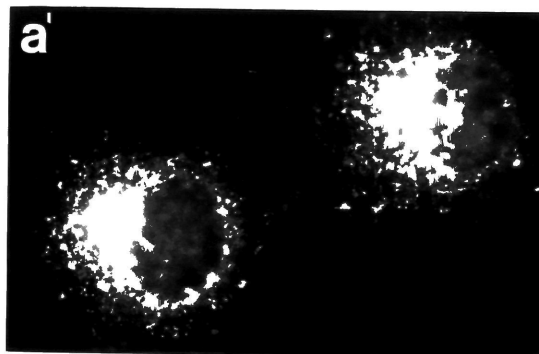
Accumulation of APP in the lysosomes of chloroquine-treated cells

There is considerable evidence for a role of lysosomes in the processing of APP. In PC12 cells, the majority of mature full length APP molecules are proteolytically degraded in a chloroquine-sensitive cellular compartment that is distinct from the site where APP secretory cleavage occurs (Caporaso *et al.*, 1992a; Chapter 3). It

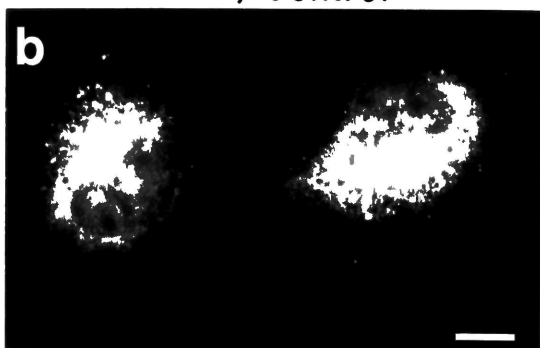
Figure 37. Comparison of the distributions of APP, Tf-R, and BiP by immunofluorescence microscopy in control COS cells and in COS cells treated with BFA. Cells were untreated (*a, a', c, c'*) or treated with 10 $\mu\text{g/ml}$ BFA for 30 min (*b, b', d, d'*), washed, fixed, and double-labeled for APP (antibody 369A) (*a, b, c, d*) and Tf-R (*a', b'*) or BiP (*c', d'*). Bars represent 10 μm .



APP, Control



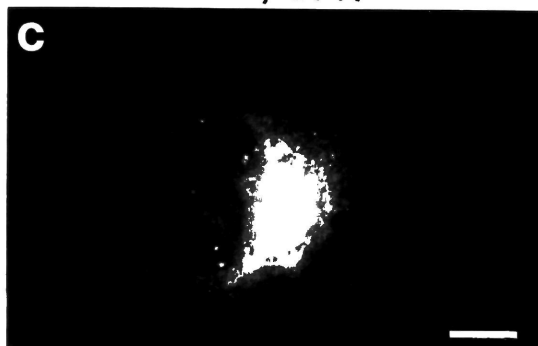
Tf-R, Control



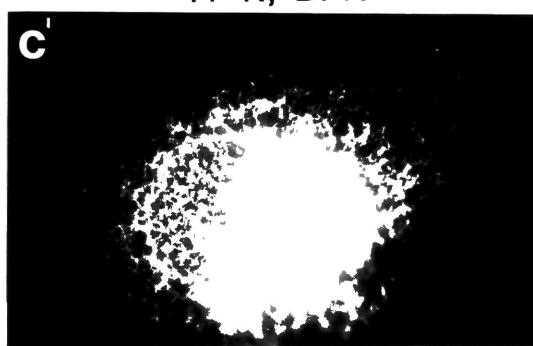
APP, BFA



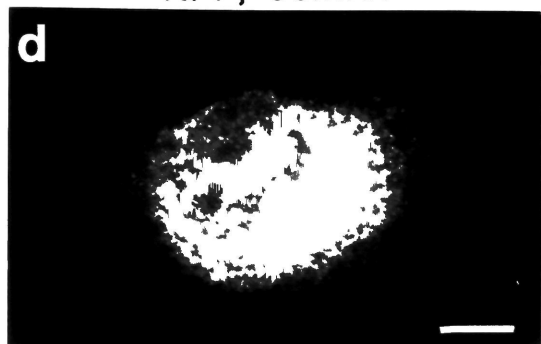
Tf-R, BFA



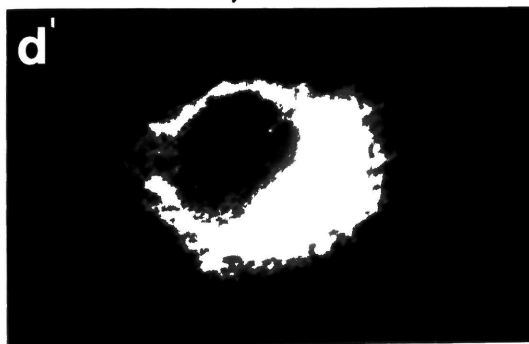
APP, Control



BiP, Control



APP, BFA



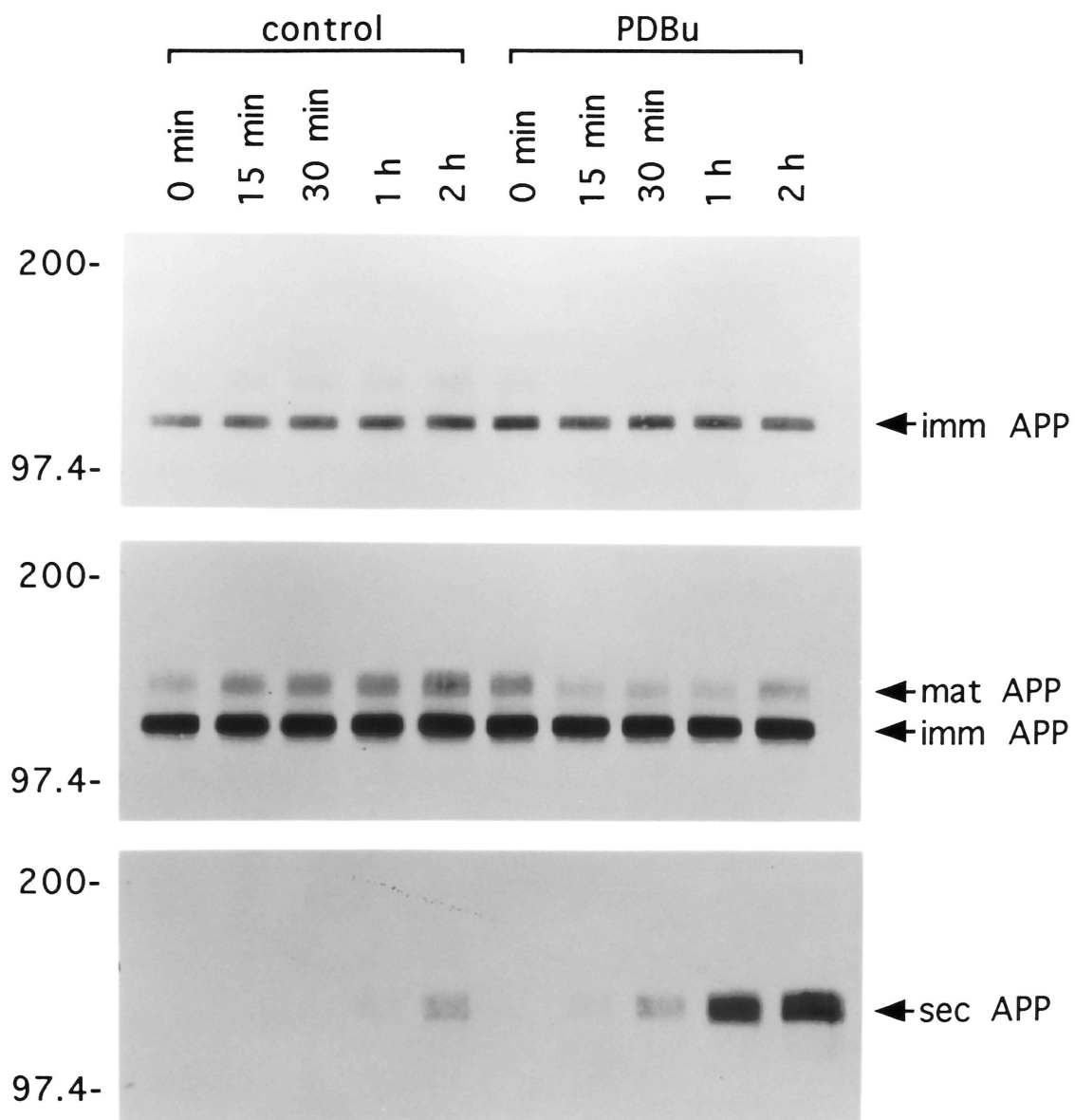
BiP, BFA

has also been shown that APP holomolecules and carboxyl-terminal fragments can be recovered from a subcellular fraction enriched in lysosomes (Haass *et al.*, 1992a). In addition, CCVs purified from PC12 cells are enriched in mature full-length APP and the carboxyl-terminal APP fragment resulting from secretory cleavage, indicating that these proteins are targeted to the endosomal system and, presumably, to lysosomes as their final destination (Nordstedt *et al.*, 1993).

To establish a role for lysosomes in APP metabolism in CHO cells, cells were double-labeled for APP and lgp120, an integral membrane protein of lysosomes (Lewis *et al.*, 1985). In untreated cells, lgp120 immunostaining was punctate and dispersed throughout the cytoplasm, but was most prevalent at a juxtannuclear location that coincided with the region enriched in APP (Figure 39, *a'*). However, within this region the lgp120-positive puncta were clearly different from the more diffuse APP immunoreactivity. The lgp120-positive puncta have been shown to represent individual lysosomes (Lewis *et al.*, 1985). There was little or no co-localization of APP immunoreactivity and the punctate lgp120 immunoreactivity in untreated cells (Figure 39, *a* and *a'*).

Following a 4-h incubation in the presence of the weakly-basic lysosomotropic agent chloroquine (de Duve *et al.*, 1974), lgp120 immunoreactivity was no longer dispersed throughout the cytoplasm, but consisted of scattered clumps of punctate staining (Figure 39, *b'*). This is consistent with the lysosomal swelling seen in cells treated with weak bases (Ohkuma and Poole, 1981). APP immunostaining in the Golgi region was still present (Figure 39, *b*). However, there was

Figure 38. Immunoblot analysis of CHO cells treated with phorbol ester. Cells were incubated with medium alone or with medium containing 1 μ M PDBu for the indicated times. Proteins from cell lysates (50 μ g) or culture medium were separated on 7.5% SDS-polyacrylamide gels, transferred to nitrocellulose, and probed with antibody 22C11. Full-length immature and mature APP appear in cell lysates as 128- and 145-kDa proteins, respectively (*top* and *middle*), and secreted APP appears in conditioned medium as a 134-kDa protein (*bottom*). The *top* and *middle* panels represent different length exposures of the same immunoblot to optimize signal clarity for immature and mature APP, respectively. Relative molecular masses (kDa) are indicated at left.



striking co-localization of APP and lgp120 staining. Immunoblot analysis revealed an accumulation of mature APP and the 14-kDa carboxyl-terminal APP fragment, but no change in immature APP levels, in cells treated with chloroquine (Figure 40).

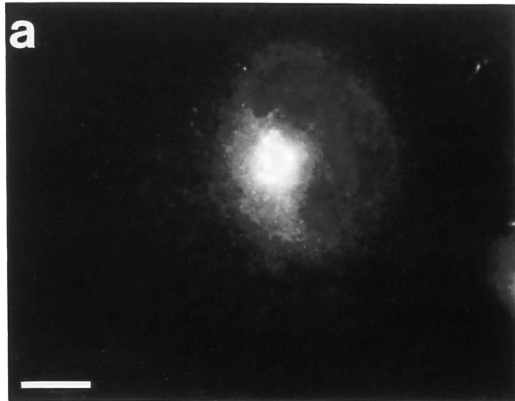
Conclusions

Much has been learned about the cell biology of APP since the cloning of its gene and elucidation of its structure (Kang *et al.*, 1987). Nevertheless, investigative efforts have not yet yielded a comprehensive scheme for the cellular trafficking and metabolic pathways of this molecule. In this chapter, the cellular trafficking of APP was investigated by examining the relationship between the subcellular localization of APP and its biochemical processing.

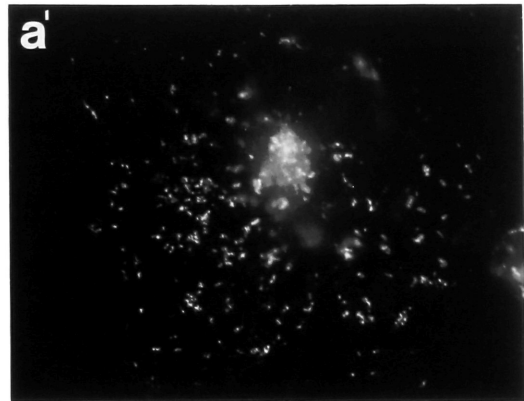
A striking feature of the distribution of APP within the cell is its high concentration in the region of the Golgi complex. In rat brain, in primary cultures of rat hippocampal neurons, and in cultures of several non-neuronal mammalian cell lines, APP immunoreactivity was localized to the region of the Golgi complex as demonstrated by several Golgi markers. A concentration of APP in the Golgi complex is in agreement with the perinuclear distribution for APP reported previously (Card *et al.*, 1988; Martin *et al.*, 1991; Schubert *et al.*, 1991; Haass *et al.*, 1992a). In those earlier studies, however, the precise localization of APP in the perinuclear area was not investigated.

The present data are consistent with a model in which APP is concentrated in the *trans*-Golgi and TGN during its transit through the central vacuolar system (Palade, 1975). Unfortunately, the

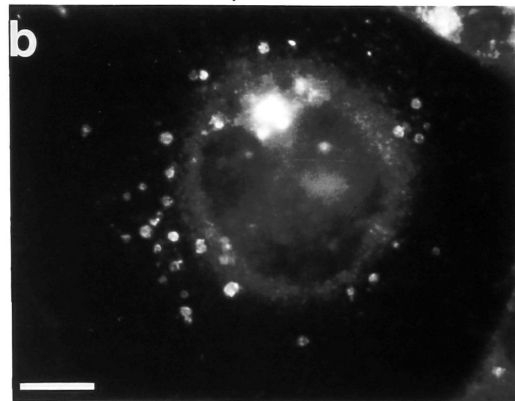
Figure 39. Comparison of the distributions of APP and lgp120 by immunofluorescence microscopy in control CHO cells and in CHO cells treated with chloroquine. Cells were untreated (*a, a'*) or treated with 50 μ M chloroquine for 4 h (*b, b'*), fixed, and double-labeled for APP (antibody 369A) (*a, b*) and lgp120 (*a', b'*). Bars represent 10 μ m.



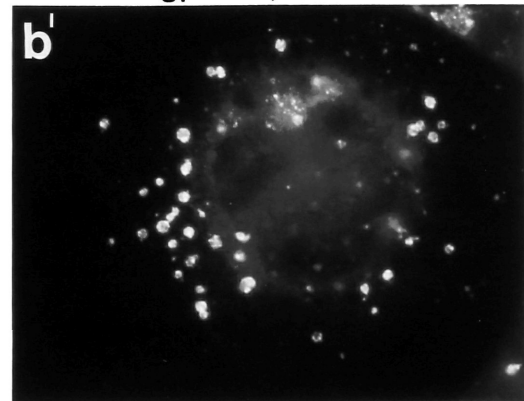
APP, Control



Lgp120, Control



APP, Chloroquine



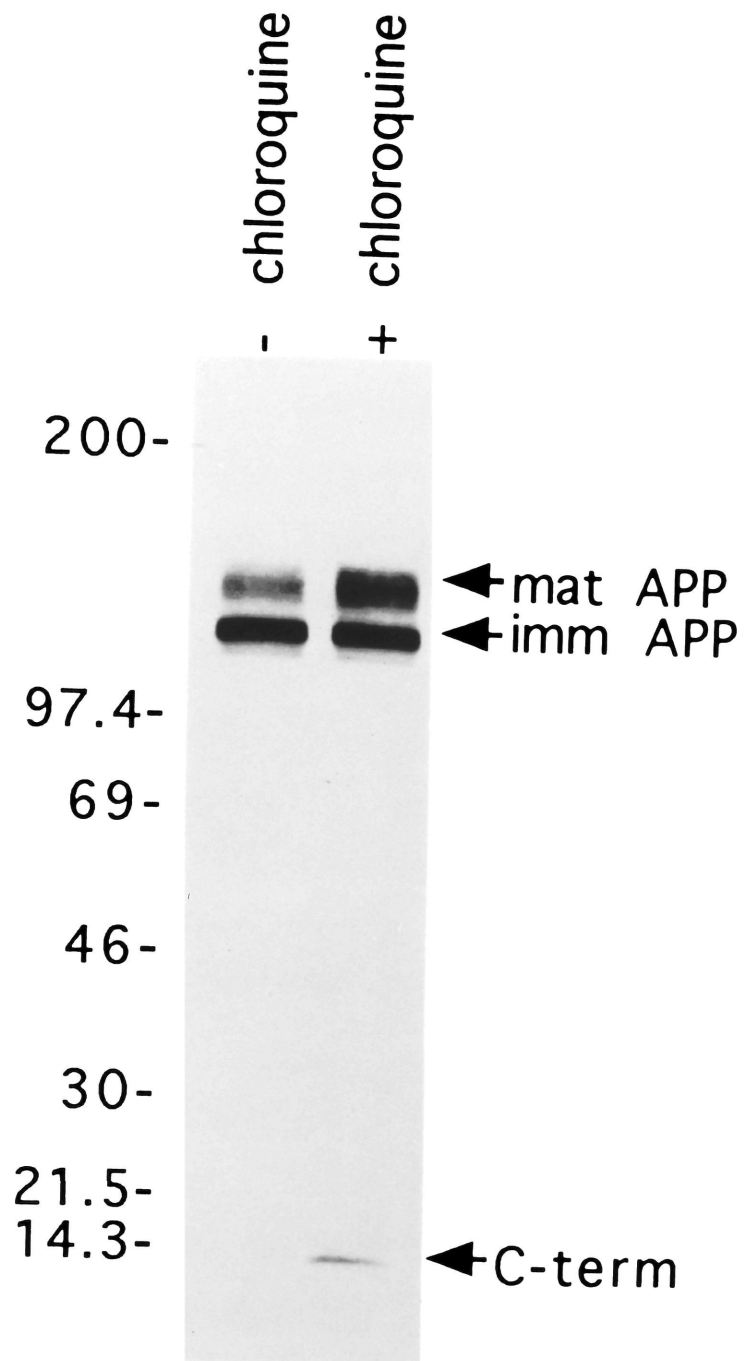
Lgp120, Chloroquine

presence of APP at the TGN could not be assessed by immunoelectron microscopy, because the experimental procedure resulted in the disruption of the TGN. Other experimental protocols (*i.e.*, ultrathin frozen sectioning) did not allow sufficient labeling of APP with the antibodies used.

Concentration of the protein as it moves through the most distal Golgi compartments would occur prior to its dispersal in carrier vesicles to the cell surface or endocytic compartment (Griffiths and Simons, 1986). In addition to the intense Golgi staining, there was visible throughout the cell diffuse punctate APP immunoreactivity, which most likely represents these carrier vesicles. Concentration of immunoreactivity in the *trans* regions of the Golgi complex can be observed for proteins that travel through the secretory pathway and that are destined for secretion (Farquhar, 1985; Griffiths and Simons, 1986). Thus, this localization is in agreement with what is known about the biochemical processing of APP.

Our results with BFA argue against the possibility that accumulation of APP in the distal Golgi complex reflects a recycling of mature APP, or of its carboxyl-terminal fragment, between the TGN and early endosomes. Although BFA induced the formation of a reticulum between the TGN and endosomal system--as identified by Tf-R, a marker for early endosomes (Stoorvogel *et al.*, 1988; Cameron *et al.*, 1991)--no APP immunoreactivity was present in this structure. BFA treatment also resulted in accumulation of full-length APP and inhibition of APP secretion. These results are in agreement with inhibition by BFA of the secretion and transport to the plasma membrane of several proteins (Takatsuki and Tamura, 1985; Misumi

Figure 40. Immunoblot analysis of CHO cells treated with chloroquine. Cells were incubated with medium alone or with medium containing 50 μ M chloroquine for 4 h. Proteins from cell lysates (50 μ g) were separated on a 4-15% SDS-polyacrylamide gel, transferred to nitrocellulose, and probed with antibody 369A. Full-length immature and mature APP appear as 128- and 145-kDa proteins, respectively, and the carboxyl-terminal APP fragment resulting from secretory cleavage appears as an approximately 14-kDa protein. Relative molecular masses (kDa) are indicated at left.



et al., 1986; Magner and Papagiannes, 1988; Fujiwara *et al.*, 1988), as well as with the relocation without functional impairment of Golgi enzymes to the ER (Doms *et al.*, 1989). Since BFA has been shown to dissect functionally the *trans*-Golgi from the TGN (Chege and Pfeffer, 1990), the present results indicate that APP secretory cleavage occurs distal to the *trans*-Golgi.

It seems unlikely that APP is a resident-Golgi protein. In contrast to some resident Golgi proteins such as mannosidase II or galactosyltransferase, which have half-lives of about 20 h (Moremen and Touster, 1985; Strous and Berger, 1982), APP was shown by pulse-chase analysis in PC12 cells to turn over with a half-life of less than two hours (Weidemann *et al.*, 1989; Caporaso *et al.*, 1992a; Chapter 3). In addition, a resident Golgi localization would suggest that APP possesses a Golgi function in addition to its proposed role as a secreted protein (Oltersdorf *et al.*, 1989; Van Nostrand *et al.*, 1989; Saitoh *et al.*, 1989). Finally, although APP immunoreactivity was present in axons and nerve terminals (Figures 29 and 31), the Golgi complex is believed to be excluded from these structures (De Camilli *et al.*, 1986).

The precise mechanism by which phorbol ester affects APP proteolytic processing is not yet understood. Activation of PKC by phorbol ester stimulates the turnover of mature full-length APP in PC12 cells (Buxbaum *et al.*, 1990) and increases APP secretion (Caporaso *et al.*, 1992b; Chapter 4). Mature full-length APP and carboxyl-terminal APP fragments have been shown to be substrates for PKC (Gandy *et al.*, 1988; Suzuki *et al.*, 1992), but the significance, if any, of APP phosphorylation on its processing remains to be

determined. Alternatively, PDBu might exert its effect on a component of the APP processing apparatus. In an attempt to assess whether phorbol ester exerts its effect on APP processing by altering the movement of APP molecules, it was examined whether APP cellular immunoreactivity could be redistributed by treatment of cells with PDBu. No change in APP immunolocalization was observed when examined with different carboxyl-terminal APP antibodies. However, any redistribution of mature APP due to PDBu might not be discernible by light microscopy, since immunoblot data showed that CHO cells contain mostly immature APP and that PDBu exerts its effects only on the mature forms of APP (Figure 38).

The present study provides strong evidence that APP is targeted to lysosomes for proteolytic processing. In cells treated with the weak base chloroquine (de Duve *et al.*, 1974), there was extensive co-localization of APP and the lysosomal integral membrane protein lgp120 (Lewis *et al.*, 1985), though little or no co-localization was seen in untreated cells (Figure 39). There was no accumulation of APP immunoreactivity in the region of the Golgi complex, indicating that the effects of chloroquine on APP processing do not occur at the TGN, which is an acidic cellular compartment that might be sensitive to weak bases (Anderson and Pathak, 1985). Also, the results suggest that APP is rapidly proteolyzed in lysosomes, since APP could only be seen in these structures when lysosomal proteolysis was inhibited by chloroquine. This was apparent by the accumulation in cell lysates of mature full-length APP and the carboxyl-terminal APP fragment resulting from secretory cleavage (Figure 40). These results agree with other

studies indicating that lysosomotropic agents can affect APP proteolytic processing (Cole *et al.*, 1989; Golde *et al.*, 1992; Caporaso *et al.*, 1992a; Chapter 3; Knops *et al.*, 1992) or cause accumulation of APP and APP degradation products in vesicular structures identified as lysosomes (Haass *et al.*, 1992a). The conclusion that lysosomes play a role in the pathogenesis of Alzheimer disease, however, would require definitive evidence that lysosome-specific enzymes can produce β /A4 amyloid peptide *in vitro* or in cell-free preparations. The recent demonstration that lysosomotropic agents can alter the production of β /A4 peptide from cultured cells (Shoji *et al.*, 1992) should facilitate the study of the precise cellular locus for the production of β /A4 amyloid.

An intriguing finding from this study was the immunoelectron microscopic localization of APP to medium-sized, apparently invaginated vesicles in axons and dendrites (Figure 31). The punctate APP staining seen in the proximal segments of axons (Figure 29) and in the processes of hippocampal neurons (Figure 30) might at least be partially accounted for by these vesicles. These structures may be carrier vesicles for APP, though it remains to be established whether they are migrating from the Golgi complex to the cell periphery or *vice versa* or both. Studies with ligated rat sciatic nerve revealed that APP undergoes anterograde fast axonal transport, but the organelles responsible for this transport were not identified (Koo *et al.*, 1990). Structures ("compound double vesicles") similar to the ones observed in the present report have been seen in the cell body and axon of the giant cerebral neuron of *Aplysia*, and have been suggested to be vesicles on their way to nerve terminals

(Shkolnik and Schwartz, 1980). Schubert *et al.* (1991) reported an association of APP with presynaptic vesicles. The present data argue against the presence of significant amounts of APP in synaptic vesicles and do not indicate a concentration of APP at central nervous system synapses (Figure 31).

On the other hand, the APP-positive vesicles may mediate retrograde transport of APP or its carboxyl-terminal fragment. The inner membranes of these structures appear to arise by invagination of the outer membranes and therefore bear similarity to multivesicular bodies (late endosomes), which are known to be involved in retrograde axonal flow (Tsukita and Ishikawa, 1980; Parton *et al.*, 1992). In addition, trafficking through multivesicular bodies could provide a means by which APP is targeted to lysosomes and by which it is released from the membrane so that proteolytic processing to β /A4 peptide could occur (Gandy *et al.*, 1992). Further study is required to clarify the role of these structures in APP trafficking.

Chapter 7

Concluding Remarks

The goal of this research project has been to gain a basic understanding of the cellular trafficking and processing pathways of APP. A comprehensive scheme for these pathways is not yet available, but several aspects of APP processing have been defined during the course of this study. Further, the model of APP trafficking that has emerged provides a starting point from which to begin examining particular facets of APP metabolism. Rather than recapitulate all the findings of the study at this point, it might be worth discussing some issues regarding APP processing and trafficking that have not yet been explained, but which deserve further investigation.

The present study and studies by other researchers have shown that several APP features resemble characteristics each of secretory, lysosomal, and resident plasma-membrane proteins. Like these families of proteins, which are post-translationally modified as they proceed through the ER and Golgi complex, APP is glycosylated and sulfated while it travels through the central vacuolar system. The pulse-chase experiments with monensin and BFA described in Chapter 3 indicate that the covalent additions that result in final APP maturation occur in the *trans*-Golgi and/or TGN. Although it is not known whether these modifications are necessary for normal APP proteolytic processing, inhibition of complete maturation with either

monensin or BFA was found to result in the accumulation of full-length APP and the abolition of APP secretion and degradation. It remains to be determined if only the mature form of APP is recognized by the secretory and degradative apparatus, or if the effects of monensin and BFA can simply be explained by a spatial separation of APP and the processing machinery. Although the immunocytochemical data reported in Chapter 6 are consistent with the latter theory, evaluation of the former possibility awaits either the isolation and *in vitro* assaying of the enzymes responsible for APP processing, or the examination of secretion and degradation for APP constructs that are mutationally defective in maturation.

The concentration of APP in the distal Golgi complex might be related to its sorting to different processing pathways, since secretory, cell-surface, and lysosomal proteins are directed to their final destinations at the TGN (Griffiths and Simons, 1986). The mechanisms by which most proteins are sorted in the TGN are poorly understood. Soluble lysosomal acid hydrolases receive a covalently-attached phosphate moiety, which serves as a "tag" to ensure efficient identification and sorting to lysosomes. Integral membrane proteins of lysosomes may be directed to the prelysosomal compartment either directly via CCVs (Kornfeld and Mellman, 1989) or indirectly via the plasma membrane (Lippincott-Schwartz and Fambrough, 1986). It has recently been shown that one of these proteins, the cation-independent mannose 6-phosphate receptor, possesses at least two signals for lysosomal sorting in its cytoplasmic domain: a pair of tyrosine residues that mediates endocytosis from the cell surface and a pair of leucine residues that probably mediates

interactions with the TGN population of CCVs (Johnson and Kornfeld, 1992). The Igp family of lysosomal membrane proteins seems to rely on a glycine-tyrosine motif for efficient lysosomal targeting (Harter and Mellman, 1992).

APP has at least one sequence in its cytoplasmic domain that is a candidate for a targeting signal, the endocytosis motif NPXY. This and the presence of mature full-length APP in CCVs supports the internalization of APP from the plasma membrane. However, there are other residues that could theoretically be involved in APP sorting, such as the APP phosphorylation sites. Mutational analysis may be useful in evaluating the efficacy of these residues in targeting APP to different cellular destinations. Several AD researchers have recently reported that deletion of the entire APP cytoplasmic domain, or of the carboxyl terminus beginning at the NPXY sequence, results in enhanced basal APP secretion. However, the imprecise nature of these preliminary studies prevents the assignment of targeting function to any specific residue or motif in the APP molecule. Site-directed mutational analysis is required to clarify the role of individual residues in cellular targeting, and could also be useful in examining other aspects of APP processing. For example, mutation of the APP phosphorylation sites could be informative in determining the role of APP phosphorylation in regulating its metabolic fate.

The routes that APP takes either to the cell surface for secretion or to the endosomal/lysosomal compartment for degradation are not known. In addition to possible sorting upon exit from the TGN, the plasma membrane represents another site where

APP targeting could occur. That is, secretory cleavage might take place in the TGN; uncleaved, full-length APP and the carboxyl-terminal APP fragment resulting from secretory proteolysis would then travel to prelysosomes via CCVs for lysosomal degradation, while the amino-terminal fragment would be carried to the cell surface via constitutive secretory vesicles. Alternatively, cleavage might occur at the plasma membrane, with the APP ectodomain released into the medium and remaining APP species endocytosed for lysosomal proteolysis. The results of the CCV experiments described in Chapter 5 are consistent with either of these models.

Attempts at determining whether all APP molecules initially arrive at the plasma membrane--prior to secretory processing or to endocytosis for lysosomal delivery--have not yielded an unambiguous conclusion. Some APP molecules at the cell surface, identified by biotin-labeling, are rapidly endocytosed (G. Caporaso, S. Gandy, J. Buxbaum, and P. Greengard, unpublished observations). In addition, Haass *et al.* (1992a) have reported that biotin-labeled APP can be recovered in purified lysosomes, and Sisodia (1992) has demonstrated that surface-labeled APP is quickly released into the medium of cultured cells. However, quantitative evaluation of the percentage of APP molecules present at the plasma membrane or of the fraction of molecules that travel through the cell surface *en route* to their final destinations has not been successfully performed.

The possible roles for these processing pathways in the pathogenesis of AD are becoming apparent. As discussed in Chapter 4, the secretory pathway represents a non-amyloidogenic route for APP molecules. The finding that APP molecules can be directed to

secretion by activation of PKC suggests targets for therapeutic intervention. However, it has also been shown that excessive upregulation of cellular phosphorylation may result in production of APP carboxyl-terminal fragments possessing an intact β /A4 amyloid domain (Buxbaum *et al.*, 1990; Suzuki *et al.*, 1992). Also, several research groups have recently demonstrated that production of β /A4 amyloid might not be an aberration of cellular processing at all. Intact β /A4 peptide has been recovered from CSF and blood plasma, as well as from the medium of cultured cells (Haass *et al.*, 1992b; Seubert *et al.*, 1992; Shoji *et al.*, 1992). Treatment of cells with lysosomotropic agents affects β /A4 secretion, suggesting that endosomes and/or lysosomes might be the site(s) of this proteolytic processing (Shoji *et al.*, 1992). Future investigative efforts will be directed at determining whether an increased amount of β /A4 amyloid is produced in the brains of AD patients, or whether there is a defect in clearance and removal of β /A4 from the cellular milieu. Moreover, release of β /A4 amyloid into the circulatory and central nervous systems suggests a physiological function for this peptide, which had been assumed to be a potentially toxic by-product of an underlying pathological defect (*e.g.*, genetic mutations in the APP gene). Synthetic β /A4 peptide has recently been reported to bind complement and activate the complement pathway in the absence of antibody, and complement proteins such as C1q are associated with senile plaques (Rogers *et al.*, 1992). It is not clear, however, whether the association of β /A4 amyloid with complement reflects a physiologically meaningful function for the peptide; alternatively, β /A4 amyloid activation of complement might provide a mechanism

for β /A4-mediated cell injury. Careful examination of the processing pathways that lead to production of β /A4 amyloid should further extend our understanding of cerebral amyloidogenesis and its role in the pathogenesis of AD.

References

- Ahle, S., A. Mann, U. Eichelsbacher, and E. Ungewickell. 1988. Structural relationships between clathrin assembly proteins from the Golgi and the plasma membrane. *EMBO (Eur. Mol. Biol. Organ.) J.* 7:919-929.
- Alzheimer. 1907. Über eine eigenartige Erkrankung der Hirnrinde. *Allgemeine Zeitschrift für Psychiatrie und Psychisch-Gerichtlich Medicin.* 64:146-148. English translation from Wilkins and Brody, 1969.
- Anderson, R. G. W., and R. K. Pathak. 1985. Vesicles and cisternae in the *trans* Golgi apparatus of human fibroblasts are acidic compartments. *Cell.* 40:635-643.
- Anderson, J. P., F. S. Esch, P. S. Keim, K. Sambamurti, I. Lieberburg, and N. K. Robakis. 1991. Exact cleavage site of Alzheimer amyloid precursor in neuronal PC-12 cells. *Neurosci. Lett.* 128:126-128.
- Baeuerle, P. A., and W. B. Huttner. 1987. Tyrosine sulfation is a *trans*-Golgi-specific protein modification. *J. Cell Biol.* 105:2655-2664.
- Banker, G. A., and W. M. Cowan. 1977. Rat hippocampal neurons in

dispersed cell culture. *Brain Res.* 126:397-425.

Bartlett, W. P., and G. A. Banker. 1984. An electron microscopic study of the development of axons and dendrites by hippocampal neurons in culture. I. Cells which develop without intercellular contacts. *J. Neurosci.* 4:1944-1953.

Beguino, L., J. A. Hanover, S. Ito, N. D. Richert, M. C. Willingham, and I. Pastan. 1985. Phorbol esters induce transient internalization without degradation of unoccupied epidermal growth factor receptors. *Proc. Natl. Acad. Sci. USA.* 82:2774-2778.

Benowitz, L. I., W. Rodriguez, P. Paskevich, E. J. Mufson, D. Schenk, and R. L. Neve. 1989. The amyloid precursor protein is concentrated in neuronal lysosomes in normal and Alzheimer disease subjects. *Exp. Neurology.* 106:237-250.

Bielschowsky, M. 1911. Zur Kenntnis der Alzheimerschen Krankheit (präsenilen Demenz mit Herdsymptomen). *J. Psychol. Neurol.* 18:273-292.

Biernat, J., E.-M. Mandelkow, C. Schröter, B. Lichtenberg-Kraag, B. Steiner, B. Berling, H. Meyer, M. Mercken, A. Vandermeeren, M. Goedert, and E. Mandelkow. 1992. The switch of tau protein to an Alzheimer-like state includes the phosphorylation of two serine-proline motifs upstream of the microtubule binding region. *EMBO (Eur. Mol. Biol. Organ.) J.* 11:1593-1597.

- Blessed, G., B. E. Tomlinson, and M. Roth. 1968. The association between quantitative measures of dementia and of senile change in the cerebral grey matter of elderly subjects. *Brit. J. Psychiat.* 114:797-811.
- Blocq, P., and G. Marinesco. 1892. Sur les lésions et la pathogénie de l'épilepsie dite essentielle. *Semaine Méd.* 12:445-446.
- Bole, D. G., L. M. Hendershot, and J. F. Kearney. 1986. Posttranslational association of immunoglobulin heavy chain binding protein with nascent heavy chains in nonsecreting and secreting hybridomas. *J. Cell Biol.* 102:1558-1566.
- Brachmann, R., P. B. Lindquist, M. Nagashima, W. Kohr, T. Lipari, M. Napier, and R. Derynck. 1989. Transmembrane TGF- α precursors activate EGF/TGF- α receptors. *Cell.* 56:691-700.
- Bradford, M. M. 1976. A rapid and sensitive method for the quantitation of microgram quantities of protein utilizing the principle of protein-dye binding. *Anal. Biochem.* 72:248-254.
- Brodsky, F. M. 1988. Living with clathrin: Its role in intracellular membrane traffic. *Science (Wash. DC).* 242:1396-1402.
- Buckley, K., and R. B. Kelly. 1985. Identification of a transmembrane glycoprotein specific for secretory vesicles of neural and endocrine cells. *J. Cell Biol.* 100:1284-1294.

Bush, A. I., R. N. Martins, B. Rumble, R. Moir, S. Fuller, E. Milward, J. Currie, D. Ames, A. Weidemann, P. Fischer, G. Multhaup, K. Beyreuther, and C. L. Masters. 1990. The amyloid precursor protein of Alzheimer's disease is released by human platelets. *J. Biol. Chem.* 265:15977-15983.

Buxbaum, J. D., S. E. Gandy, P. Cicchetti, M. E. Ehrlich, A. J. Czernik, R. P. Fracasso, T. V. Ramabhadran, A. J. Unterbeck, and P. Greengard. 1990. Processing of Alzheimer β /A4 amyloid precursor protein: Modulation by agents that regulate protein phosphorylation. *Proc. Natl. Acad. Sci. USA.* 87:6003-6006.

Buxbaum, J. D., M. Oishi, H. I. Chen, R. Pinkas-Kramarski, E. A. Jaffe, S. E. Gandy, and P. Greengard. 1992. Cholinergic agonists and interleukin 1 regulate processing and secretion of the Alzheimer β /A4 amyloid protein precursor. *Proc. Natl. Acad. Sci. USA.* 89:10075-10078.

Caceres, A., and K. S. Kosik. 1990. Inhibition of neurite polarity by tau antisense oligonucleotides in primary cerebellar neurons. *Nature (Lond.).* 343:461-463.

Cameron, P. L., T. C. Südhof, R. Jahn, and P. De Camilli. 1991. Colocalization of synaptophysin with transferrin receptors: Implications for synaptic vesicle biogenesis. *J. Cell Biol.* 115:151-164.

Campbell, C., J. Squicciarini, M. Shia, P. F. Pilch, and R. E. Fine. 1984. Identification of a protein kinase as an intrinsic component of rat liver coated vesicles. *Biochemistry*. 23:4420-4426.

Caporaso, G. L., S. E. Gandy, J. D. Buxbaum, and P. Greengard. 1992a. Chloroquine inhibits intracellular degradation but not secretion of Alzheimer β /A4 amyloid precursor protein. *Proc. Natl. Acad. Sci. USA*. 89:2252-2256.

Caporaso, G. L., S. E. Gandy, J. D. Buxbaum, T. V. Ramabhadran, and P. Greengard. 1992b. Protein phosphorylation regulates secretion of Alzheimer β /A4 amyloid precursor protein. *Proc. Natl. Acad. Sci. USA*. 89:3055-3059.

Caporaso, G. L., K. Takei, S. E. Gandy, M. Matteoli, O. Mundigl, P. Greengard, and P. De Camilli. 1993. Microscopic and biochemical examination of the intracellular trafficking of the Alzheimer β /A4 amyloid precursor protein. Submitted for publication.

Card, J. P., R. P. Meade, and L. G. Davis. 1988. Immunocytochemical localization of the precursor protein for β -amyloid in the rat central nervous system. *Neuron*. 1:835-846.

Casanova, J. E., P. P. Breitfeld, S. A. Ross, and K. E. Mostov. 1990. Phosphorylation of the polymeric immunoglobulin receptor required for its efficient transcytosis. *Science (Wash. DC)*. 248:742-745.

Castagna, M., Y. Takai, K. Kaibuchi, K. Sano, U. Kikkawa, and Y. Nishizuka. 1982. Direct activation of calcium-activated, phospholipid-dependent protein kinase by tumor-promoting phorbol esters. *J. Biol. Chem.* 257:7847-7851.

Chanat, E., and W. B. Huttner. 1991. Milieu-induced, selective aggregation of regulated secretory proteins in the *trans*-Golgi network. *J. Cell Biol.* 115:1505-1519.

Chartier-Harlin, M.-C., F. Crawford, H. Houlden, A. Warren, D. Hughes, L. Fidani, A. Goate, M. Rossor, P. Roques, J. Hardy, and M. Mullan. 1991. Early-onset Alzheimer's disease caused by mutations at codon 717 of the β -amyloid precursor protein gene. *Nature (Lond.)*. 353:844-846.

Chege, N. W., and S. R. Pfeffer. 1990. Compartmentation of the Golgi complex: Brefeldin-A distinguishes *trans*-Golgi cisternae from the *trans*-Golgi network. *J. Cell Biol.* 111:893-899.

Chen, W.-J., J. L. Goldstein, and M. S. Brown. 1990. NPXY, a sequence often found in cytoplasmic tails, is required for coated pit-mediated internalization of the low density lipoprotein receptor. *J. Biol. Chem.* 265:3116-3123.

Citron, M., T. Oltersdorf, C. Haass, L. McConlogue, A. Y. Hung, P. Seubert, C. Vigo-Pelfrey, I. Lieberburg, and D. J. Selkoe. 1992. Mutation of the β -amyloid precursor protein in familial Alzheimer's

disease increases β -protein production. *Nature (Lond.)*. 360:672-674.

Clark, M. J., J. Gagnon, A. F. Williams, and A. N. Barclay. 1985. MRC OX-2 antigen: A lymphoid/neuronal membrane glycoprotein with a structure like a single immunoglobulin light chain. *EMBO (Eur. Mol. Biol. Organ.) J.* 4:113-118.

Cohen, D. H., H. Feiner, O. Jensson, and B. Frangione. 1983. Amyloid fibril in hereditary cerebral hemorrhage with amyloidosis (HCHWA) is related to the gastroentero-pancreatic neuroendocrine protein, gamma trace. *J. Exp. Med.* 158:623-628.

Cohen, P., C. F. B. Holmes, and Y. Tsukitani. 1990. Okadaic acid: A new probe for the study of cellular regulation. *Trends Biochem. Sci.* 15:98-102.

Cole, G. M., T. V. Huynh, and T. Saitoh. 1989. Evidence for lysosomal processing of amyloid β -protein precursor in cultured cells. *Neurochem. Res.* 14:933-939.

Cotman, C. W., C. J. Pike, and A. Copani. 1992. β -amyloid neurotoxicity: A discussion of in vitro findings. *Neurobiol. Aging.* 13:587-590.

De Camilli, P., R. Cameron, and P. Greengard. 1983a. Synapsin I (protein I), a nerve terminal-specific phosphoprotein. I. Its general

distribution in synapses of the central and peripheral nervous system demonstrated by immunofluorescence in frozen and plastic sections. *J. Cell Biol.* 96:1337-1354.

De Camilli, P., S. M. Harris, Jr., W. B. Huttner, and P. Greengard. 1983b. Synapsin I (protein I), a nerve terminal-specific phosphoprotein. II. Its specific association with synaptic vesicles demonstrated by immunocytochemistry in agarose-embedded synaptosomes. *J. Cell Biol.* 96:1355-1373.

De Camilli, P., M. Moretti, S. Denis Donini, U. Walter, and S. M. Lohmann. 1986. Heterogeneous distribution of the cAMP receptor protein RII in the nervous system: Evidence for its intracellular accumulation on microtubules, microtubule-organizing centers, and in the area of the Golgi complex. *J. Cell Biol.* 103:189-203.

de Duve, C., T. de Barsey, B. Poole, A. Trouet, P. Tulkens, and F. Van Hoof. 1974. Commentary. Lysosomotropic drugs. *Biochem. Pharmacol.* 23:2495-2531.

Derynck, R. 1988. Transforming growth factor α . *Cell.* 54:593-595.

de Sauvage, F., and J.-N. Octave. 1989. A novel mRNA of the A4 amyloid precursor gene coding for a possibly secreted protein. *Science (Wash. DC)*. 245:651-653.

Doms, R. W., G. Russ, and J. W. Yewdell. 1989. Brefeldin A

redistributes resident and itinerant Golgi proteins to the endoplasmic reticulum. *J. Cell Biol.* 109:61-72.

Downing, J. R., M. F. Roussel, and C. J. Sherr. 1989. Ligand and protein kinase C downmodulate the colony-stimulating factor 1 receptor by independent mechanisms. *Mol. Cell. Biol.* 9:2890-2896.

Drewes, G., B. Lichtenberg-Kraag, F. Döring, E.-M. Mandelkow, J. Biernat, J. Goris, M. Dorée, and E. Mandelkow. 1992. Mitogen activated protein (MAP) kinase transforms tau protein into an Alzheimer-like state. *EMBO (Eur. Mol. Biol. Organ.) J.* 11:2131-2138.

Eaton, D. L., and J. B. Baker. 1983. Phorbol ester and mitogens stimulate human fibroblast secretions of plasmin-activatable plasminogen activator and protease nexin, an antiactivator/antiplasmin. *J. Cell Biol.* 97:323-328.

Efrat, S., S. Linde, H. Kofod, D. Spector, M. Delannoy, S. Grant, D. Hanahan, and S. Baekkeskov. 1988. Beta-cell lines derived from transgenic mice expressing a hybrid insulin gene-oncogene. *Proc. Natl. Acad. Sci. USA.* 85:9037-9041.

Ehlers, M. R. W., and J. F. Riordan. 1991. Membrane proteins with soluble counterparts: Role of proteolysis in the release of transmembrane proteins. *Biochemistry.* 30:10065-10074.

Esch, F. S., P. S. Keim, E. C. Beattie, R. W. Blacher, A. R. Culwell, T.

Oltersdorf, D. McClure, and P. J. Ward. 1990. Cleavage of amyloid β peptide during constitutive processing of its precursor. *Science* (Wash. DC). 248:1122-1124.

Evans, D. A., H. H. Funkenstein, M. S. Albert, P. A. Scherr, N. R. Cook, M. J. Chown, L. E. Hebert, C. H. Hennekens, and J. O. Taylor. 1989. Prevalence of Alzheimer's disease in a community population of older persons. Higher than previously reported. *JAMA*. 262:2551-2556.

Farquhar, M. G. 1985. Progress in unraveling pathways of Golgi traffic. *Ann. Rev. Cell Biol.* 1:447-488.

Friedreich, N., and A. Kekulé. 1859. Zur amyloidfrage. *Arch. Pathol. Anat. Physiol. Klin. Med.* 16:50-65.

Fujiwara, T., K. Oda, S. Yokota, A. Takatsuki, and Y. Ikehara. 1988. Brefeldin A causes disassembly of the Golgi complex and accumulation of secretory proteins in the endoplasmic reticulum. *J. Biol. Chem.* 263:18545-18552.

Gallis, B., A. Lewis, J. Wignall, A. Alpert, D. Y. Mochizuki, D. Cosman, T. Hopp, and D. Urdal. 1986. Phosphorylation of the human interleukin-2 receptor and a synthetic peptide identical to its C-terminal, cytoplasmic domain. *J. Biol. Chem.* 261:5075-5080.

Gandy, S., A. J. Czernik, and P. Greengard. 1988. Phosphorylation of

Alzheimer disease amyloid precursor peptide by protein kinase C and Ca^{2+} /calmodulin-dependent protein kinase II. *Proc. Natl. Acad. Sci. USA.* 85:6218-6221.

Gandy, S. E., J. D. Buxbaum, and P. Greengard. 1991. Signal transduction and the pathobiology of Alzheimer's disease. *In* Alzheimer's Disease: Basic Mechanisms, Diagnosis and Therapeutic Strategies. K. Iqbal, D. R. Crapper McLachlan, B. Winblad, and H. M. Wisniewski, editors. John Wiley & Sons Ltd., New York. 155-172.

Gandy, S. E., J. D. Buxbaum, and P. Greengard. 1992. A cell biological approach to the therapy of Alzheimer-type cerebral β /A4-amyloidosis. *In* Alzheimer's Disease. New Treatment Strategies. Z. S. Khachaturian and J. P. Blass, editors. Marcel Dekker, Inc., New York. 175-192.

Gazdar, A. F., W. L. Chick, H. K. Oie, H. L. Sims, D. L. King, G. C. Weir, and V. Lauris. 1980. Continuous, clonal, insulin- and somatostatin-secreting cell lines established from a transplantable rat islet cell tumor. *Proc. Natl. Acad. Sci. USA.* 77:3519-3523.

Geddes, J. W., K. J. Anderson, and C. W. Cotman. 1986. Senile plaques as aberrant sprout-stimulating structures. *Exp. Neurol.* 94:767-776.

Giaccone, G., F. Tagliavini, G. Linoli, C. Bouras, L. Frigerio, B. Frangione, and O. Bugiani. 1989. Down patients: Extracellular preamyloid deposits precede neuritic degeneration and senile plaques. *Neurosci.*

Lett. 97:232-238.

Gillespie, S. L., T. E. Golde, and S. G. Younkin. 1992. Secretory processing of the Alzheimer amyloid β /A4 protein precursor is increased by protein phosphorylation. *Biochem. Biophys. Res. Commun.* 187:1285-1290.

Glennner, G. G., and C. W. Wong. 1984a. Alzheimer's disease: Initial report of the purification and characterization of a novel cerebrovascular amyloid protein. *Biochem. Biophys. Res. Commun.* 120:885-890.

Glennner, G. G., and C. W. Wong. 1984b. Alzheimer's disease and Down's syndrome: Sharing of a unique cerebrovascular amyloid fibril protein. *Biochem. Biophys. Res. Commun.* 122:1131-1135.

Goate, A., M.-C. Chartier-Harlin, M. Mullan, J. Brown, F. Crawford, L. Fidani, L. Giuffra, A. Haynes, N. Irving, L. James, R. Mant, P. Newton, K. Rooke, P. Roques, C. Talbot, M. Pericak-Vance, A. Roses, R. Williamson, M. Rossor, M. Owen, and J. Hardy. 1991. Segregation of a missense mutation in the amyloid precursor protein gene with familial Alzheimer's disease. *Nature (Lond.)*. 349:704-706.

Goedert, M., C. M. Wischik, R. A. Crowther, J. E. Walker, and A. Klug. 1988. Cloning and sequencing of the cDNA encoding a core protein of the paired helical filament of Alzheimer disease: Identification as the microtubule-associated protein tau. *Proc. Natl. Acad. Sci. USA*.

85:4051-4055.

Golde, T. E., S. Estus, M. Usiak, L. H. Younkin, and S. G. Younkin. 1990. Expression of β amyloid protein precursor mRNAs: Recognition of a novel alternatively spliced form and quantitation in Alzheimer's disease using PCR. *Neuron*. 4:253-267.

Golde, T. E., S. Estus, L. H. Younkin, D. J. Selkoe, and S. G. Younkin. 1992. Processing of the amyloid protein precursor to potentially amyloidogenic derivatives. *Science (Wash. DC)*. 255:728-730.

Goldgaber, D., M. I. Lerman, O. W. McBride, U. Saffiotti, and D. C. Gajdusek. 1987. Characterization and chromosomal localization of a cDNA encoding brain amyloid of Alzheimer's disease. *Science (Wash. DC)*. 235:877-880.

Goldgaber, D., H. W. Harris, T. Hla, T. Maciag, R. J. Donnelly, J. S. Jacobsen, M. P. Vitek, and D. C. Gajdusek. 1989. Interleukin 1 regulates synthesis of amyloid β -protein precursor mRNA in human endothelial cells. *Proc. Natl. Acad. Sci. USA*. 86:7606-7610.

Goldstein, J. L., M. S. Brown, R. G. W. Anderson, D. W. Russell, and W. J. Schneider. 1985. Receptor-mediated endocytosis: Concepts emerging from the LDL receptor system. *Annu. Rev. Cell Biol.* 1:1-39.

Green, S. A., and R. B. Kelly. 1992. Low density lipoprotein receptor

and cation-independent mannose 6-phosphate receptor are transported from the cell surface to the Golgi apparatus at equal rates in PC12 cells. *J. Cell Biol.* 117:47-55.

Greenberg, S. G., and P. Davies. 1990. A preparation of Alzheimer paired helical filaments that displays distinct τ proteins by polyacrylamide gel electrophoresis. *Proc. Natl. Acad. Sci. USA.* 87:5827-5831.

Greene, L. A., and A. S. Tischler. 1976. Establishment of a noradrenergic clonal line of rat adrenal pheochromocytoma cells which respond to nerve growth factor. *Proc. Natl. Acad. Sci. USA.* 73:2424-2428.

Greene, L. A., M. M. Sobeih, and K. K. Teng. 1991. Methodologies for the culture and experimental use of the PC12 rat pheochromocytoma cell line. *In Culturing Nerve Cells.* G. Banker and K. Goslin, editors. MIT Press, Cambridge, MA. 207-226.

Griffiths, G., P. Quinn, and G. Warren. 1983. Dissection of the Golgi complex. I. Monensin inhibits the transport of viral membrane proteins from *medial* to *trans* Golgi cisternae in baby hamster kidney cells infected with Semliki Forest virus. *J. Cell Biol.* 96:835-850.

Griffiths, G., and K. Simons. 1986. The *trans* Golgi network: Sorting at the exit site of the Golgi complex. *Science (Wash. DC).* 234:438-443.

Grundke-Iqbal, I., K. Iqbal, Y.-C. Tung, M. Quinlan, H. M. Wisniewski, and L. I. Binder. 1986. Abnormal phosphorylation of the microtubule-associated protein τ (tau) in Alzheimer cytoskeletal pathology. *Proc. Natl. Acad. Sci. USA.* 83:4913-4917.

Haass, C., A. Y. Hung, and D. J. Selkoe. 1991. Processing of β -amyloid precursor protein in microglia and astrocytes favors an internal localization over constitutive secretion. *J. Neurosci.* 11:3783-3793.

Haass, C., E. H. Koo, A. Mellon, A. Y. Hung, and D. J. Selkoe. 1992a. Targeting of cell-surface β -amyloid precursor protein to lysosomes: Alternative processing into amyloid-bearing fragments. *Nature (Lond.)*. 357:500-503.

Haass, C., M. G. Schlossmacher, A. Y. Hung, C. Vigo-Pelfrey, A. Mellon, B. L. Ostaszewski, I. Lieberburg, E. H. Koo, D. Schenk, D. B. Teplow, and D. J. Selkoe. 1992b. Amyloid β -peptide is produced by cultured cells during normal metabolism. *Nature (Lond.)*. 359:322-325.

Harter, C., and I. Mellman. 1992. Transport of the lysosomal membrane glycoprotein lgp120 (lgp-A) to lysosomes does not require appearance on the plasma membrane. *J. Cell Biol.* 117:311-325.

Hasegawa, M., T. Arai, and Y. Ihara. 1990. Immunochemical evidence that fragments of phosphorylated MAP5 (MAP1B) are bound to neurofibrillary tangles in Alzheimer's disease. *Neuron*.

4:909-918.

Hendriks, L., C. M. van Duijn, P. Cras, M. Cruts, W. Van Hul, F. van Harskamp, A. Warren, M. G. McInnis, S. E. Antonarakis, J.-J. Martin, A. Hofman, and C. Van Broeckhoven. 1992. Presenile dementia and cerebral haemorrhage linked to a mutation at codon 692 of the β -amyloid precursor protein gene. *Nature Genet.* 1:218-221.

Himmler, A. 1989. Structure of the bovine tau gene: Alternatively spliced transcripts generate a protein family. *Mol. Cell. Biol.* 9:1389-1396.

Himmler, A., D. Drechsel, M. W. Kirschner, and D. W. Martin, Jr. 1989. Tau consists of a set of proteins with repeated C-terminal microtubule-binding domains and variable N-terminal domains. *Mol. Cell. Biol.* 9:1381-1388.

Hunter, T., N. Ling, and J. A. Cooper. 1984. Protein kinase C phosphorylation of the EGF receptor at a threonine residue close to the cytoplasmic face of the plasma membrane. *Nature (Lond.)*. 311:480-483.

Ishiguro, K., M. Takamatsu, K. Tomizawa, A. Omori, M. Takahashi, M. Arioka, T. Uchida, and K. Imahori. 1992. Tau protein kinase I converts normal tau protein into A68-like component of paired helical filaments. *J. Biol. Chem.* 267:10897-10901.

Jacobsen, J. S., H. A. Muenkel, A. J. Blume, and M. P. Vitek. 1991. A novel species-specific RNA related to alternatively spliced amyloid precursor protein mRNAs. *Neurobiol. Aging*. 12:575-583.

Jaken, S., and P. H. Black. 1981. Regulation of plasminogen activator in 3T3 cells: Effect of phorbol myristate acetate on subcellular distribution and molecular weight. *J. Cell Biol.* 90:727-731.

Joachim, C. L., J. H. Morris, and D. J. Selkoe. 1989. Diffuse senile plaques occur commonly in the cerebellum in Alzheimer's disease. *Am. J. Pathol.* 135:309-319.

Joachim, C. L., and D. J. Selkoe. 1992. The seminal role of β -amyloid in the pathogenesis of Alzheimer disease. *Alzheimer Disease and Associated Disorders*. 6:7-34.

Johnson, K. F., and S. Kornfeld. 1992. The cytoplasmic tail of the mannose 6-phosphate/insulin-like growth factor-II receptor has two signals for lysosomal enzyme sorting in the Golgi. *J. Cell Biol.* 119:249-257.

Kang, J., H.-G. Lemaire, A. Unterbeck, J. M. Salbaum, C. L. Masters, K.-H. Grzeschik, G. Multhaup, K. Beyreuther, and B. Müller-Hill. 1987. The precursor of Alzheimer's disease amyloid A4 protein resembles a cell-surface receptor. *Nature (Lond.)*. 325:733-736.

Kaplan, H. I., and B. J. Sadock. 1988. Synopsis of Psychiatry.

Behavioral Sciences. Clinical Psychiatry. Fifth edition. Williams & Wilkins, Baltimore.

Katzman, R. 1986. Alzheimer's disease. *N. Engl. J. Med.* 314:964-973.

Khachaturian, Z. S. 1985. Diagnosis of Alzheimer's disease. *Arch. Neurol.* 42:1097-1105.

Kidd, M. 1963. Paired helical filaments in electron microscopy of Alzheimer's disease. *Nature (Lond.)*. 197:192-193.

Kidd, M. 1964. Alzheimer's disease--An electron microscopical study. *Brain.* 87:307-320.

Kikkawa, U., and Y. Nishizuka. 1986. The role of protein kinase C in transmembrane signalling. *Ann. Rev. Cell Biol.* 2:149-178.

Kishimoto, T. K., M. A. Jutila, E. L. Berg, and E. C. Butcher. 1989. Neutrophil Mac-1 and MEL-14 adhesion proteins inversely regulated by chemotactic factors. *Science (Wash. DC)*. 245:1238-1241.

Kitaguchi, N., Y. Takahashi, Y. Tokushima, S. Shiojiri, and H. Ito. 1988. Novel precursor of Alzheimer's disease amyloid protein shows protease inhibitory activity. *Nature (Lond.)*. 331:530-532.

Klausner, R. D., and R. Sitia. 1990. Protein degradation in the

endoplasmic reticulum. *Cell*. 62:611-614.

Klausner, R. D., J. G. Donaldson, and J. Lippincott-Schwartz. 1992. Brefeldin A: Insights into the control of membrane traffic and organelle structure. *J. Cell Biol.* 116:1071-1080.

Knops, J., K. S. Kosik, G. Lee, J. D. Pardee, L. Cohen-Gould, and L. McConlogue. 1991. Overexpression of tau in a nonneuronal cell induces long cellular processes. *J. Cell Biol.* 114:725-733.

Knops, J., I. Lieberburg, and S. Sinha. 1992. Evidence for a nonsecretory, acidic degradation pathway for amyloid precursor protein in 293 cells. Identification of a novel, 22-kDa, β -peptide-containing intermediate. *J. Biol. Chem.* 267:16022-16024.

Koh, J.-y., L. L. Yang, and C. W. Cotman. 1990. β -amyloid protein increases the vulnerability of cultured cortical neurons to excitotoxic damage. *Brain Res.* 533:315-320.

Koo, E. H., S. S. Sisodia, D. R. Archer, L. J. Martin, A. Weidemann, K. Beyreuther, P. Fischer, C. L. Masters, and D. L. Price. 1990. Precursor of amyloid protein in Alzheimer disease undergoes fast anterograde axonal transport. *Proc. Natl. Acad. Sci. USA.* 87:1561-1565.

Kornfeld, S., and I. Mellman. 1989. The biogenesis of lysosomes. *Annu. Rev. Cell Biol.* 5:483-525.

Kosik, K. S., C. L. Joachim, and D. J. Selkoe. 1986. Microtubule-associated protein tau (τ) is a major antigenic component of paired helical filaments in Alzheimer disease. *Proc. Natl. Acad. Sci. USA*. 83:4044-4048.

Kosik, K. S., L. D. Orecchio, L. Binder, J. Q. Trojanowski, V. M.-Y. Lee, and G. Lee. 1988. Epitopes that span the tau molecule are shared with paired helical filaments. *Neuron*. 1:817-825.

Kraepelin, E. 1910. *Psychiatrie*. J. A. Barth, Leipzig.

Ksiezak-Reding, H., L. I. Binder, and S.-H. Yen. 1990. Alzheimer disease proteins (A β 8) share epitopes with tau but show distinct biochemical properties. *J. Neurosci. Res*. 25:420-430.

Laemmli, U. K. 1970. Cleavage of structural proteins during the assembly of the head of bacteriophage T4. *Nature (Lond.)*. 227:680-685.

Lantz, M., U. Gullberg, E. Nilsson, and I. Olsson. 1990. Characterization in vitro of a human tumor necrosis factor-binding protein. A soluble form of a tumor necrosis factor receptor. *J. Clin. Invest*. 86:1396-1402.

Lazarovits, J., and M. Roth. 1988. A single amino acid change in the cytoplasmic domain allows the influenza virus hemagglutinin to be endocytosed through coated pits. *Cell*. 53:743-752.

Lee, V. M.-Y., B. J. Balin, L. Otvos, Jr., and J. Q. Trojanowski. 1991. A68: A major subunit of paired helical filaments and derivatized forms of normal tau. *Science (Wash. DC)*. 251:675-678.

Lemaire, H. G., J. M. Salbaum, G. Multhaup, J. Kang, R. M. Bayney, A. Unterbeck, K. Beyreuther, and B. Müller-Hill. 1989. The PreA4₆₉₅ precursor protein of Alzheimer's disease A4 amyloid is encoded by 16 exons. *Nucleic Acids Res.* 17:517-522.

Levy, E., M. D. Carmen, I. J. Fernandez-Madrid, M. D. Power, I. Lieberburg, S. G. van Duinen, G. Th. A. M. Bots, W. Luyendijk, and B. Frangione. 1990. Mutation of the Alzheimer's disease amyloid gene in hereditary cerebral hemorrhage, Dutch type. *Science (Wash. DC)*. 248:1124-1126.

Lewis, V., S. A. Green, M. Marsh, P. Vihko, A. Helenius, and I. Mellman. 1985. Glycoproteins of the lysosomal membrane. *J. Cell Biol.* 100:1839-1847.

Lin, C. R., W. S. Chen, C. S. Lazar, C. D. Carpenter, G. N. Gill, R. M. Evans, and M. G. Rosenfeld. 1986. Protein kinase C phosphorylation at Thr 654 of the unoccupied EGF receptor and EGF binding regulate functional receptor loss by independent mechanisms. *Cell*. 44:839-848.

Lindwall, G., and R. D. Cole. 1984. Phosphorylation affects the ability of tau protein to promote microtubule assembly. *J. Biol. Chem.*

259:5301-5305.

Lippincott-Schwartz, J., and D. M. Fambrough. 1986. Lysosomal membrane dynamics: Structure and interorganellar movement of a major lysosomal membrane glycoprotein. *J. Cell Biol.* 102:1593-1605.

Lippincott-Schwartz, J., J. S. Bonifacino, L. C. Yuan, and R. D. Klausner. 1988. Degradation from the endoplasmic reticulum: Disposing of newly synthesized proteins. *Cell.* 54:209-220.

Lippincott-Schwartz, J., L. C. Yuan, J. S. Bonifacino, and R. D. Klausner. 1989. Rapid redistribution of Golgi proteins into the ER in cells treated with brefeldin A: Evidence for membrane cycling from Golgi to ER. *Cell.* 56:801-813.

Lippincott-Schwartz, J., L. Yuan, C. Tipper, M. Amherdt, L. Orci, and R. D. Klausner. 1991. Brefeldin A's effects on endosomes, lysosomes, and the TGN suggest a general mechanism for regulating organelle structure and membrane traffic. *Cell.* 67:601-616.

Lobel, P., K. Fujimoto, R. D. Ye, G. Griffiths, and S. Kornfeld. 1989. Mutations in the cytoplasmic domain of the 275 kd mannose 6-phosphate receptor differentially alter lysosomal enzyme sorting and endocytosis. *Cell.* 57:787-796.

Low, D. A., J. B. Baker, W. C. Koonce, and D. C. Cunningham. 1981.

Released protease-nexin regulates cellular binding, internalization, and degradation of serine proteases. *Proc. Natl. Acad. Sci. USA.* 78:2340-2344.

Lund, K. A., C. S. Lazar, W. S. Chen, B. J. Walsh, J. B. Welsh, J. J. Herbst, G. M. Walton, M. G. Rosenfeld, G. N. Gill, and H. S. Wiley. 1990. Phosphorylation of the epidermal growth factor receptor at threonine 654 inhibits ligand-induced internalization and down-regulation. *J. Biol. Chem.* 265:20517-20523.

Luo, L., L. E. Martin-Morris, and K. White. 1990. Identification, secretion, and neural expression of APPL, a *Drosophila* protein similar to human amyloid protein precursor. *J. Neurosci.* 10:3849-3861.

Luo, L., T. Tully, and K. White. 1992. Human amyloid precursor protein ameliorates behavioral deficit of flies deleted for *Appl* gene. *Neuron.* 9:595-605.

Magner, J. A., and E. Papagiannes. 1988. Blockade by brefeldin A of intracellular transport of secretory proteins in mouse pituitary cells: Effects on the biosynthesis of thyrotropin and free α -subunits. *Endocrinology.* 122:912-920.

Manetto, V., G. Perry, M. Tabaton, P. Mulvihill, V. A. Fried, H. T. Smith, P. Gambetti, and L. Autilio-Gambetti. 1988. Ubiquitin is associated with abnormal cytoplasmic filaments characteristic of

neurodegenerative diseases. *Proc. Natl. Acad. Sci. USA.* 85:4501-4505.

Mann, D. M. A., and M. M. Esiri. 1989. The pattern of acquisition of plaques and tangles in the brains of patients under 50 years of age with Down's syndrome. *J. Neurol. Sci.* 89:169-179.

Martin, L. J., S. S. Sisodia, E. H. Koo, L. C. Cork, T. L. Dellovade, A. Weidemann, K. Beyreuther, C. Masters, and D. L. Price. 1991. Amyloid precursor protein in aged nonhuman primates. *Proc. Natl. Acad. Sci. USA.* 88:1461-1465.

Masliah, E., R. D. Terry, M. Mallory, M. Alford, and L. A. Hansen. 1990. Diffuse plaques do not accentuate synapse loss in Alzheimer's disease. *Am. J. Pathol.* 137:1293-1297.

Masters, C. L., G. Simms, N. A. Weinman, G. Multhaup, B. L. McDonald, and K. Beyreuther. 1985. Amyloid plaque protein in Alzheimer disease and Down syndrome. *Proc. Natl. Acad. Sci. USA.* 82:4245-4249.

Mattson, M. P., B. Cheng, D. Davis, K. Bryant, I. Lieberburg, and R. E. Rydel. 1992. β -amyloid peptides destabilize calcium homeostasis and render human cortical neurons vulnerable to excitotoxicity. *J. Neurosci.* 12:376-389.

May, W. S., S. Jacobs, and P. Cuatrecasas. 1984. Association of

phorbol ester-induced hyperphosphorylation and reversible regulation of transferrin membrane receptors in HL60 cells. *Proc. Natl. Acad. Sci. USA.* 81:2016-2020.

May, W. S., N. Sahyoun, S. Jacobs, M. Wolf, and P. Cuatrecasas. 1985. Mechanism of phorbol diester-induced regulation of surface transferrin receptor involves the action of activated protein kinase C and an intact cytoskeleton. *J. Biol. Chem.* 260:9419-9426.

McGraw, T. E., K. W. Dunn, and F. R. Maxfield. 1988. Phorbol ester treatment increases the exocytic rate of the transferrin receptor recycling pathway independent of serine-24 phosphorylation. *J. Cell Biol.* 106:1061-1066.

McKhann, G., D. Drachman, M. Folstein, R. Katzman, D. Price, and E. M. Stadlan. 1984. Clinical diagnosis of Alzheimer's disease: Report of the NINCDS-ADRDA Work Group under the auspices of Department of Health and Human Services Task Force on Alzheimer's Disease. *Neurology.* 34:939-944.

Misumi, Y., Y. Misumi, K. Miki, A. Takatsuki, G. Tamura, and Y. Ikehara. 1986. Novel blockade by brefeldin A of intracellular transport of secretory proteins in cultured rat hepatocytes. *J. Biol. Chem.* 261:11398-11403.

Moremen, K. W., and O. Touster. 1985. Biosynthesis and modification of Golgi mannosidase II in HeLa and 3T3 cells. *J. Biol. Chem.*

260:6654-6662.

Mori, H., J. Kondo, and Y. Ihara. 1987. Ubiquitin is a component of paired helical filaments in Alzheimer's disease. *Science (Wash. DC)*. 235:1641-1644.

Moriyama, Y., T. Takano, and S. Ohkuma. 1982. Acridine orange as a fluorescent probe for lysosomal proton pump. *J. Biochem.* 92:1333-1336.

Mullan, M., F. Crawford, K. Axelman, H. Houlden, L. Lilius, B. Winblad, and L. Lannfelt. 1992. A pathogenic mutation for probable Alzheimer's disease in the APP gene at the N-terminus of β -amyloid. *Nature Genet.* 1:345-347.

Murrell, J., M. Farlow, B. Ghetti, and M. D. Benson. 1991. A mutation in the amyloid precursor protein associated with hereditary Alzheimer's disease. *Science (Wash. DC)*. 254:97-99.

Nairn, A. C., H. C. Hemmings, Jr., and P. Greengard. 1985. Protein kinases in the brain. *Ann. Rev. Biochem.* 54:931-976.

Nandi, P. K., G. Irace, P. P. Van Jaarsveld, R. E. Lippoldt, and H. Edelhoch. 1982. Instability of coated vesicles in concentrated sucrose solutions. *Proc. Natl. Acad. Sci. USA.* 79:5881-5885.

Naruse, S., S. Igarashi, H. Kobayashi, K. Aoki, T. Inuzuka, K. Kaneko, T.

Shimizu, K. Iihara, T. Kojima, T. Miyatake, and S. Tsuji. 1991. Mis-sense mutation Val—>Ile in exon 17 of amyloid precursor protein gene in Japanese familial Alzheimer's disease. *Lancet*. 337:978-979.

Nestler, E. J., and P. Greengard. 1984. Protein Phosphorylation in the Nervous System. John Wiley & Sons, Inc., New York.

Nestler, E. J., S. I. Walaas, and P. Greengard. 1984. Neuronal phosphoproteins: Physiological and clinical implications. *Science (Wash. DC)*. 225:1357-1364.

Neve, R. L., E. A. Finch, and L. R. Dawes. 1988. Expression of the Alzheimer amyloid precursor gene transcripts in the human brain. *Neuron*. 1:669-677.

Niederau, C., and J. H. Grendell. 1988. Intracellular vacuoles in experimental acute pancreatitis in rats and mice are an acidified compartment. *J. Clin. Invest.* 81:229-236.

Nitsch, R. M., B. E. Slack, R. J. Wurtman, and J. H. Growdon. 1992. Release of Alzheimer amyloid precursor derivatives stimulated by activation of muscarinic acetylcholine receptors. *Science (Wash. DC)*. 258:304-307.

Nordstedt, C., G. L. Caporaso, J. Thyberg, S. E. Gandy, and P. Greengard. 1993. Identification of the Alzheimer β /A4 amyloid precursor protein in clathrin-coated vesicles purified from PC12 cells. *J. Biol.*

Chem. 268:608-612.

Novikoff, P. M., D. R. P. Tulsiani, O. Touster, A. Yam, and A. B. Novikoff. 1983. Immunocytochemical localization of α -D-mannosidase II in the Golgi apparatus of rat liver. *Proc. Natl. Acad. Sci. USA.* 80:4364-4368.

Nukina, N., K. S. Kosik, and D. J. Selkoe. 1988. The monoclonal antibody, Alz 50, recognizes tau proteins in Alzheimer's disease brain. *Neurosci. Lett.* 87:240-246.

Ogomori, K., T. Kitamoto, J. Tateishi, Y. Sato, M. Suetsugu, and M. Abe. 1989. β -Protein amyloid is widely distributed in the central nervous system of patients with Alzheimer's disease. *Am. J. Pathol.* 134:243-251.

Ohkuma, S., and B. Poole. 1981. Cytoplasmic vacuolation of mouse peritoneal macrophages and the uptake into lysosomes of weakly basic substances. *J. Cell Biol.* 90:656-664.

Oltersdorf, T., L. C. Fritz, D. B. Schenk, I. Lieberburg, K. L. Johnson-Wood, E. C. Beattie, P. J. Ward, R. W. Blacher, H. F. Dovey, and S. Sinha. 1989. The secreted form of the Alzheimer's amyloid precursor protein with the Kunitz domain is protease nexin-II. *Nature (Lond.).* 341:144-147.

Oltersdorf, T., P. J. Ward, T. Henriksson, E. C. Beattie, R. Neve, I.

Lieberburg, and L. C. Fritz. 1990. The Alzheimer amyloid precursor protein. Identification of a stable intermediate in the biosynthetic/degradative pathway. *J. Biol. Chem.* 265:4492-4497.

Overly, C. C., L. C. Fritz, I. Lieberburg, and L. McConlogue. 1991. The β -amyloid precursor protein is not processed by the regulated secretory pathway. *Biochem. Biophys. Res. Comm.* 181:513-519.

Palade, G. 1975. Intracellular aspects of the process of protein synthesis. *Science (Wash. DC)*. 189:347-358.

Palmert, M. R., M. Berman Podlisny, D. S. Witker, T. Oltersdorf, L. H. Younkin, D. J. Selkoe, and S. G. Younkin. 1989. The β -amyloid protein precursor of Alzheimer disease has soluble derivatives found in human brain and cerebrospinal fluid. *Proc. Natl. Acad. Sci. USA*. 86:6338-6342.

Pandiella, A., and J. Massagué. 1991. Cleavage of the membrane precursor for transforming growth factor α is a regulated process. *Proc. Natl. Acad. Sci. USA*. 88:1726-1730.

Parton, R. G., K. Simons, and C. G. Dotti. 1992. Axonal and dendritic endocytic pathways in cultured neurons. *J. Cell Biol.* 119:123-137.

Pearse, B. M. F. 1976. Clathrin: A unique protein associated with intracellular transfer of membrane by coated vesicles. *Proc. Natl. Acad. Sci. USA*. 73:1255-1259.

Pearse, B. M. F. 1988. Receptors compete for adaptors found in plasma membrane coated pits. *EMBO (Eur. Mol. Biol. Organ.) J.* 7:3331-3336.

Pelham, H. R. B. 1991. Multiple targets for brefeldin A. *Cell.* 67:449-451.

Pericak-Vance, M. A., J. L. Bebout, P. C. Gaskell, Jr., L. H. Yamaoka, W.-Y. Hung, M. J. Alberts, A. P. Walker, R. J. Bartlett, C. A. Haynes, K. A. Welsh, N. L. Earl, A. Heyman, C. M. Clark, and A. D. Roses. 1991. Linkage studies in familial Alzheimer disease: Evidence for chromosome 19 linkage. *Am. J. Hum. Genet.* 48:1034-1050.

Podlisny, M. B., D. R. Tolan, and D. J. Selkoe. 1991. Homology of the amyloid beta protein precursor in monkey and human supports a primate model for beta amyloidosis in Alzheimer's disease. *Am. J. Pathol.* 138:1423-1435.

Ponte, P., P. Gonzalez-DeWhitt, J. Schilling, J. Miller, D. Hsu, B. Greenberg, K. Davis, W. Wallace, I. Lieberburg, F. Fuller, and B. Cordell. 1988. A new A4 amyloid mRNA contains a domain homologous to serine proteinase inhibitors. *Nature (Lond.).* 331:525-527.

Poole, B., and S. Ohkuma. 1981. Effect of weak bases on the intralysosomal pH in mouse peritoneal macrophages. *J. Cell Biol.* 90:665-669.

Powers, R. E., R. G. Struble, M. F. Casanova, D. T. O'Connor, C. A. Kitt, and D. L. Price. 1988. Innervation of human hippocampus by noradrenergic systems: Normal anatomy and structural abnormalities in aging and in Alzheimer's disease. *Neuroscience*. 25:401-417.

Prelli, F., E. Castaño, G. G. Glenner, and B. Frangione. 1988. Differences between vascular and plaque core amyloid in Alzheimer's disease. *J. Neurochem.* 51:648-651.

Price, D. L., E. H. Koo, and A. Unterbeck. 1989. Cellular and molecular biology of Alzheimer's disease. *BioEssays*. 10:69-74.

Quon, D., Y. Wang, R. Catalano, J. Marian Scardina, K. Murakami, and B. Cordell. 1991. Formation of β -amyloid protein deposits in brains of transgenic mice. *Nature (Lond.)*. 352:239-241.

Reaves, B., and G. Banting. 1992. Perturbation of the morphology of the *trans*-Golgi network following brefeldin A treatment: Redistribution of a TGN-specific integral membrane protein, TGN38. *J. Cell Biol.* 116:85-94.

Régnier-Vigouroux, A., S. A. Tooze, and W. B. Huttner. 1991. Newly synthesized synaptophysin is transported to synaptic-like microvesicles via constitutive secretory vesicles and the plasma membrane. *EMBO (Eur. Mol. Biol. Organ.) J.* 10:3589-3601.

Ridgway, N. D., P. A. Dawson, Y. K. Ho, M. S. Brown, and J. L. Goldstein. 1992. Translocation of oxysterol binding protein to Golgi apparatus triggered by ligand binding. *J. Cell Biol.* 116:307-319.

Robakis, N. K., N. Ramakrishna, G. Wolfe, and H. M. Wisniewski. 1987. Molecular cloning and characterization of a cDNA encoding the cerebrovascular and the neuritic plaque amyloid peptides. *Proc. Natl. Acad. Sci. USA.* 84:4190-4194.

Roder, H. M., and V. M. Ingram. 1991. Two novel kinases phosphorylate tau and the KSP site of heavy neurofilament subunits in high stoichiometric ratios. *J. Neurosci.* 11:3325-3343.

Rogers, J., N. R. Cooper, S. Webster, J. Schultz, P. L. McGeer, S. D. Styren, W. H. Civin, L. Brachova, B. Bradt, P. Ward, and I. Lieberburg. 1992. Complement activation by β -amyloid in Alzheimer disease. *Proc. Natl. Acad. Sci. USA.* 89:10016-10020.

Rosen, D. R., L. Martin-Morris, L. Luo, and K. White. 1989. A *Drosophila* gene encoding a protein resembling the human β -amyloid protein precursor. *Proc. Natl. Acad. Sci. USA.* 86:2478-2482.

Rumble, B., R. Retallack, C. Hilbich, G. Simms, G. Multhaup, R. Martins, A. Hockey, P. Montgomery, K. Beyreuther, and C. L. Masters. 1989. Amyloid A4 protein and its precursor in Down's syndrome and Alzheimer's disease. *N. Eng. J. Med.* 320:1446-1452.

Saitoh, T., M. Sundsmo, J.-M. Roch, N. Kimura, G. Cole, D. Schubert, T. Oltersdorf, and D. B. Schenk. 1989. Secreted form of amyloid β protein precursor is involved in the growth regulation of fibroblasts. *Cell*. 58:615-622.

Schellenberg, G. D., T. D. Bird, E. M. Wijsman, D. K. Moore, M. Boehnke, E. M. Bryant, T. H. Lampe, D. Nochlin, S. M. Sumi, S. S. Deeb, K. Beyreuther, and G. M. Martin. 1988. Absence of linkage of chromosome 21q21 markers to familial Alzheimer's disease. *Science (Wash. DC)*. 241:1507-1510.

Schellenberg, G. D., M. Boehnke, E. M. Wijsman, D. K. Moore, G. M. Martin, and T. D. Bird. 1992a. Genetic association and linkage analysis of the apolipoprotein CII locus and familial Alzheimer's disease. *Ann. Neurol.* 31:223-227.

Schellenberg, G. D., T. D. Bird, E. M. Wijsman, H. T. Orr, L. Anderson, E. Nemens, J. A. White, L. Bonnycastle, J. L. Weber, M. E. Alonso, H. Potter, L. L. Heston, and G. M. Martin. 1992b. Genetic linkage evidence for a familial Alzheimer's disease locus on chromosome 14. *Science (Wash. DC)*. 258:668-671.

Schubert, W., R. Prior, A. Weidemann, H. Dirksen, G. Multhaup, C. L. Masters, and K. Beyreuther. 1991. Localization of Alzheimer β A4 amyloid precursor protein at central and peripheral synaptic sites. *Brain Res.* 563:184-194.

Schwartz, P., J. Kurucz, and A. Kurucz. 1965. Fluorescence microscopy demonstration of cerebrovascular and pancreatic insular amyloid in presenile and senile states. *J. Am. Geriatr. Soc.* 13:199-205.

Selkoe, D. J. 1989a. Molecular pathology of amyloidogenic proteins and the role of vascular amyloidosis in Alzheimer's disease. *Neurobiol. Aging.* 10:387-395.

Selkoe, D. J. 1989b. Biochemistry of altered brain proteins in Alzheimer's disease. *Ann. Rev. Neurosci.* 12:463-490.

Selkoe, D. J. 1991. The molecular pathology of Alzheimer's disease. *Neuron.* 6:487-498.

Selkoe, D. J., Y. Ihara, and F. J. Salazar. 1982. Alzheimer's disease: Insolubility of partially purified paired helical filaments in sodium dodecyl sulfate and urea. *Science (Wash. DC).* 215:1243-1245.

Selkoe, D. J., D. S. Bell, M. B. Podlisny, D. L. Price, and L. C. Cork. 1987. Conservation of brain amyloid proteins in aged mammals and humans with Alzheimer's disease. *Science (Wash. DC).* 235:873-877.

Seubert, P., C. Vigo-Pelfrey, F. Esch, M. Lee, H. Dovey, D. Davis, S. Sinha, M. Schlossmacher, J. Whaley, C. Swindlehurst, R. McCormack, R. Wolfert, D. Selkoe, I. Lieberburg, and D. Schenk. 1992. Isolation and quantification of soluble Alzheimer's β -peptide from biological fluids.

Nature (Lond.). 359:325-327.

Shackelford, D. A., and I. S. Trowbridge. 1986. Identification of lymphocyte integral membrane proteins as substrates for protein kinase C. *J. Biol. Chem.* 261:8334-8341.

Shenoy, S., J.-K. Choi, S. Bagrodia, T. D. Copeland, J. L. Maller, and D. Shalloway. 1989. Purified maturation promoting factor phosphorylates pp60^{c-src} at the sites phosphorylated during fibroblast mitosis. *Cell*. 57:763-774.

Shivers, B. D., C. Hilbich, G. Multhaup, M. Salbaum, K. Beyreuther, and P. H. Seeburg. 1988. Alzheimer's disease amyloidogenic glycoprotein: Expression pattern in rat brain suggests a role in cell contact. *EMBO (Eur. Mol. Biol. Organ.) J.* 7:1365-1370.

Shkolnik, L. J., and J. H. Schwartz. 1980. Genesis and maturation of serotonergic vesicles in identified giant cerebral neuron of *Aplysia*. *J. Neurophysiol.* 43:945-967.

Shoji, M., T. E. Golde, J. Ghiso, T. T. Cheung, S. Estus, L. M. Shaffer, X.-D. Cai, D. M. McKay, R. Tintner, B. Frangione, and S. G. Younkin. 1992. Production of the Alzheimer amyloid β protein by normal proteolytic processing. *Science (Wash. DC)*. 258:126-129.

Simchowicz, T. 1911. Histologische Studien über die senile Demenz. *Histol. Histopathol. Arb. Grosshirnrinde*. 4:267-444.

Sipe, J. D. 1992. Amyloidosis. *Annu. Rev. Biochem.* 61:947-975.

Sisodia, S. S. 1992. β -amyloid precursor protein cleavage by a membrane-bound protease. *Proc. Natl. Acad. Sci. USA.* 89:6075-6079.

Sisodia, S. S., E. H. Koo, K. Beyreuther, A. Unterbeck, and D. L. Price. 1990. Evidence that β -amyloid protein in Alzheimer's disease is not derived by normal processing. *Science (Wash. DC).* 248:492-495.

Slot, J. W., and H. J. Geuze. 1985. A new method of preparing gold probes for multiple-labeling cytochemistry. *Eur. J. Cell Biol.* 38:87-93.

Smith, R. P., D. A. Higuchi, and G. J. Broze, Jr. 1990. Platelet coagulation factor XI_a-inhibitor, a form of Alzheimer amyloid precursor protein. *Science (Wash. DC).* 248:1126-1128.

Stein, J., and C. W. Rettenmier. 1991. Proteolytic processing of a plasma membrane-bound precursor to human macrophage colony-stimulating factor (CSF-1) is accelerated by phorbol ester. *Oncogene.* 6:601-605.

Sternberger, N. H., L. A. Sternberger, and J. Ulrich. 1985. Aberrant neurofilament phosphorylation in Alzheimer disease. *Proc. Natl. Acad. Sci. USA.* 82:4274-4276.

St George-Hyslop, P. H., R. E. Tanzi, R. J. Polinsky, J. L. Haines, L. Nee, P. C. Watkins, R. H. Myers, R. G. Feldman, D. Pollen, D. Drachman, J. Growdon, A. Bruni, J.-F. Foncin, D. Salmon, P. Frommelt, L. Amaducci, S. Sorbi, S. Piacentini, G. D. Stewart, W. J. Hobbs, P. M. Conneally, and J. F. Gusella. 1987. The genetic defect causing familial Alzheimer's disease maps on chromosome 21. *Science (Wash. DC)*. 235:885-890.

St George-Hyslop, P. H., J. L. Haines, L. A. Farrer, R. Polinsky, C. Van Broeckhoven, A. Goate, D. R. Crapper McLachlan, H. Orr, A. C. Bruni, S. Sorbi, I. Rainero, J.-F. Foncin, D. Pollen, J.-M. Cantu, R. Tupler, N. Voskresenskaya, R. Mayeux, J. Growdon, V. A. Fried, R. H. Myers, L. Nee, H. Backhoven, J.-J. Martin, M. Rossor, M. J. Owen, M. Mullan, M. E. Percy, H. Karlinsky, S. Rich, L. Heston, M. Montesi, M. Mortilla, N. Nacmias, J. F. Gusella, J. A. Hardy, and other members of the FAD Collaborative Study group. 1990. Genetic linkage studies suggest that Alzheimer's disease is not a single homogeneous disorder. *Nature (Lond.)*. 347:194-197.

Stoorvogel, W., H. J. Geuze, J. M. Griffith, and G. J. Strous. 1988. The pathways of endocytosed transferrin and secretory protein are connected in the *trans*-Golgi reticulum. *J. Cell Biol.* 106:1821-1829.

Strous, G. J. A. M., and E. G. Berger. 1982. Biosynthesis, intracellular transport, and release of the Golgi enzyme galactosyltransferase (lactose synthetase A protein) in HeLa cells. *J. Biol. Chem.* 257:7623-7628.

Struble, R. G., R. E. Powers, M. F. Casanova, C. A. Kitt, E. C. Brown, and D. L. Price. 1987. Neuropeptidergic systems in plaques of Alzheimer's disease. *J. Neuropathol. Exp. Neurol.* 46:567-584.

Suenaga, T., A. Hirano, J. F. Llena, S.-H. Yen, and D. W. Dickson. 1990. Modified Bielschowsky stain and immunohistochemical studies on striatal plaques in Alzheimer's disease. *Acta Neuropathol.* 80:280-286.

Suzuki, T., A. C. Nairn, S. E. Gandy, and P. Greengard. 1992. Phosphorylation of Alzheimer amyloid precursor protein by protein kinase C. *Neuroscience.* 48:755-761.

Takatsuki, A., and G. Tamura. 1985. Brefeldin A, a specific inhibitor of intracellular translocation of vesicular stomatitis virus G protein: Intracellular accumulation of high-mannose type G protein and inhibition of its cell surface expression. *Agric. Biol. Chem.* 49:899-902.

Takei, K., H. Stukenbrok, A. Metcalf, G. A. Mignery, T. C. Südhof, P. Volpe, and P. De Camilli. 1992. Ca^{2+} stores in Purkinje neurons: Endoplasmic reticulum subcompartments demonstrated by the heterogeneous distribution of the InsP_3 receptor, Ca^{2+} -ATPase, and calsequestrin. *J. Neurosci.* 12:489-505.

Tanzi, R. E., J. F. Gusella, P. C. Watkins, G. A. P. Bruns, P. St George-Hyslop, M. L. Van Keuren, D. Patterson, S. Pagan, D. M. Kurnit, and R.

L. Neve. 1987. Amyloid β protein gene: cDNA, mRNA distribution, and genetic linkage near the Alzheimer locus. *Science (Wash. DC)*. 235:880-884.

Tanzi, R. E., A. I. McClatchey, E. D. Lamperti, L. Villa-Komaroff, J. F. Gusella, and R. L. Neve. 1988. Protease inhibitor domain encoded by an amyloid protein precursor mRNA associated with Alzheimer's disease. *Nature (Lond.)*. 331:528-530.

Tartakoff, A. M. 1983. Perturbation of vesicular traffic with the carboxylic ionophore monensin. *Cell*. 32:1026-1028.

Tartakoff, A. M., and P. Vassalli. 1983. Lectin-binding sites as markers of Golgi subcompartments: Proximal-to-distal maturation of oligosaccharides. *J. Cell Biol.* 97:1243-1248.

Tomlinson, B. E., and J. A. N. Corsellis. 1984. Ageing and the dementias. *In* Greenfield's Neuropathology. Fourth edition. J. H. Adams, J. A. N. Corsellis, and L. W. Duchon, editors. John Wiley & Sons, Inc., New York. 951-1025.

Towbin, H., T. Staehelin, and J. Gordon. 1979. Electrophoretic transfer of proteins from polyacrylamide gels to nitrocellulose sheets: Procedure and some applications. *Proc. Natl. Acad. Sci. USA*. 76:4350-4354.

Trojanowski, J. Q., M. L. Schmidt, L. Otvos, Jr., H. Arai, W. D. Hill, and

V. M.-Y. Lee. 1990. Vulnerability of the neuronal cytoskeleton in aging and Alzheimer disease: Widespread involvement of all three major filament systems. *Annu. Rev. Gerontol. Geriatr.* 10:167-182.

Tsukita, S., and H. Ishikawa. 1980. The movement of membranous organelles in axons. Electron microscopic identification of anterogradely and retrogradely transported organelles. *J. Cell Biol.* 84:513-530.

Turkewitz, A. P., and S. C. Harrison. 1989. Concentration of transferrin receptor in human placental coated vesicles. *J. Cell Biol.* 108:2127-2135.

Uéda, K., E. Masliah, T. Saitoh, S. L. Bakalis, H. Scoble, and K. S. Kosik. 1990. Alz-50 recognizes a phosphorylated epitope of tau protein. *J. Neurosci.* 10:3295-3304.

Van Broeckhoven, C., J. Haan, E. Bakker, J. A. Hardy, W. Van Hul, A. Wehnert, M. Vegter-Van der Vlis, and R. A. C. Roos. 1990. Amyloid β protein precursor gene and hereditary cerebral hemorrhage with amyloidosis (Dutch). *Science (Wash. DC)*. 248:1120-1122.

van Duinen, S. G., E. M. Castaño, F. Prelli, G. T. A. B. Bots, W. Luyendijk, and B. Frangione. 1987. Hereditary cerebral hemorrhage with amyloidosis in patients of Dutch origin is related to Alzheimer disease. *Proc. Natl. Acad. Sci. USA.* 84:5991-5994.

Van Nostrand, W. E., and D. D. Cunningham. 1987. Purification of protease nexin II from human fibroblasts. *J. Biol. Chem.* 262:8508-8514.

Van Nostrand, W. E., S. L. Wagner, M. Suzuki, B. H. Choi, J. S. Farrow, J. W. Geddes, C. W. Cotman, and D. D. Cunningham. 1989. Protease nexin-II, a potent antichymotrypsin, shows identity to amyloid β -protein precursor. *Nature (Lond.)*. 341:546-549.

Vinters, H. V., and J. J. Gilbert. 1983. Cerebral amyloid angiopathy: Incidence and complications in the aging brain. II. The distribution of amyloid vascular changes. *Stroke*. 14:924-928.

Virchow, R. 1855. Ueber den Gang der amyloiden Degeneration. *Arch. Pathol. Anat. Physiol. Klin. Med.* 8:364-368.

Virtanen, I., P. Ekblom, and P. Laurila. 1980. Subcellular compartmentalization of saccharide moieties in cultured normal and malignant cells. *J. Cell Biol.* 85:429-434.

Vulliet, P. R., F. L. Hall, J. P. Mitchell, and D. G. Hardie. 1989. Identification of a novel proline-directed serine/threonine protein kinase in rat pheochromocytoma. *J. Biol. Chem.* 264:16292-16298.

Wasco, W., K. Bupp, M. Magendantz, J. F. Gusella, R. E. Tanzi, and F. Solomon. 1992. Identification of a mouse brain cDNA that encodes a protein related to the Alzheimer disease-associated amyloid β

protein precursor. *Proc. Natl. Acad. Sci. USA.* 89:10758-10762.

Wattendorff, A. R., G. Th. A. M. Bots, L. N. Went, and L. J. Endtz. 1982. Familial cerebral amyloid angiopathy presenting as recurrent cerebral haemorrhage. *J. Neurol. Sci.* 55:121-135.

Weidemann, A., G. König, D. Bunke, P. Fischer, J. M. Salbaum, C. L. Masters, and K. Beyreuther. 1989. Identification, biogenesis and localization of precursors of Alzheimer's disease A4 amyloid protein. *Cell.* 57:115-126.

Whitson, J. S., D. J. Selkoe, and C. W. Cotman. 1989. Amyloid β protein enhances the survival of hippocampal neurons in vitro. *Science (Wash. DC).* 243:1488-1490.

Wilkins, R. H., and I. A. Brody. 1969. Alzheimer's disease. *Arch. Neurol.* 21:109-110.

Wischik, C. M., M. Novak, H. C. Thøgersen, P. C. Edwards, M. J. Runswick, R. Jakes, J. E. Walker, C. Milstein, M. Roth, and A. Klug. 1988a. Isolation of a fragment of tau derived from the core of the paired helical filament of Alzheimer disease. *Proc. Natl. Acad. Sci. USA.* 85:4506-4510.

Wischik, C. M., M. Novak, P. C. Edwards, A. Klug, W. Tichelaar, and R. A. Crowther. 1988b. Structural characterization of the core of the paired helical filament of Alzheimer disease. *Proc. Natl. Acad. Sci.*

USA. 85:4884-4888.

Wisniewski, K. E., A. J. Dalton, D. R. Crapper McLachlan, G. Y. Wen, and H. M. Wisniewski. 1985. Alzheimer's disease in Down's syndrome: Clinicopathologic studies. *Neurology*. 35:957-961.

Wisniewski, T., J. Ghiso, and B. Frangione. 1991. Peptides homologous to the amyloid protein of Alzheimer's disease containing a glutamine for glutamic acid substitution have accelerated amyloid fibril formation. *Biochem. Biophys. Res. Commun.* 179:1247-1254.

Wolozin, B. L., A. Pruchnicki, D. W. Dickson, and P. Davies. 1986. A neuronal antigen in the brains of Alzheimer patients. *Science (Wash. DC)*. 232:648-650.

Wong, S. T., L. F. Winchell, B. K. McCune, H. S. Earp, J. Teixidó, J. Massagué, B. Herman, and D. C. Lee. 1989. The TGF- α precursor expressed on the cell surface binds to the EGF receptor on adjacent cells, leading to signal transduction. *Cell*. 56:495-506.

Wood, S. A., J. E. Park., and W. J. Brown. 1991. Brefeldin A causes a microtubule-mediated fusion of the trans-Golgi network and early endosomes. *Cell*. 67:591-600.

Wunderlich, D., A. Lee, R. P. Fracasso, D. V. Mierz, R. M. Bayney, and T. V. Ramabhadran. 1992. Use of recombinant fusion proteins for generation and rapid characterization of monoclonal antibodies.

Application to the Kunitz domain of human β amyloid precursor protein. *J. Imm. Meth.* 147:1-11.

Yamada, T., H. Sasaki, H. Furuya, T. Miyata, I. Goto, and Y. Sakaki. 1987. Complementary DNA for the mouse homolog of the human amyloid beta protein precursor. *Biochem. Biophys. Res. Commun.* 149:665-671.

Yan, Y. C., Y. Bai, L. Wang, S. Miao, and S. S. Koide. 1990. Characterization of cDNA encoding a human sperm membrane protein related to A4 amyloid protein. *Proc. Natl. Acad. Sci. USA.* 87:2405-2408.

Yankner, B. A., L. R. Dawes, S. Fisher, L. Villa-Komaroff, M. L. Oster-Granite, and R. L. Neve. 1989. Neurotoxicity of a fragment of the amyloid precursor associated with Alzheimer's disease. *Science (Wash. DC).* 245:417-420.

Yankner, B. A., L. K. Duffy, and D. A. Kirschner. 1990a. Neurotrophic and neurotoxic effects of amyloid β protein: Reversal by tachykinin neuropeptides. *Science (Wash. DC).* 250:279-282.

Yankner, B. A., A. Caceres, and L. K. Duffy. 1990b. Nerve growth factor potentiates the neurotoxicity of β amyloid. *Proc. Natl. Acad. Sci. USA.* 87:9020-9023.

Yuan, L., J. G., Barriocanal, J. S. Bonifacino, and I. V. Sandoval. 1987.

Two integral membrane proteins located in the *cis*-middle and *trans*-part of the Golgi system acquire sialylated N-linked carbohydrates and display different turnovers and sensitivity to cAMP-dependent phosphorylation. *J. Cell Biol.* 105:215-227.

End